非平衡态物理和计算方法

极端条件下的物态演化

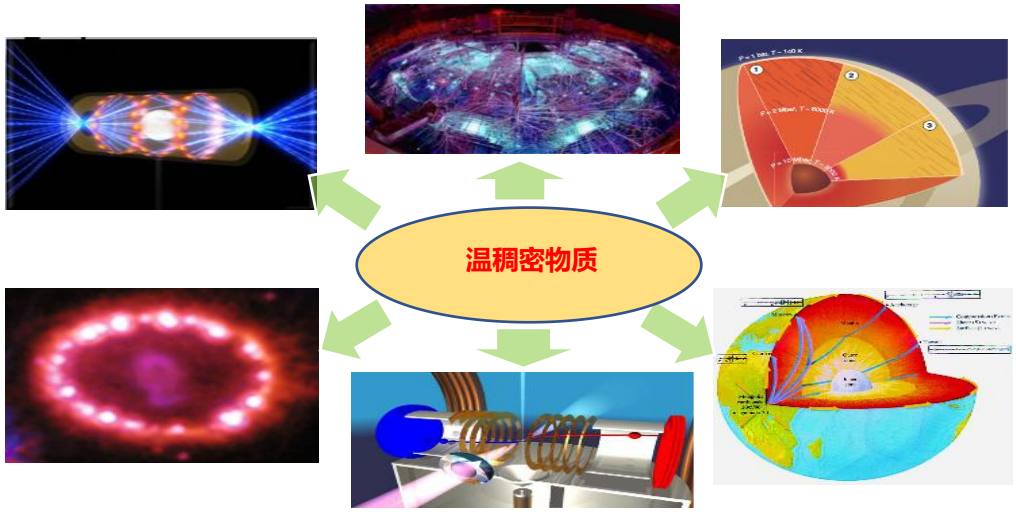

戴佳钰　国防科技大学物理系

北京计科中心

2020.11.11


星火燎

报告内容

第一部分 极端条件下的科学问题

第二部分 计算方法简述

第三部分 典型计算结果

The National Academy of Science report called the frontiers in High Energy Density Physics the X-Games of contemporary science

Inertial Confinement

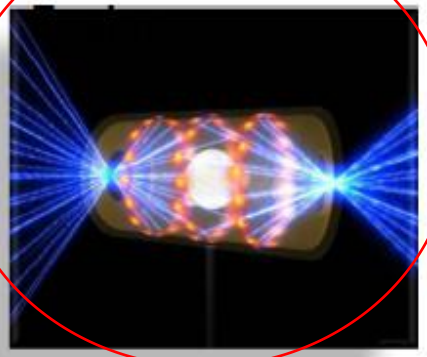

Warm Dense Matter

Quark Gluon Plasma

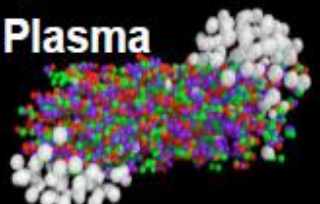

Astrophysics

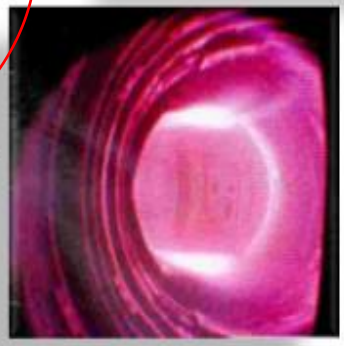

Magnetic Fusion

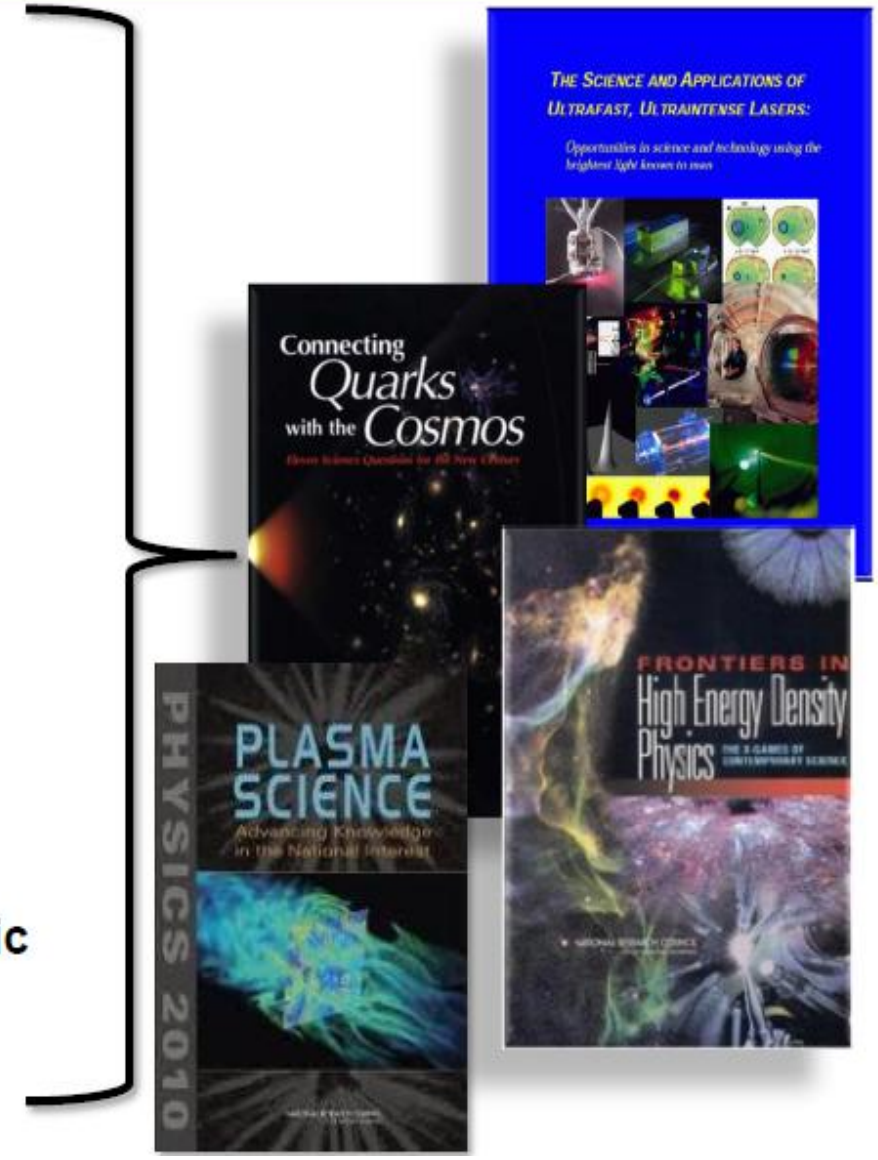

Z-pin experiments

Z

WDM materials platform

Ramp loading up to 5 Mbar,shock loading up to 40 Mbar

Validation

Long time

EOS and op mixtures in WDM state

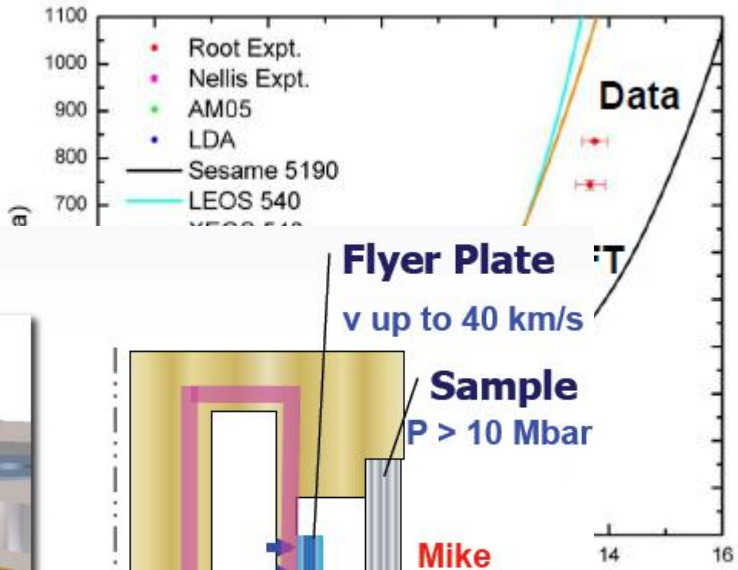

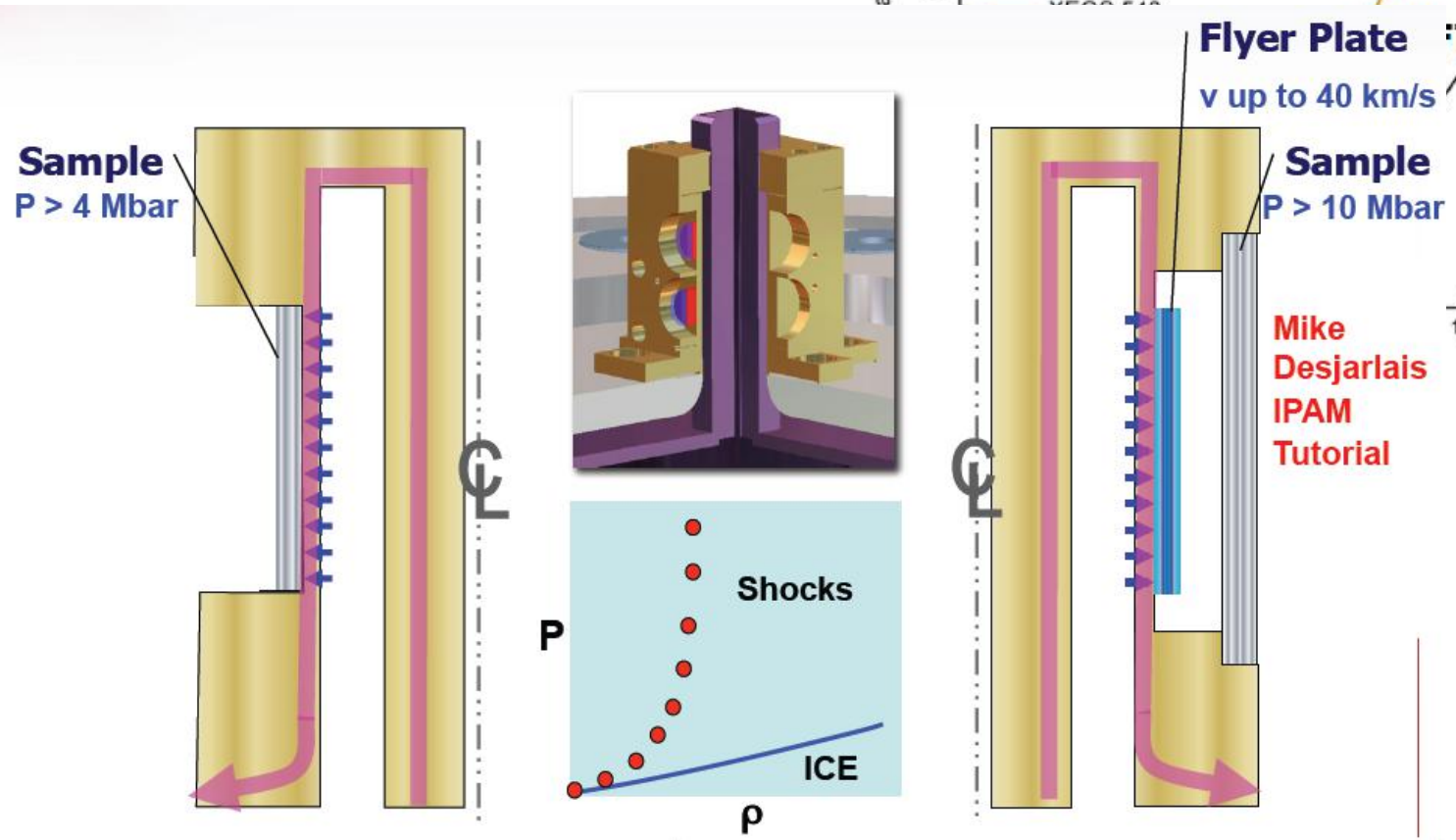

Isentropic Compression Experiments:
gradual pressure rise in sample

Shock Hugoniot Experiments:
shock wave in sample on impact

激光产生温稠密物质动态演化

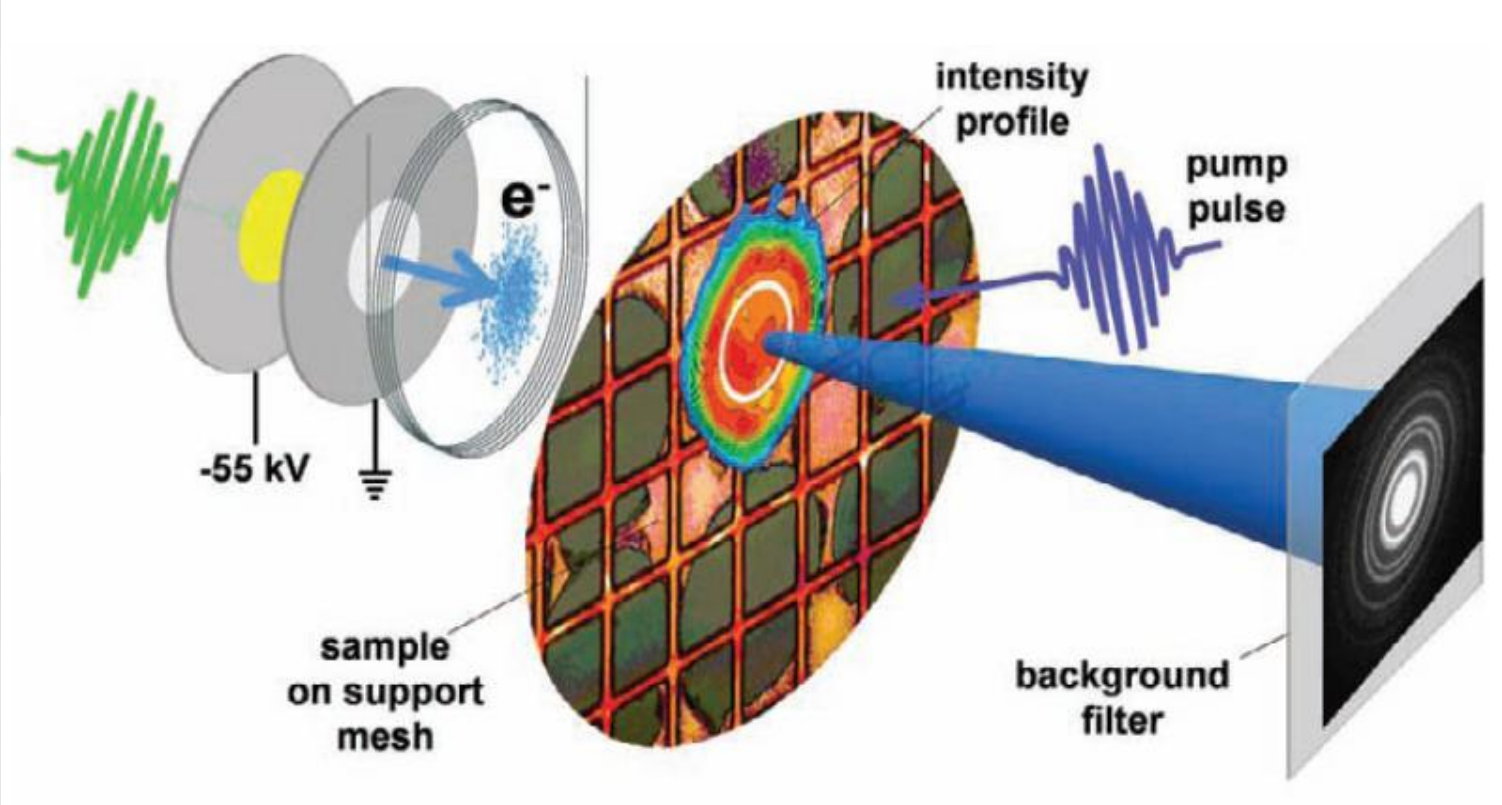

Laser induced the formation of warm dense matter:

Non-equilibrium process

Ultrafast dynamics

Ernstorfer et al. Science 323, 1033-1037 (2009)

康冬冬、戴佳钰*等. 强激光与粒子束 32: 092006 (2020)

Plasmas consist of mobile charged particles (ions, electrons,..) interacting by long-range Coulombic N-body forces

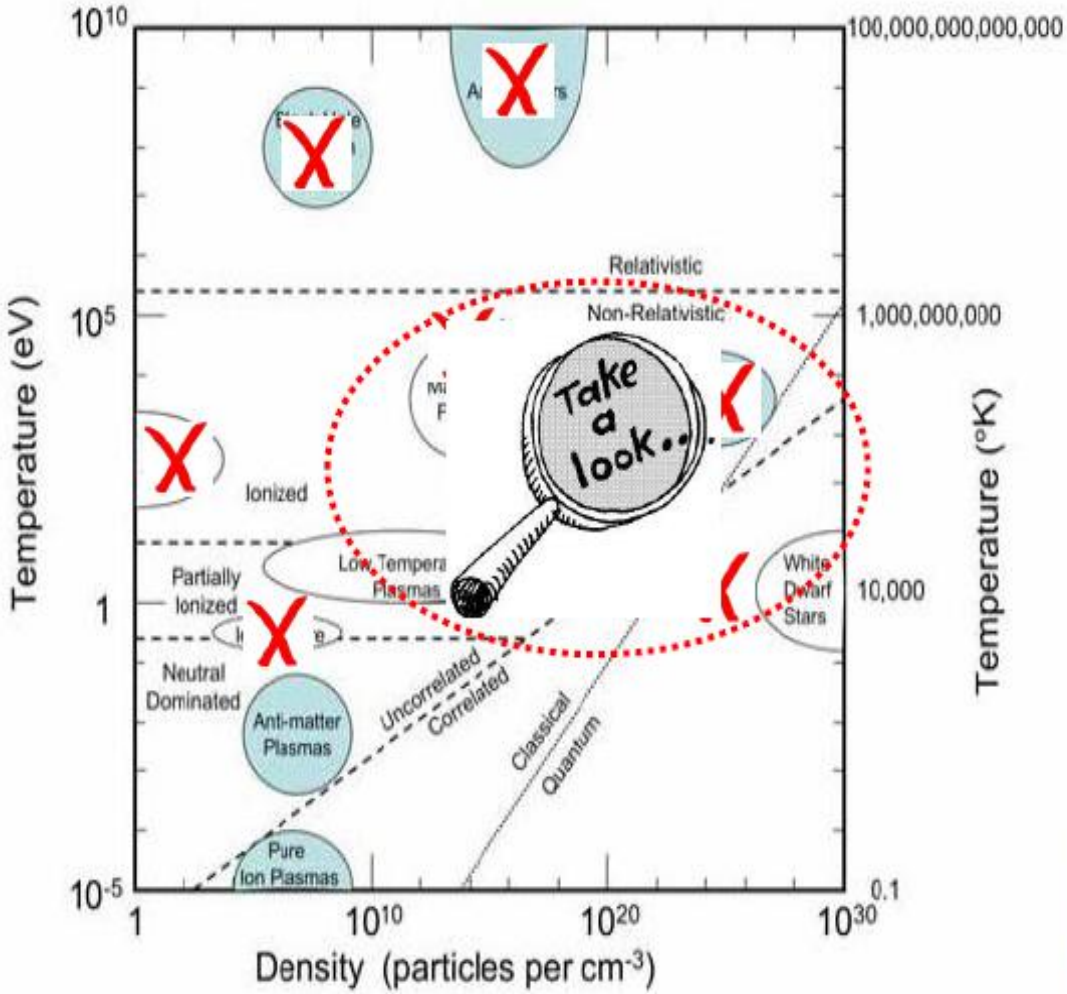

Our understanding of plasma behavior in each of these regimes differs widely

Matter in the plasma state exists in an unimaginable variety

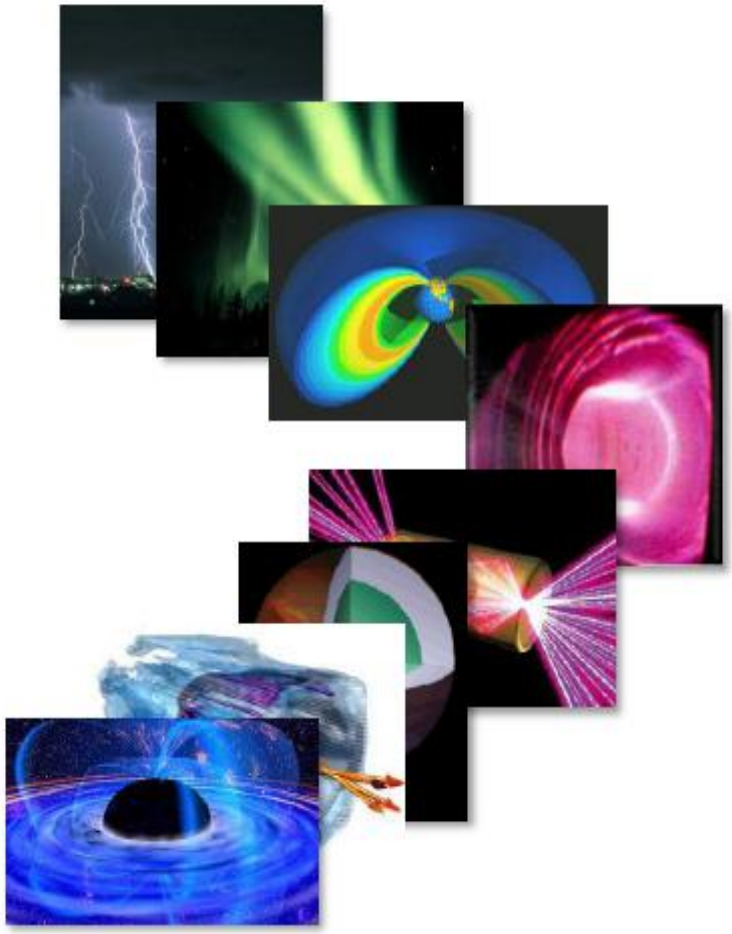

$1\,\mathrm{eV} = 1.16\times10^{4}\ \mathrm{K}$

Matter under high energy density conditions, exhibits complex behavior not typically associated with classical plasmas

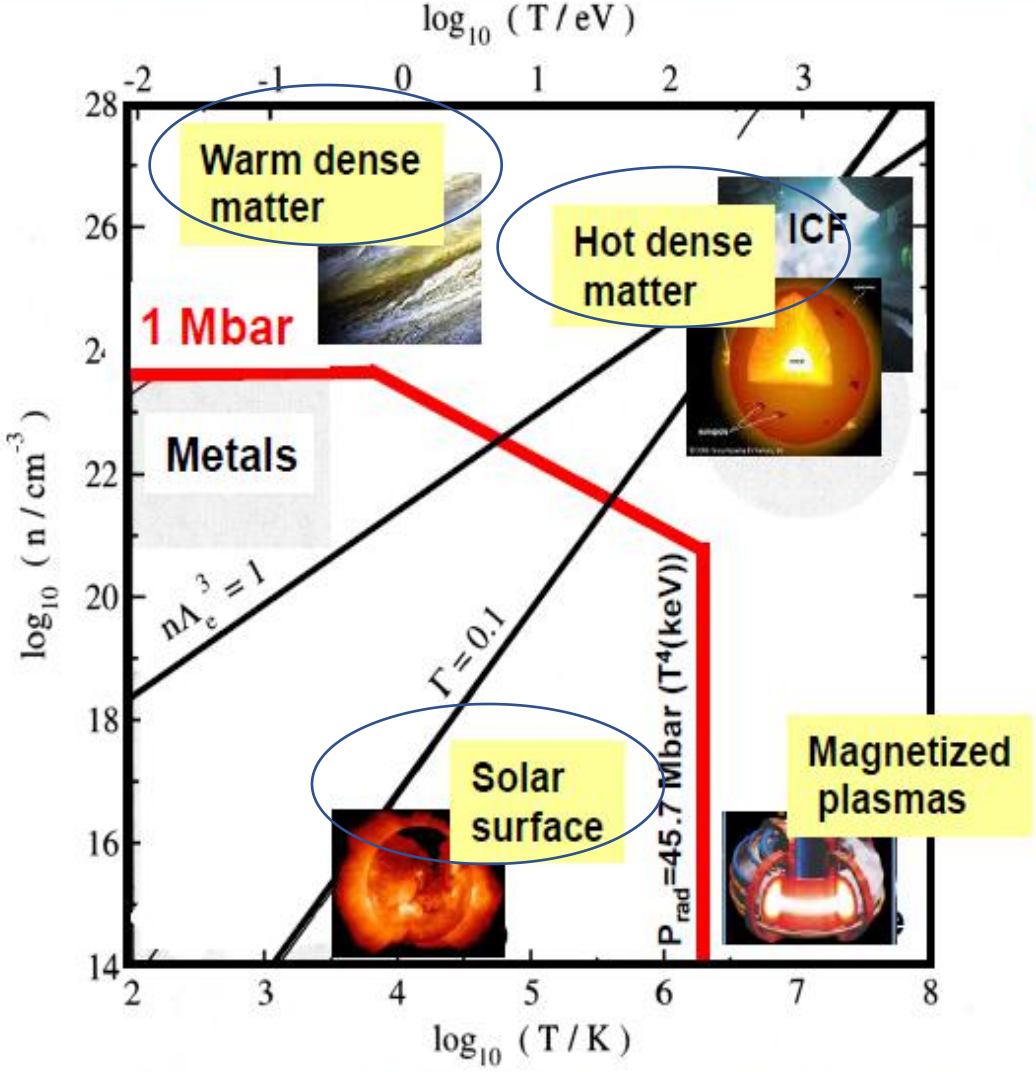

Kremp et al., *"Quantum Statistics of Non-ideal Plasmas"*, Springer-Verlag (2005)

1 Mbar = 10^{12} erg/cm^3

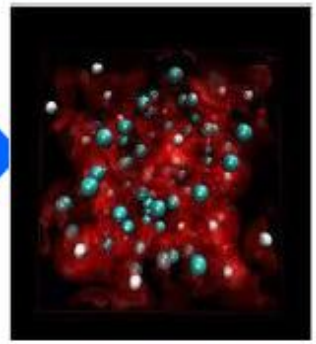

Bulk modulus ~ 1 Mbar

- Radiation dominated
- Strong correlations
- Multiple species
- Fermi degeneracy
- Hybrid quantum and classical behavior
- Bound states
- ionization

An ICF example: Spanning strongly coupled (large particle-particle correlations) to weakly coupled (Brownian motion like) regimes

Weakly coupled plasma: $\Gamma << 1$

- Collisions are long range and many body
- Weak ion-ion and electron-ion correlations
- Debye sphere is densely populated
- Kinetics is the result of the cumulative effect of many small angle weak collisions
- Theory is well developed $1/n\lambda_D^3 << 1$

Strongly coupled plasma: $\Gamma \geq 1$

- Large ion-ion and electron-ion correlations
- Particle motions are strongly influenced by nearest neighbor interactions
- Debye sphere is sparsely populated
- Large angle scattering as the result of a single encounter becomes important

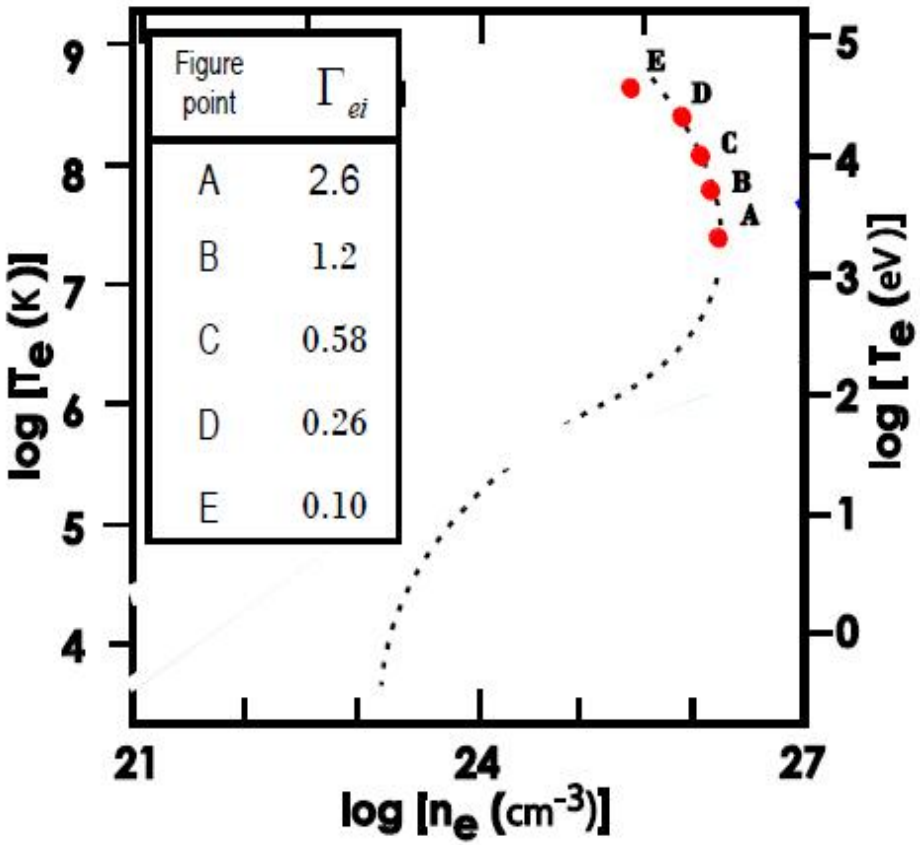

density-temperature trajectory of the DT gas in an ICF capsule

The multi-scale problem: Applications require simulation at the macro-scale but need fundamental physics information from the micro-scale

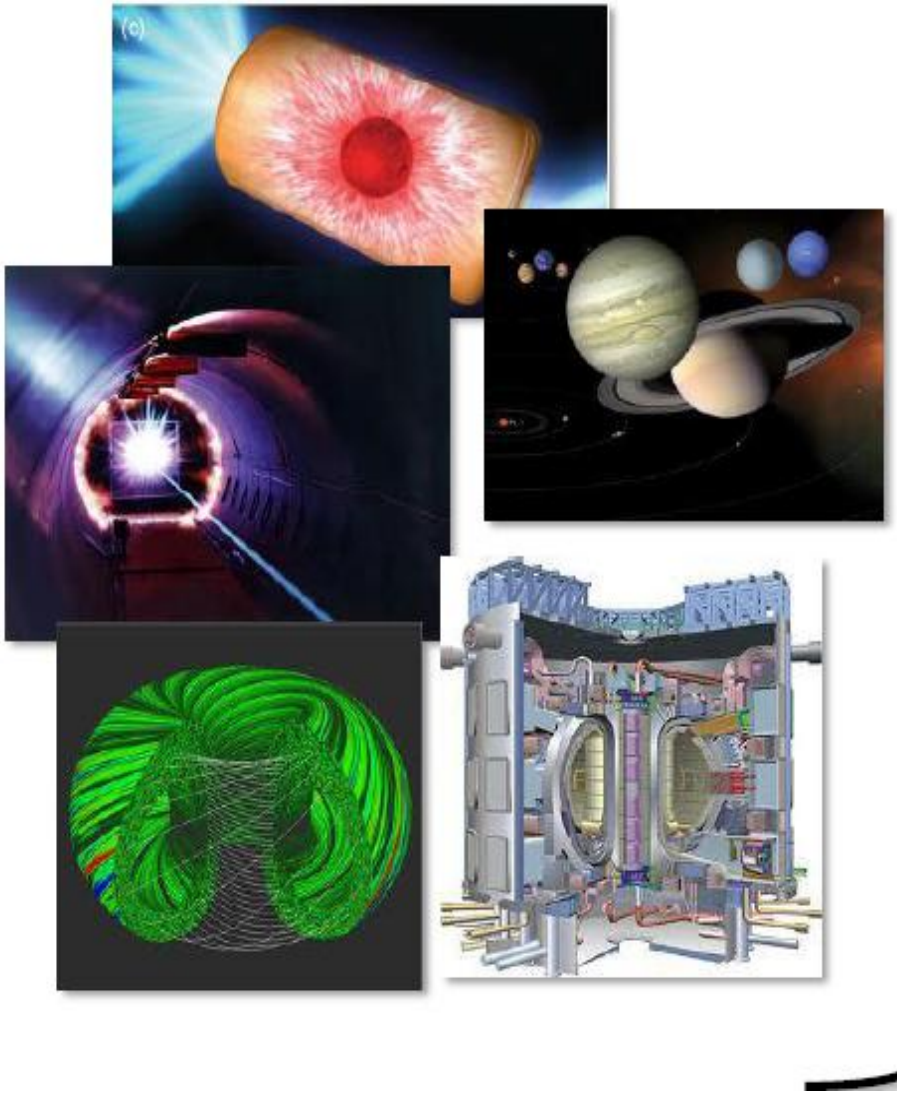

Fluid Models

Hydrodynamics

MHD

Radiation Hydrodynamics

- Equation of state
- Transport coefficients
- Stopping power
- Plasma turbulence
- opacity

The multi-scale problem: Applications require simulation at the macro-scale but need fundamental physics information from the micro-scale

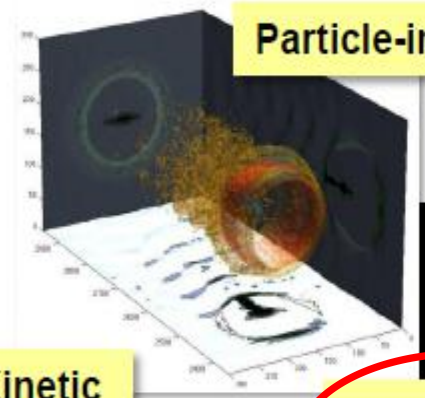

Particle-in-Cell

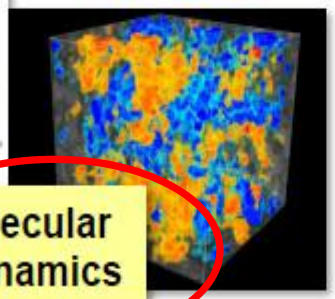

Molecular Dynamics

Kinetic Theory

Density Functional Theory

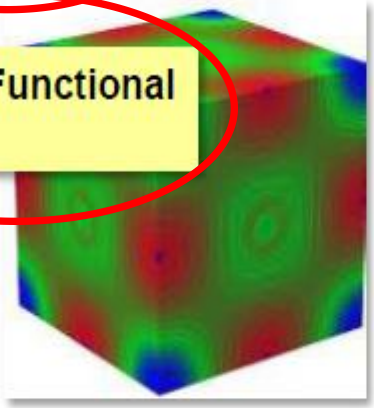

Quantum Molecular Dynamics

Equation of state

Transport coefficients

Stopping power

Plasma turbulence

Opacity

Fluid Models

Hydrodynamics

MHD

Radiation Hydrodynamics

Why is matter in the high energy density regime so interesting: The hot dense matter regime

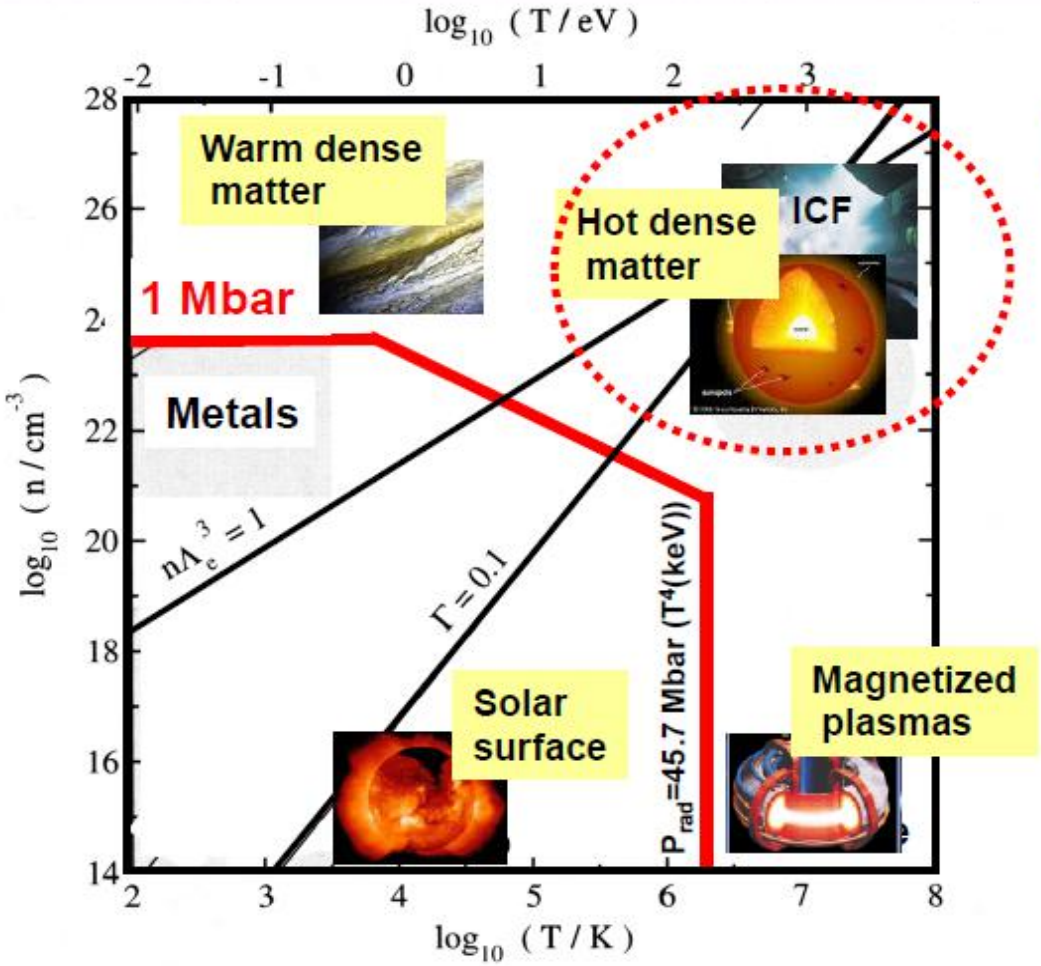

Kremp et al., *"Quantum Statistics of Non-ideal Plasmas"*, Springer-Verlag (2005)

1 Mbar = 10^{12} erg/cm^3

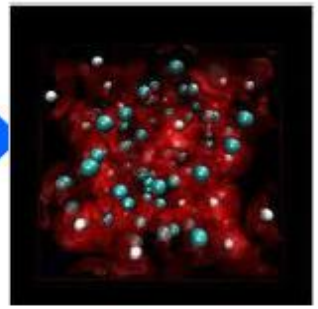

Bulk modulus ~ 1 Mbar

- Radiative processes YES
- Strong correlations MAYBE
- Multiple species YES
- Fermi degeneracy NO
- TN burn YES
- Atomic processes YES

What are the major challenges facing each of the critical areas of hot dense matter ?

Thermonuclear burn

Particle spectra (do D and T distributions remain Maxwellian?)
Electron, ion and radiation T(t)
The role of high Z impurities

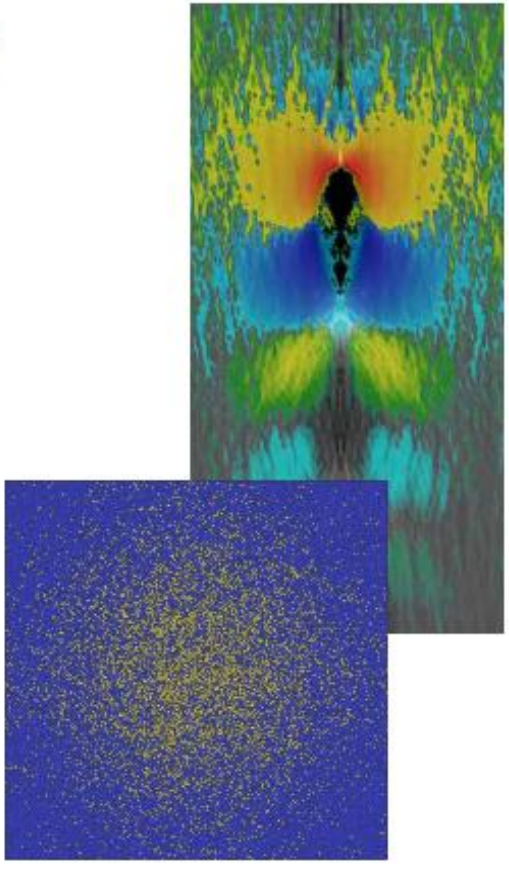

Equations of state

Thermal conductivity
Species diffusivity

Transport properties of hot dense matter

Thermal conductivity
Species diffusivity
The role of high Z impurities

Momentum and energy exchange rates

Stopping power
Electron ion coupling
The role of high Z impurities

Comprehensive theory describing hot dense matter plasmas with impurities

Strongly coupled high Z component and weakly coupled low Z component

Warm dense matter regime is at the meeting point of several distinct physical regimes- a scientifically rich area of HEDP

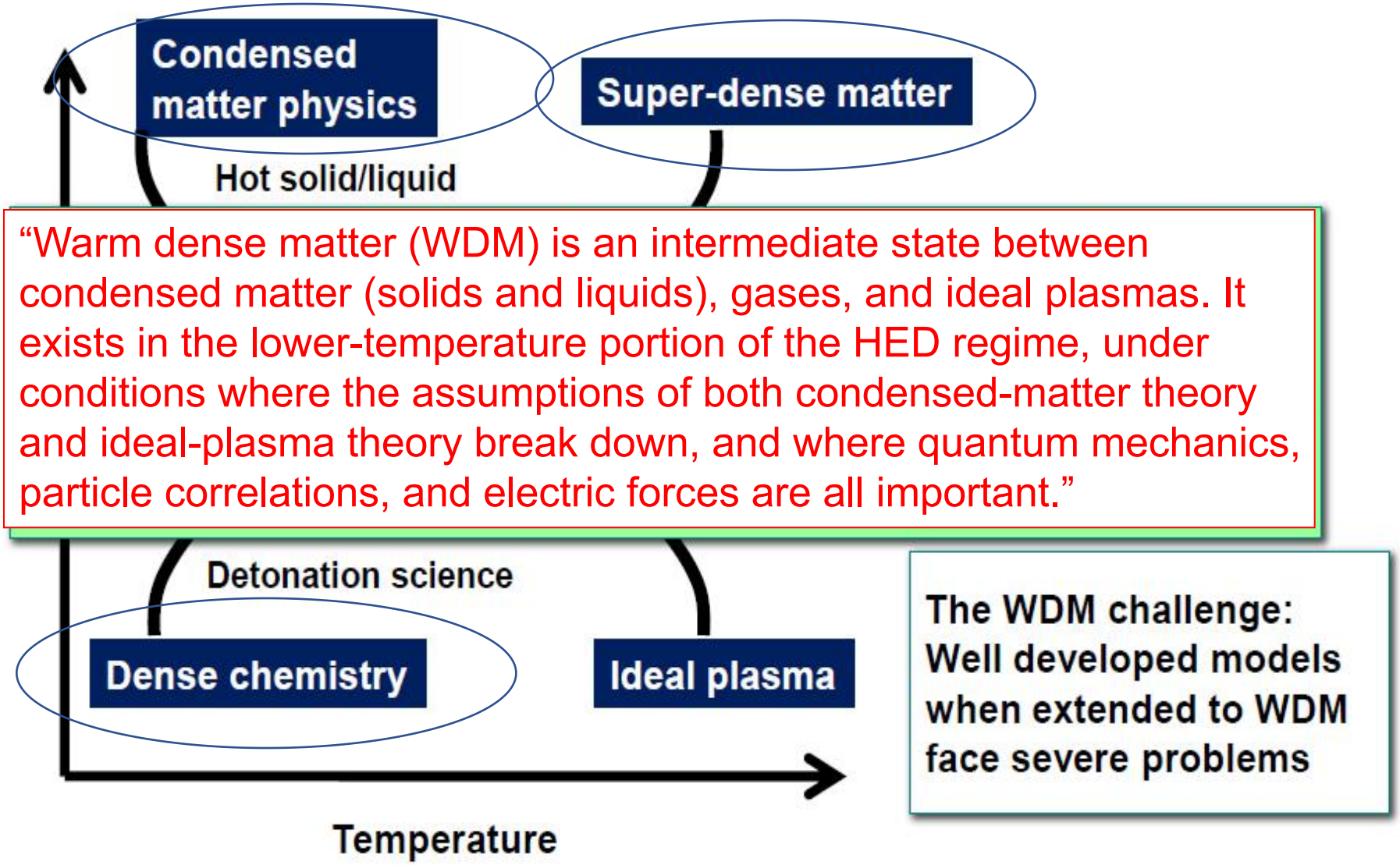

Matter in the plasma state exists in an unimaginable variety

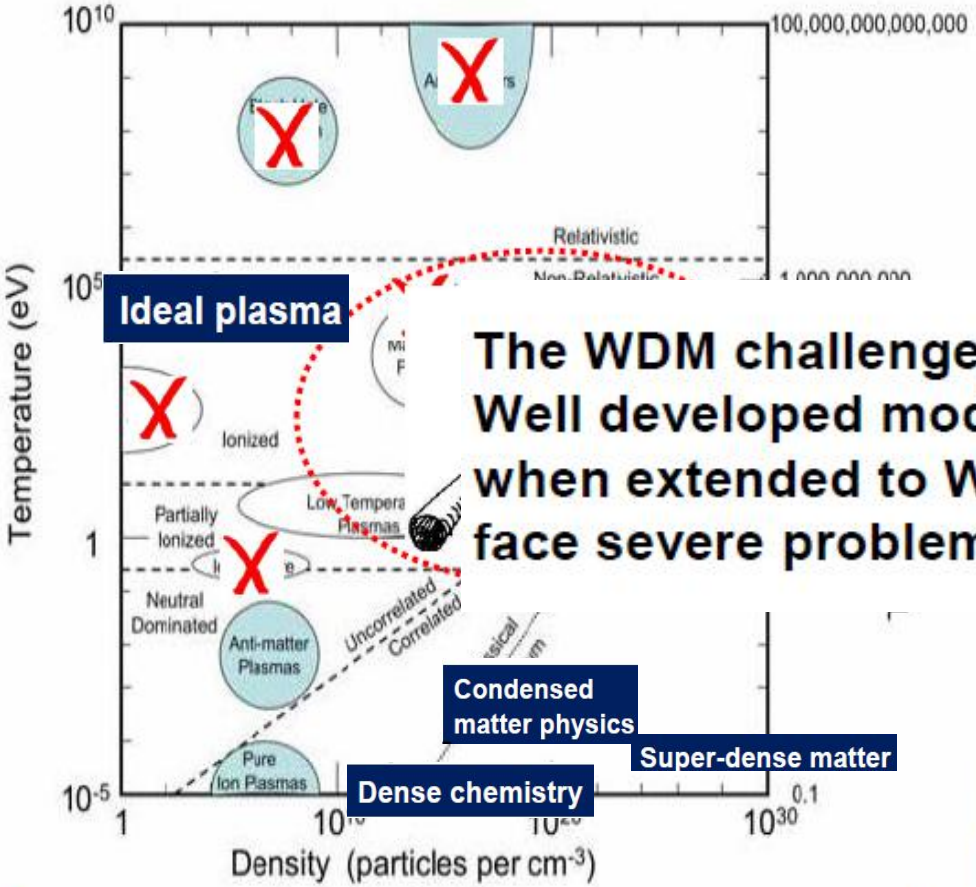

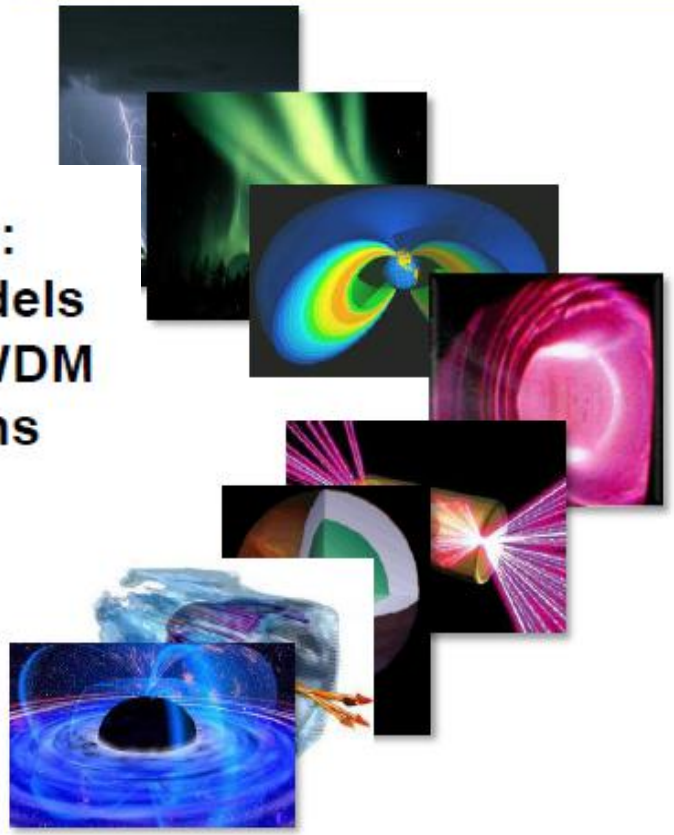

$1\,\mathrm{eV} = 1.16\times10^{4}\ \mathrm{K}$

From single atomic model to strongly coupled ions

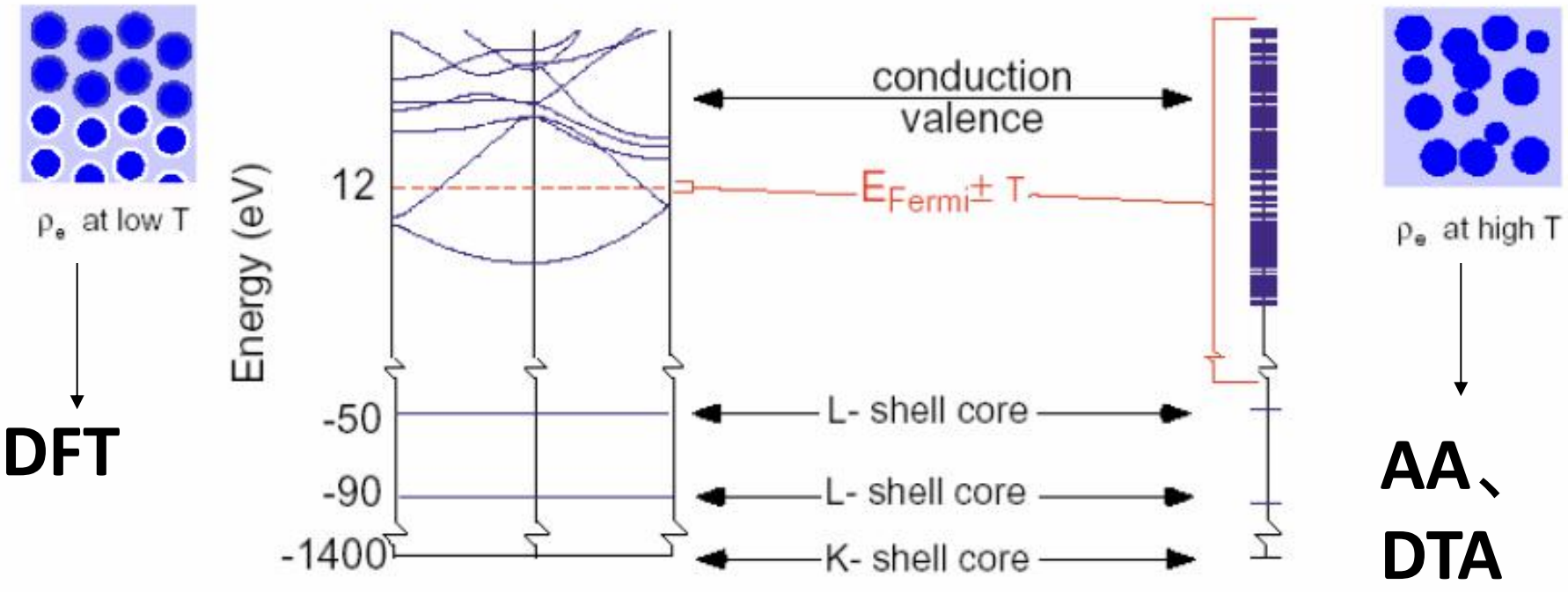

1. Interionic interaction potential in HDM with large excitations and ionizations of electrons
2. Simulations of the atomic thermomotions
3. Microfield distributions

Strongly coupled plasma: $\Gamma \geq 1$

– Large ion-ion and electron-ion correlations

– Particle motions are strongly influenced by nearest neighbor interactions

– Debye sphere is sparsely populated

– Large angle scattering as the result of a single encounter becomes important

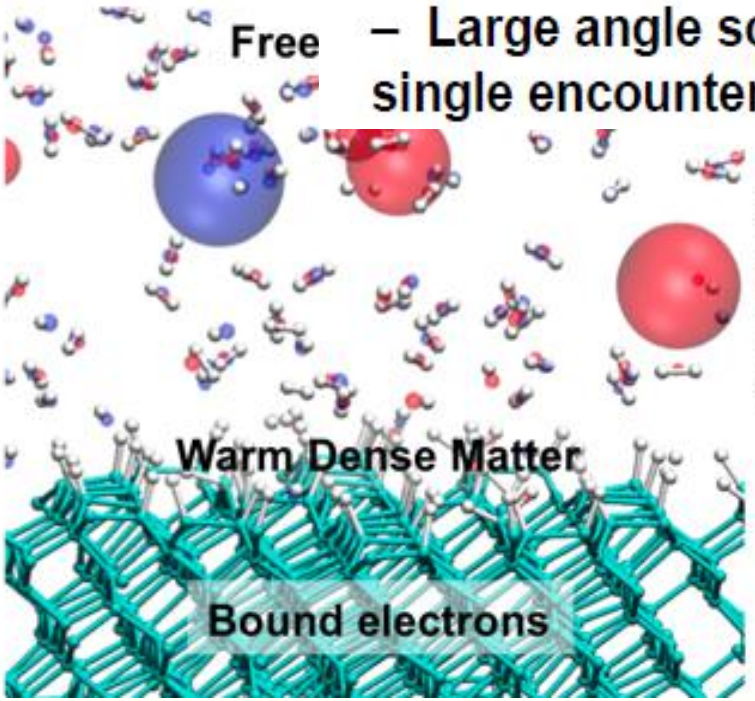

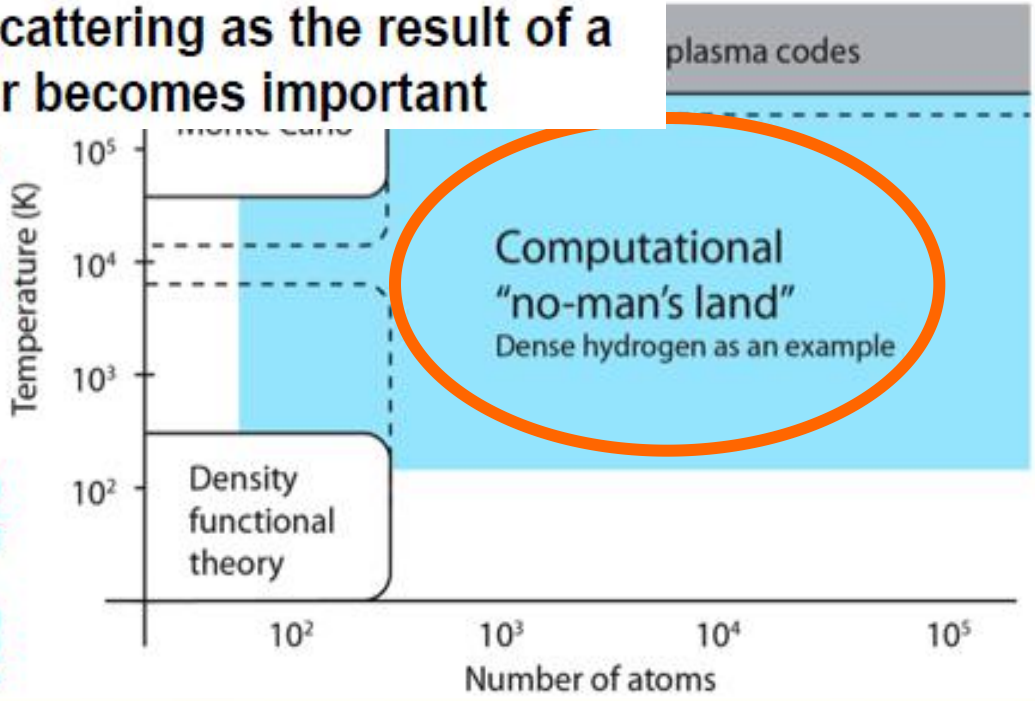

What are the major challenges facing each of the critical areas of warm dense matter ?

Phase Transitions in WDM

Melting, liquid-liquid phase transitions, plasma phase transitions

Metal-insulator transition

Equations of state and their dependence on formation history

Computation of EOS without decomposition of ionic and electronic contributions

EOS for mixtures

Transport properties of WDM

Viscosity, diffusivity, electric, ionic and thermal conductivity

Constitutive properties of warm solids

What is a solid at very high pressures?

Deformation and dissipation mechanisms (strength)

Comprehensive theory connecting WDM regions

DFT: Orbital-free, exact exchange, going beyond Born-Oppenheimer, high B fields

Particle simulation methods

What are the key questions in dense matter?

How does chemistry change at extreme densitie

- How do core electrons affect bonding?
- What is the nature of insulator-metal transitions at high

What is a solid at > 10 Mbar?

- How do melt, strength, structure, EOS change at ultra-h
- How fast can you squish a solid?

What is the nature of He or H when the interaton ~deBroglie wavelength?

- How do mixtures of H and He behave at high densities?

Simulations predict electronic localization through compression

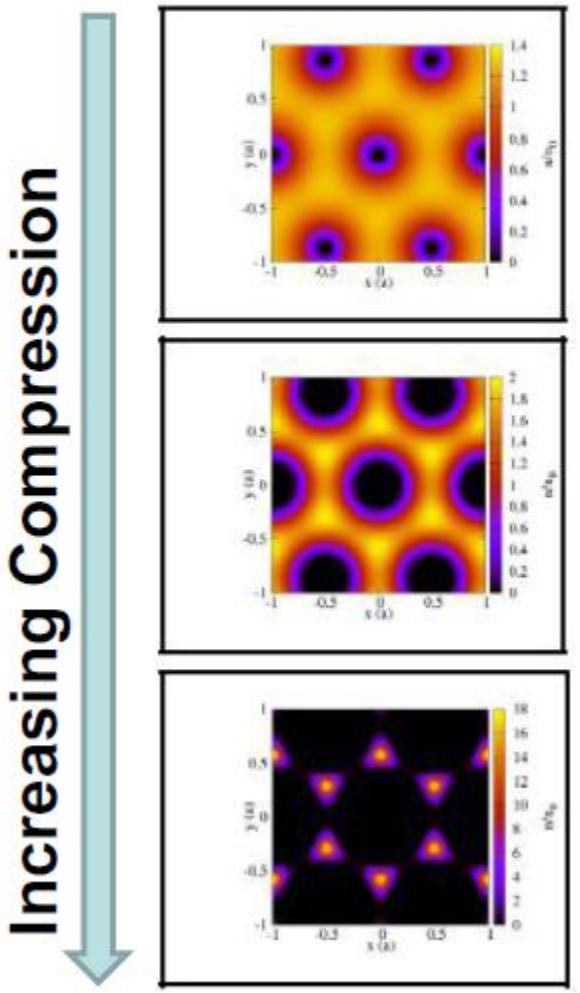

Neil Ashcroft, 2010

研究背景

极端高温高密度条件带来许多新的科学问题

状态方程　输运系数　超快过程　光学参数　状态诊断

极端条件 → 新方法和新手段

激光与物质相互作用（流体模拟/等效实验）

冷凝聚态物质 → 温热稠密物质 → 理想等离子体气

- **组成成分复杂：** 自由电子、束缚电子、团簇等
- **物理特征多样：** 电子部分简并、离子强耦合、复杂环境、动态

研究背景

随着强激光技术的发展和应用，以美国的国家点火装置和我国的点火计划为代表，有可能在实验室制备这种极端物态，甚至创造以空心原子、电子泡为代表的新物质，探索激光聚变等新能源技术和太赫兹与阿秒脉冲等新光源。

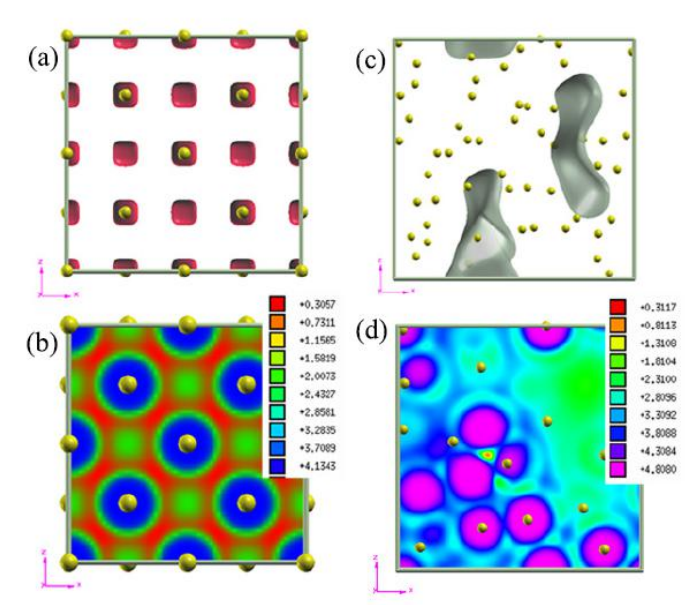

PRL， 2012

研究背景

- 精密计算物性参数
- 统一描述临界状态
- 实时诊断超快过程

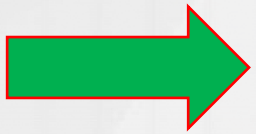

- 核武器精密化设计和新型能源开发
- 极端条件下材料应用
- 超快电子信息器件研发

- 需要构建基于离子间相互作为基础的**多尺度模拟**方法，对涉及到的**跨尺度问题**进行直接模拟和物理效应研究

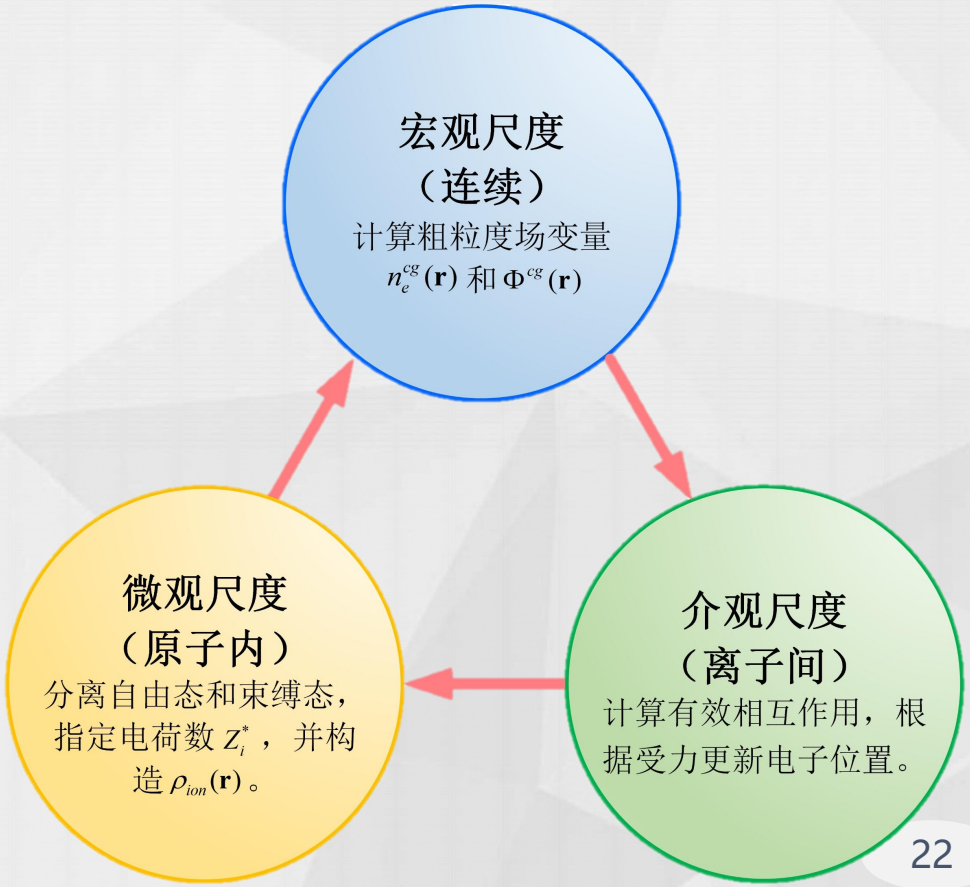

Two Approaches in our group:

First principles based on quantum mechanics:

DFT, QMC, Hartree-Fock, Field Theory……

Advantage——Accuracy

Semiclassical Method: averaged atoms model,

MD based on empirical interatomic potential,

(electron) force field…….

Advantage——Largescale, dynamics

Fe phase - Conditions under (super) earth core

Structure of Iron to 1 Gbar and 40 000 K

Departme *om*

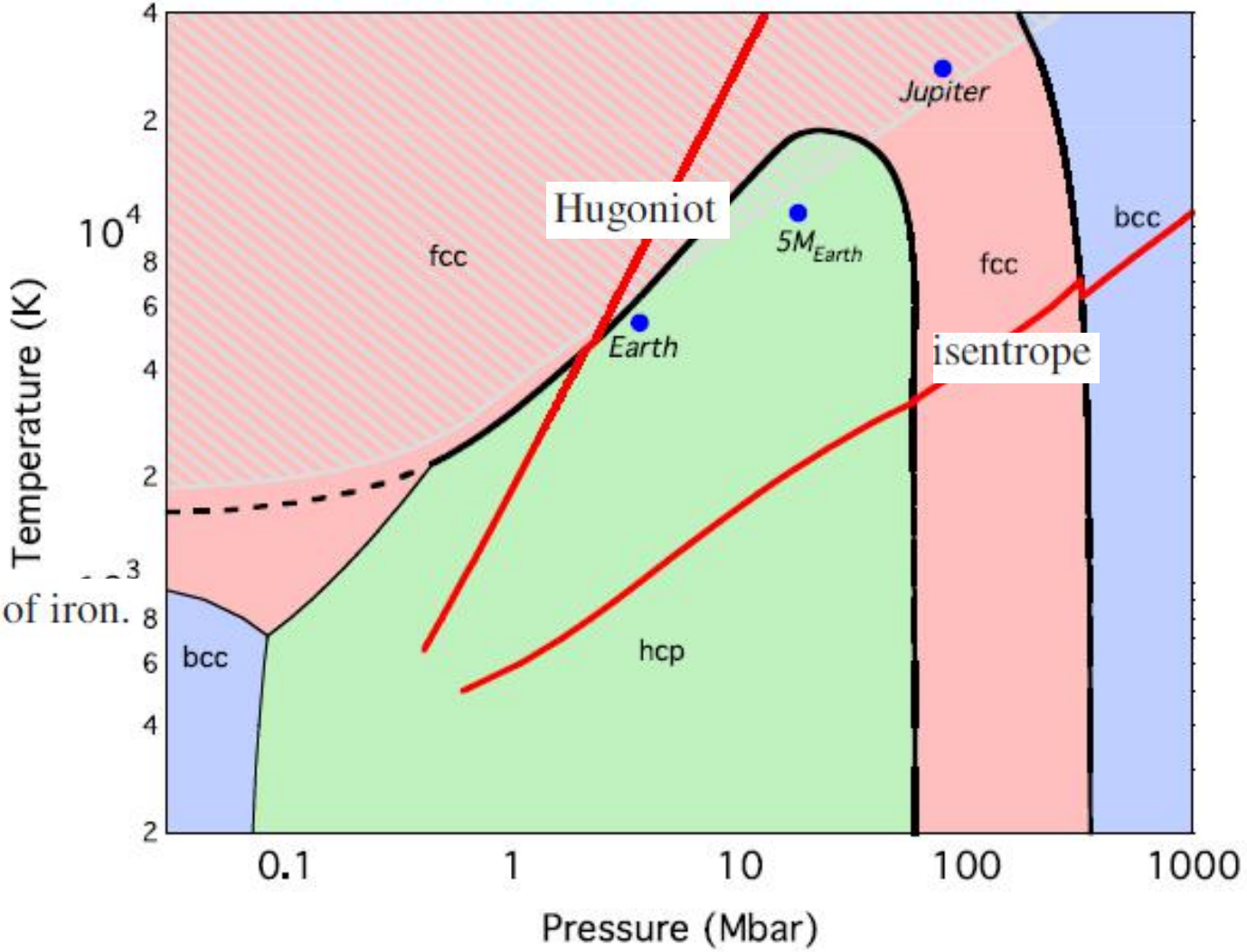

Phase diagram of iron.

What **pressures-temperatures can you achieve with drivers ?**

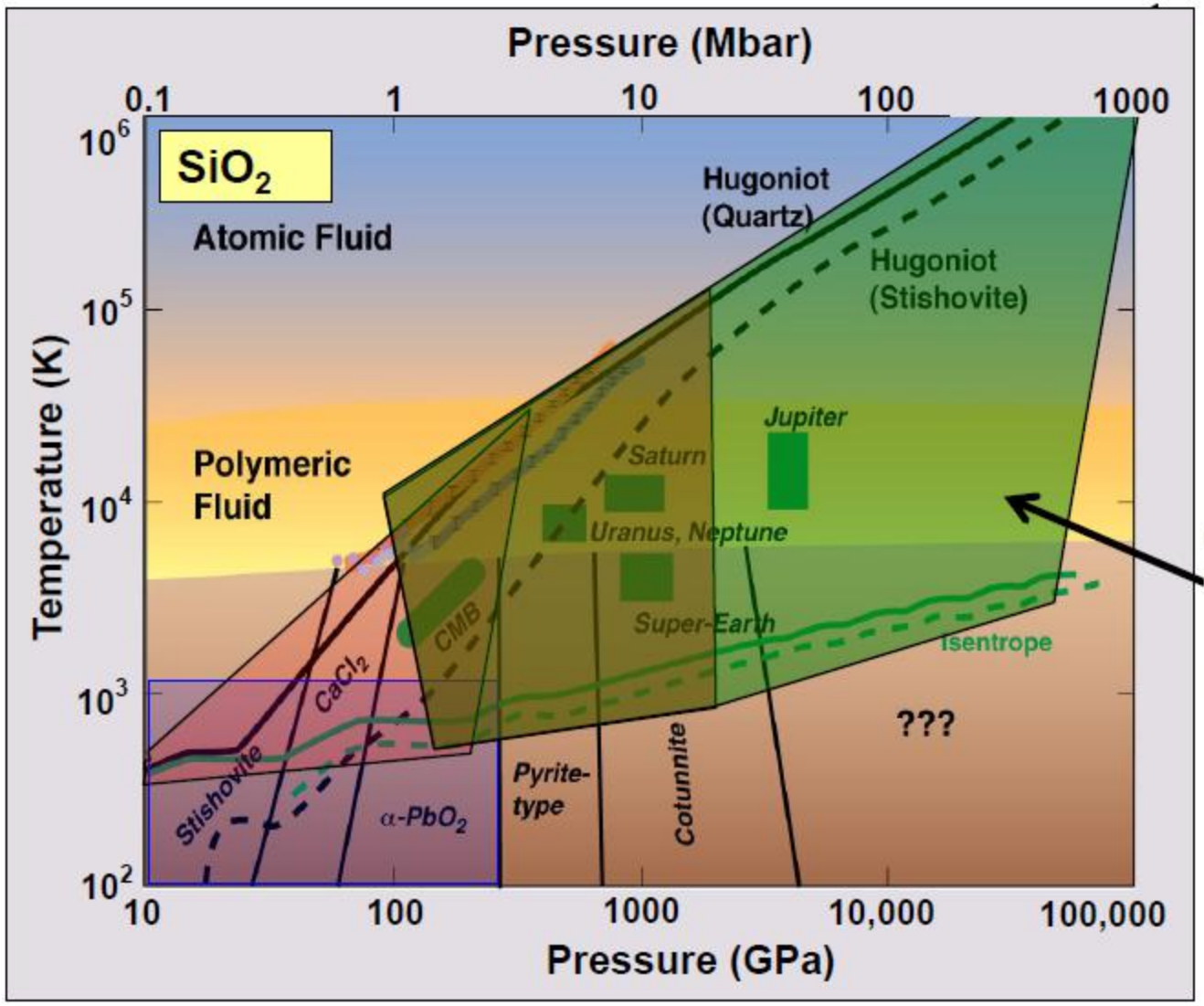

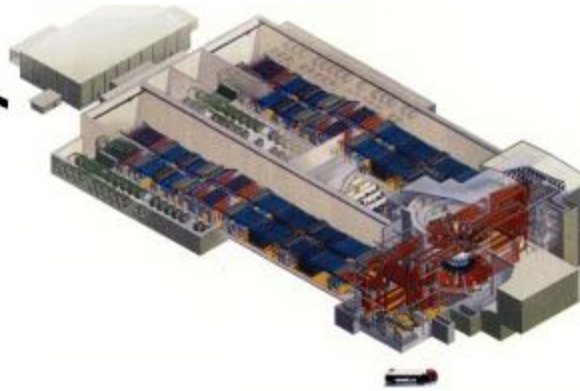

Hicks, 2006

High pressure phases of aluminum are also predicted to be complex

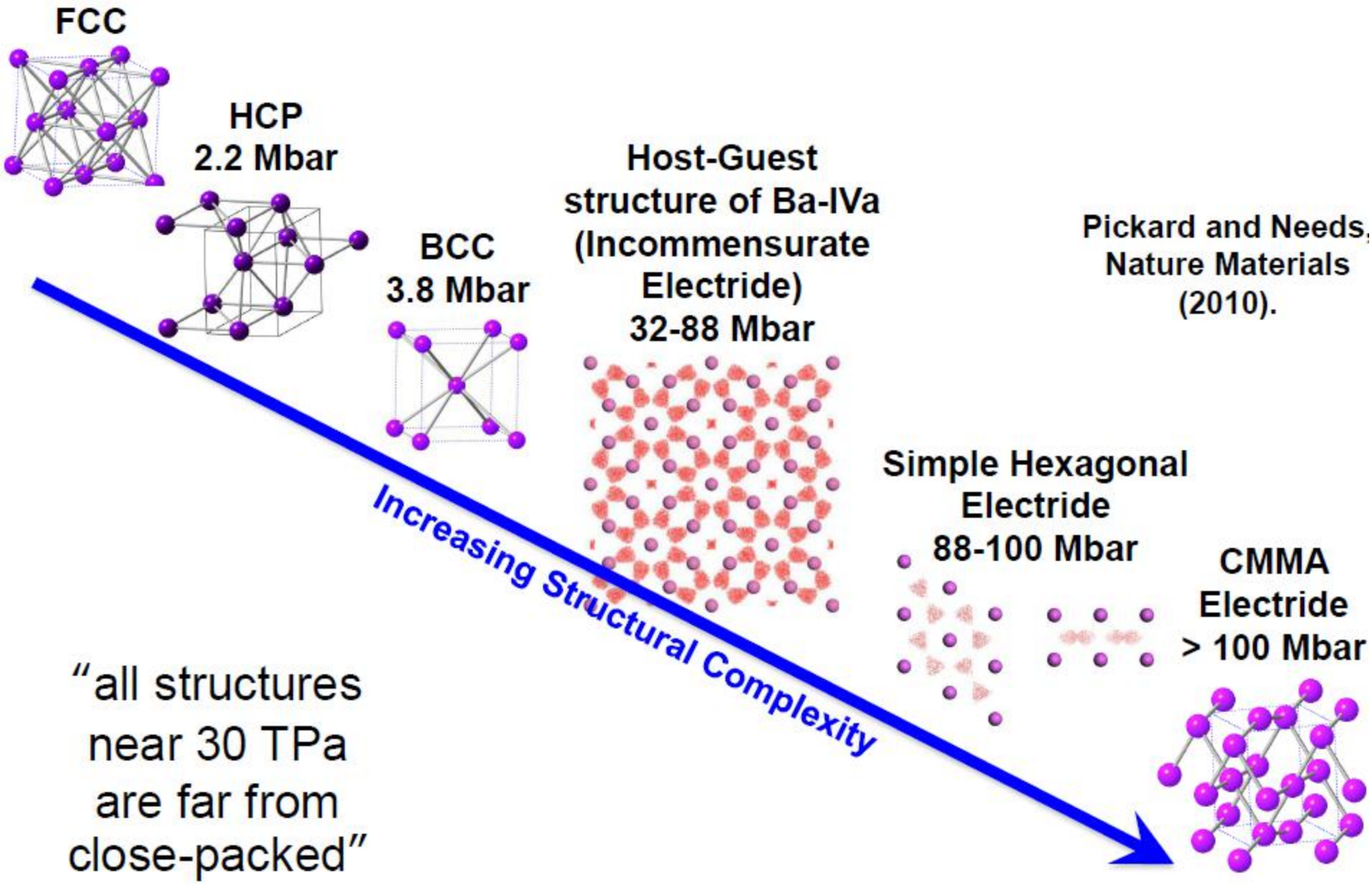

Ions in a “Sea of Hot Electrons”

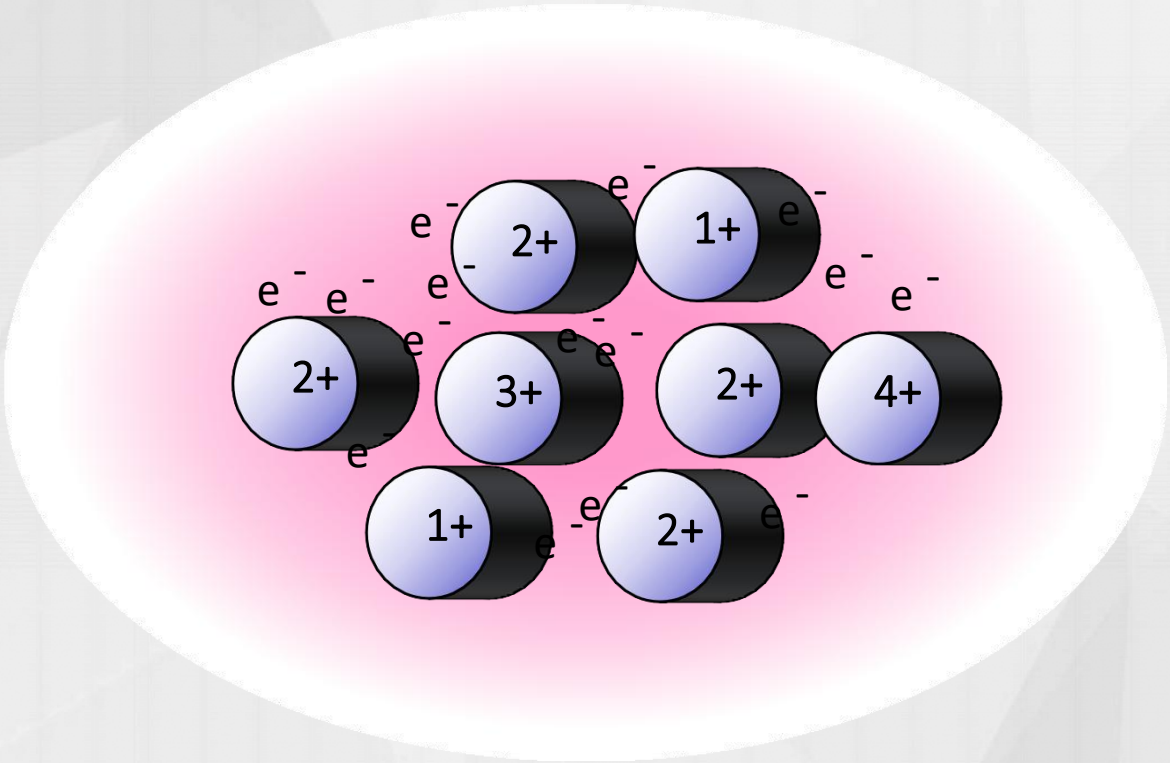

动力学碰撞——非绝热效应

分子动力学方法

- 分子动力学方法

基本思想：物质是由原子和分子组成的多粒子系统，假定粒子在由经典力学描述的特定轨道上运动，计算粒子受到的作用力，求解运动方程得到系统中全体粒子在相空间中的运动轨迹，进而计算系统的热力学参数和输运性质。

基本假设：各态历经假设

粒子为经典粒子

分子动力学方法

- 分子动力学方法

核心问题：1. 计算原子间相互作用势

2. 积分牛顿运动方程

限制： 有限观测时间

有限系统大小

[1] M. P. Allen, D. J. Tildesley, Computer Simulation of Liquids (1987)
[2] Frenkel & Smit, Understanding Molecular Simulation—From Algorithms to Applications (1996)

- A key concept to understand material properties
  - Born-Oppenheimer Approximation
  - Propagation of the nuclei on the potential energy surface (PES)
- Most popular method: *ab initio* MD

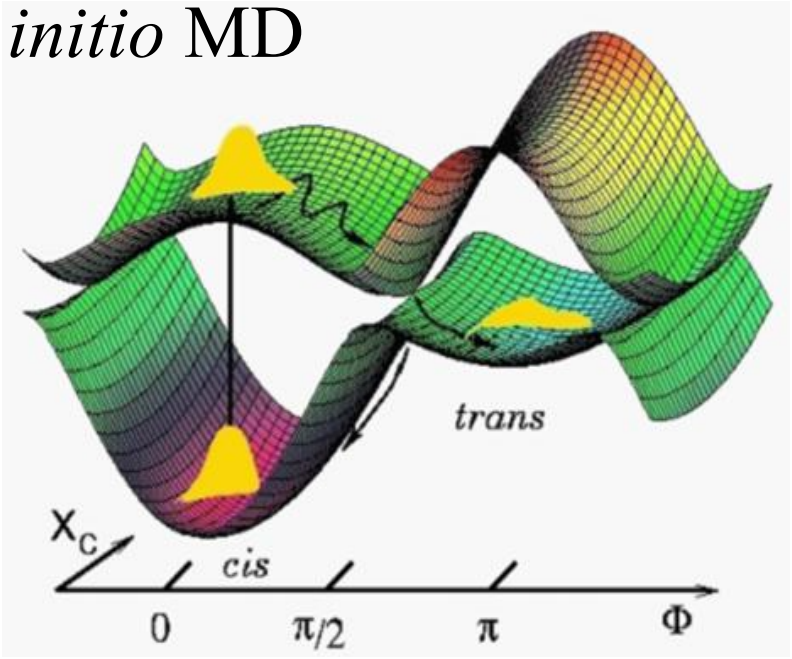

Brownian Motion: Langevin Equation

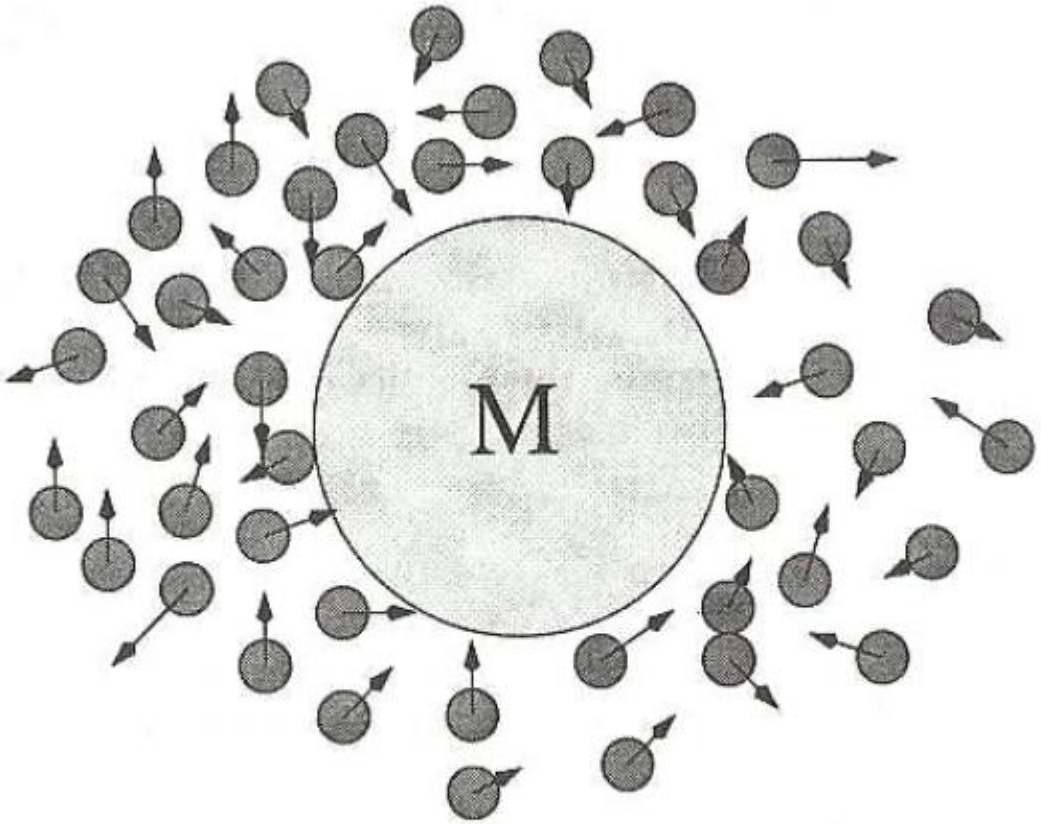

A large Brownian particle with mass M immersed in a fluid of much smaller and lighter particles.

激光产生温稠密物质动态演化

- **Non-adiabatic effects：excitation, transition, collisions et al.**
- **Electron-ion collisions induced friction (EI-CIF)**
- **Langevin Equation:**

$$M_I \ddot{\boldsymbol{R}}_I = \boldsymbol{F} - \gamma M_I \dot{\boldsymbol{R}}_I + \boldsymbol{N}_I$$

DFT　　Friction coefficient　　White noise

QLMD

- **EOS and electronic structures up to 100 eV can be studied.**

Dai and Yuan*. Phys. Rev. Lett. 104: 245001 (2010); Phys. Rev. Lett. 109: 175701 (2012)

L. G. Stanton et al. Pys. Rev. X 8, 021044 (2018);

Kang and Dai*. J. Phys.: Condens. Matter 30, 073002 (2018) (Topic Review).

Hugoniot: data from QLMD

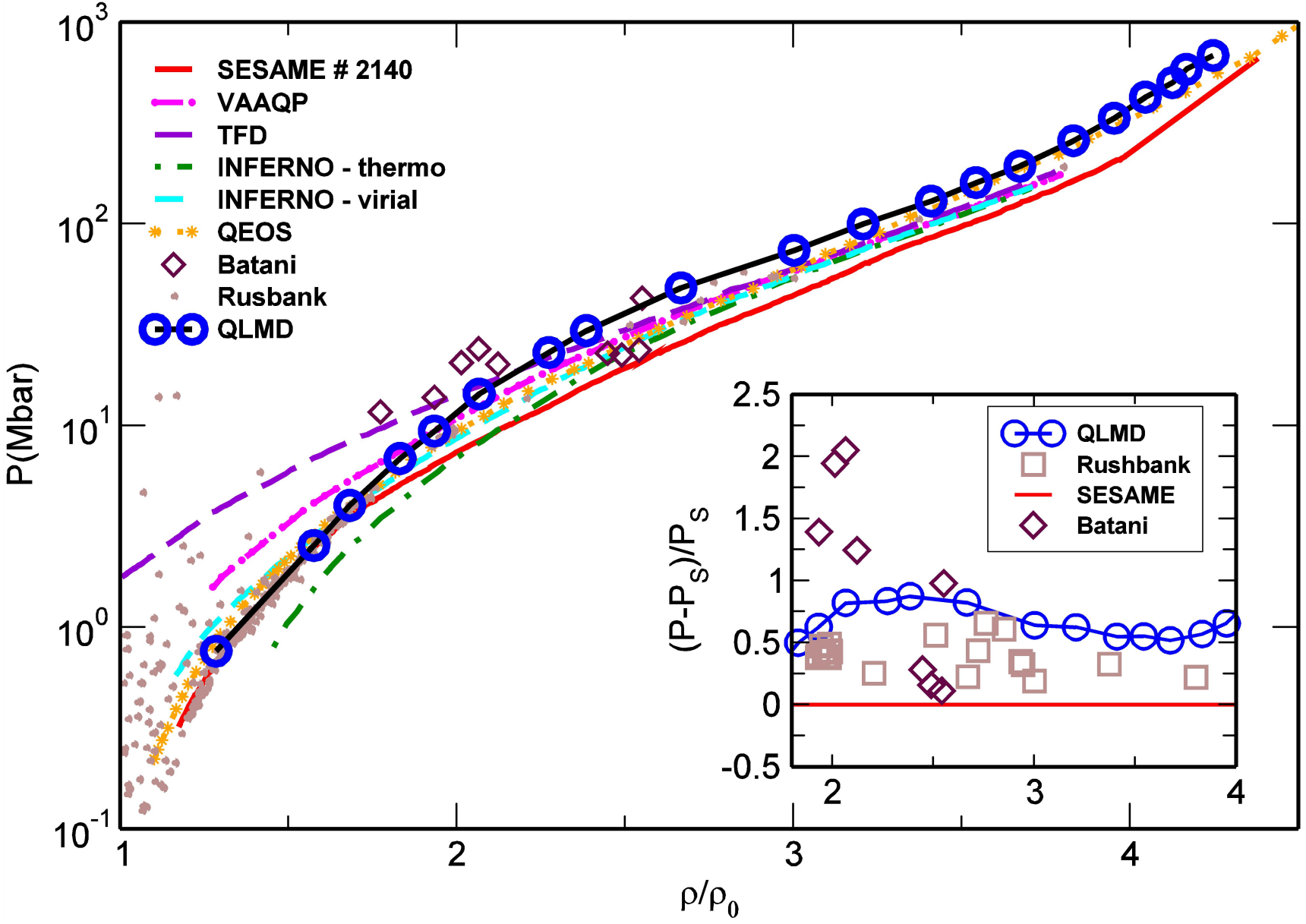

Hugoniot: structures from QLMD

and

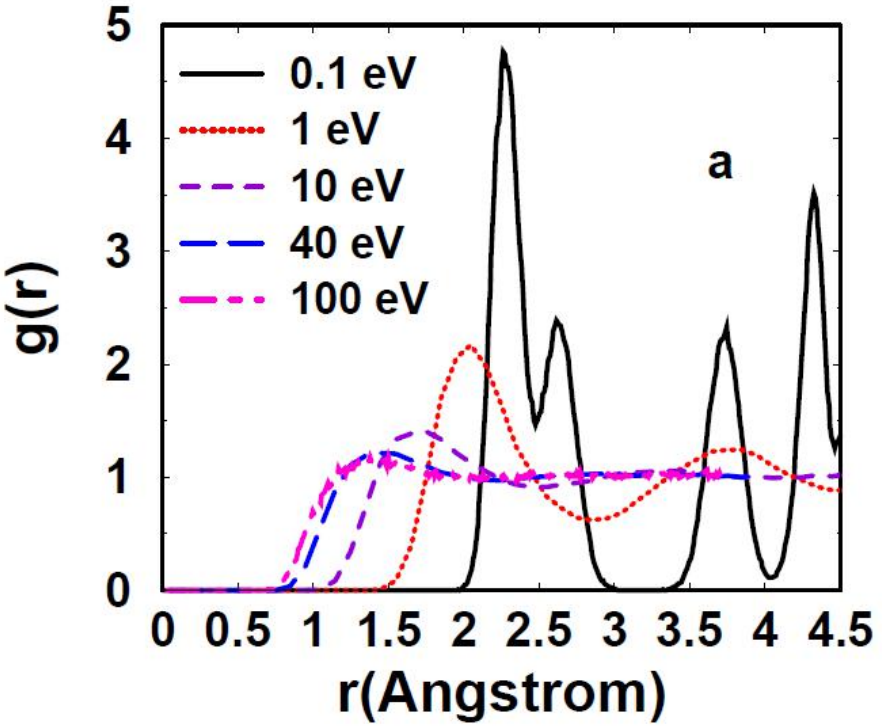

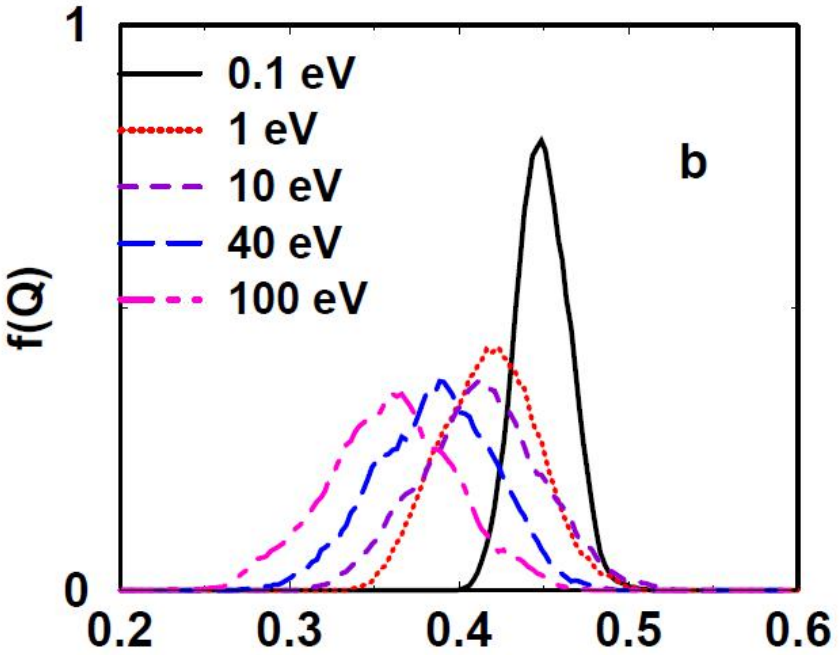

$$ECN = \frac{1}{N}\sum_{i=1}^{N} ECN_i = \frac{1}{N}\sum_{i=1}^{N}\sum_{j\neq i}\exp\left[1-\left(\frac{d_{ij}}{d_{av}^i}\right)^6\right]$$

"effective coordination numbers" (ECN)

$$d_{av}^i = \frac{\sum_j d_{ij}\exp\left[1-\left(\frac{d_{ij}}{d_{av}^i}\right)^6\right]}{\sum_j \exp\left[1-\left(\frac{d_{ij}}{d_{av}^i}\right)^6\right]}, d_{av} = \frac{1}{N}\sum_{i=1}^{N} d_{av}^i$$

Temperature effect--Ionic short ordered structures

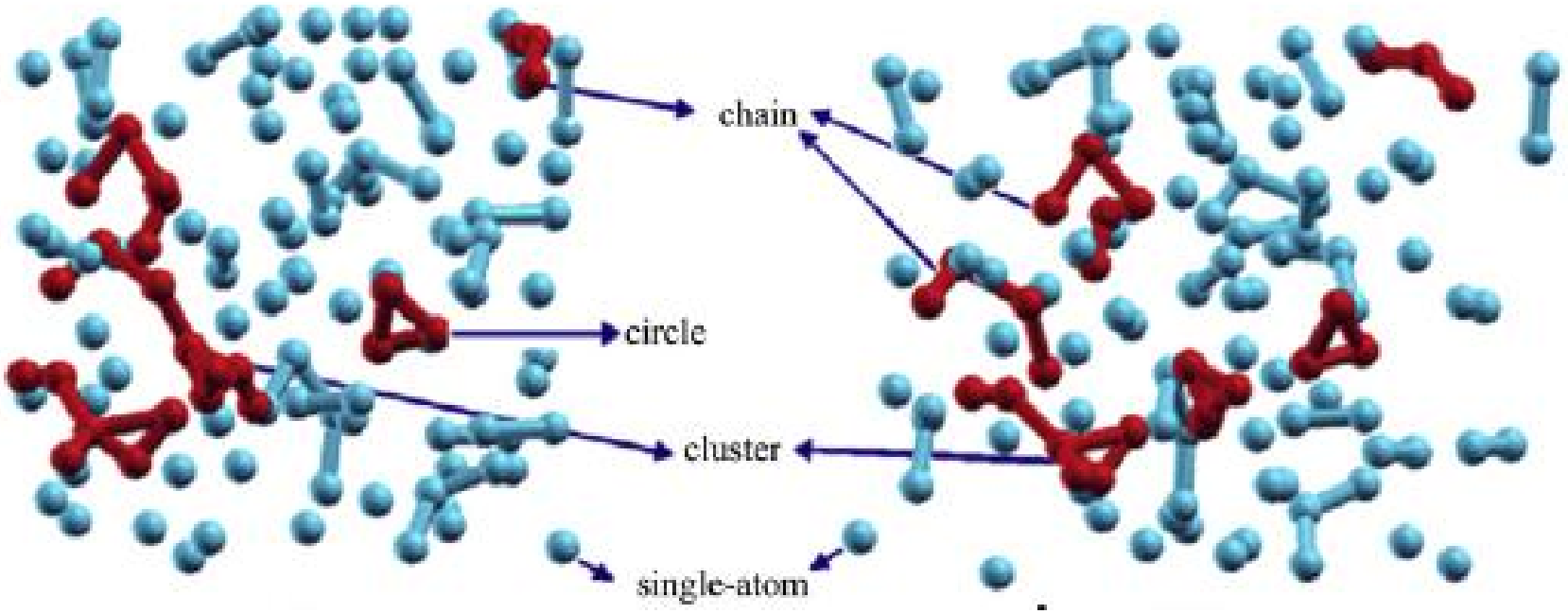

There are medium or short ordered structures in hot dense matter

Dai Jiayu et al. HEDP, 7: 84-90 (2011)

Ionic structures

T = 1 eV

ρ= 13.23 g/ccm

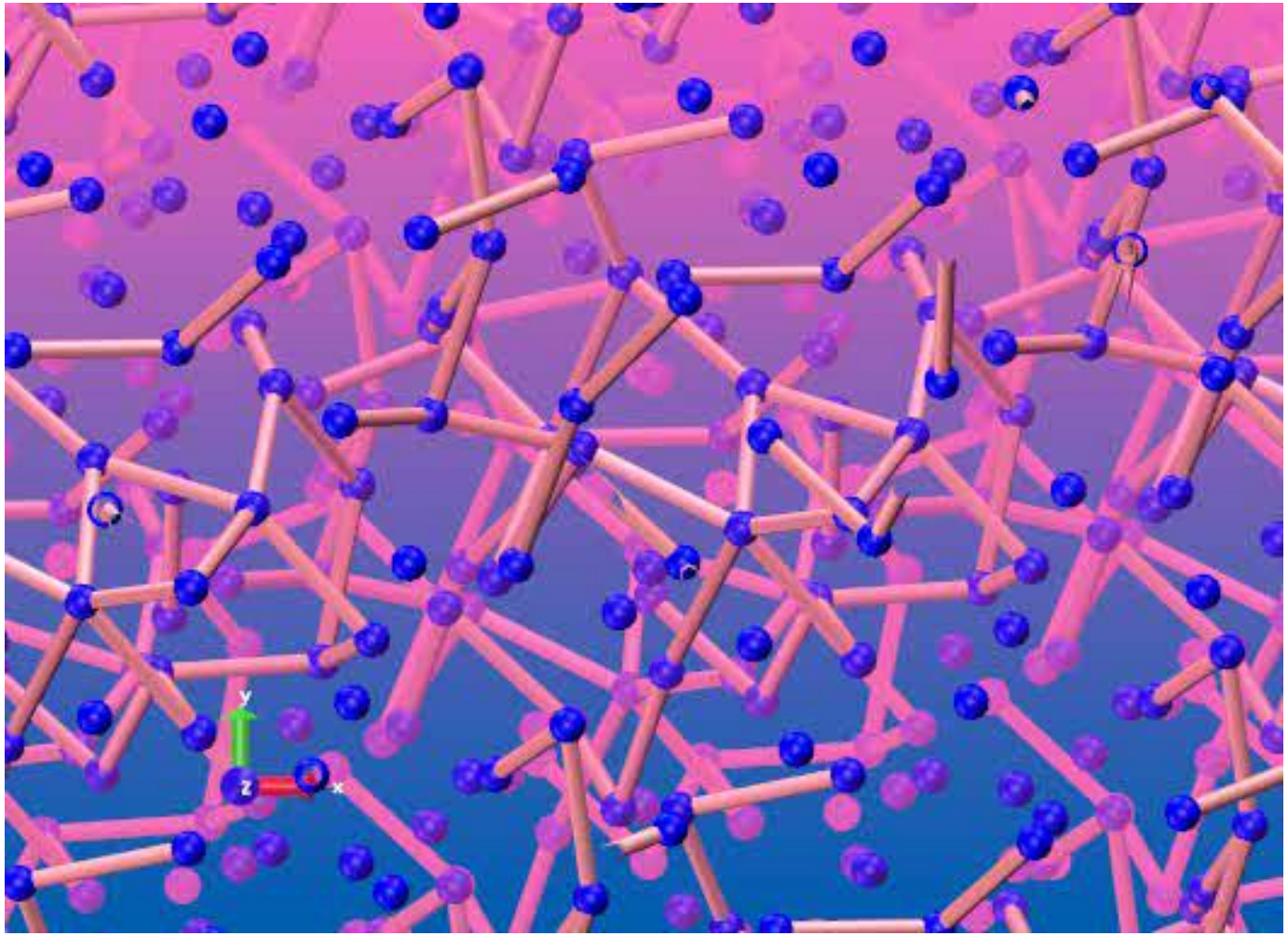

Ionic structures

T = 100 eV

ρ= 33.385 g/ccm

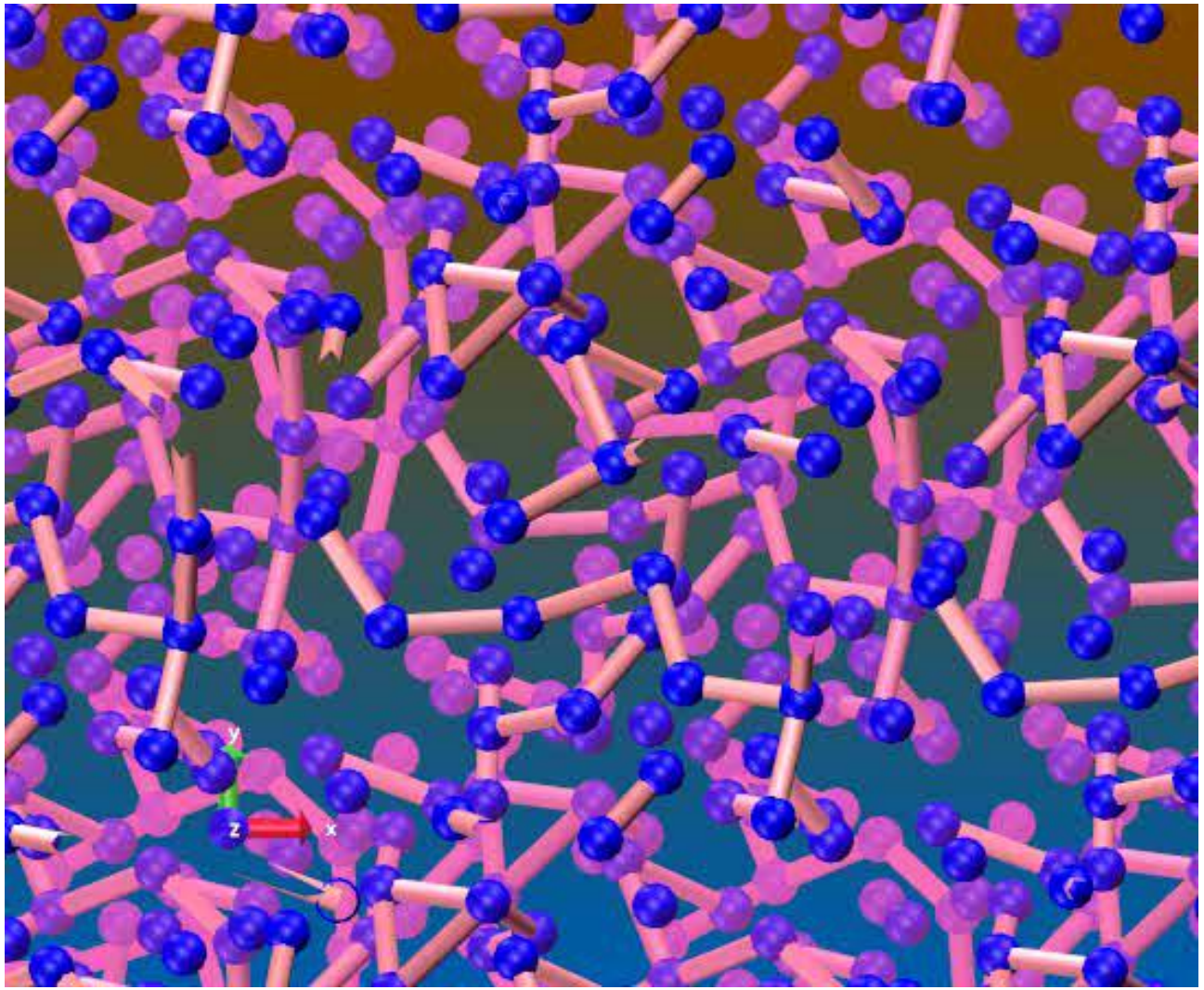

Temperature effect- -Dynamical ionic clusters with flowing electron bubbles

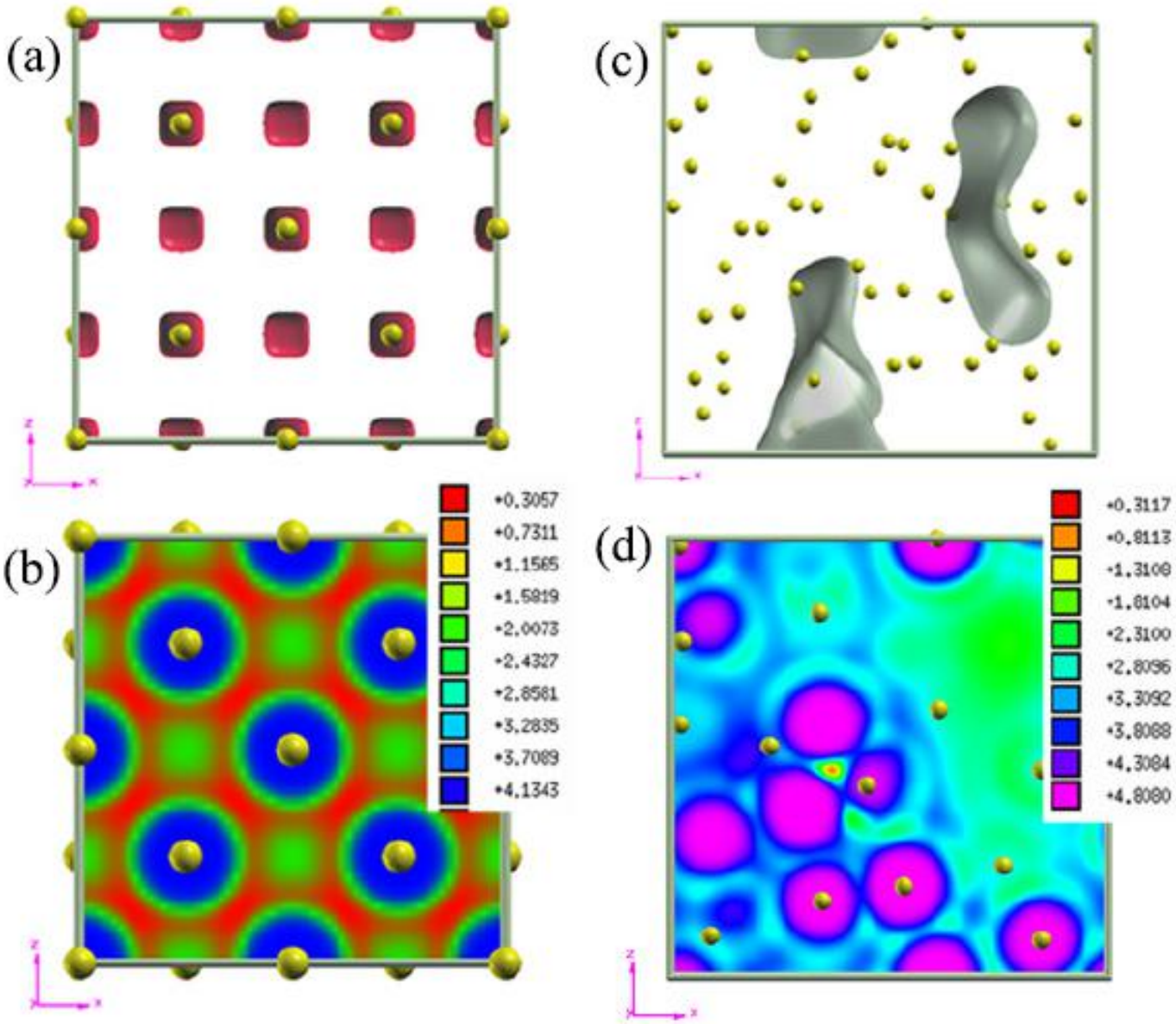

Electronic bubbles

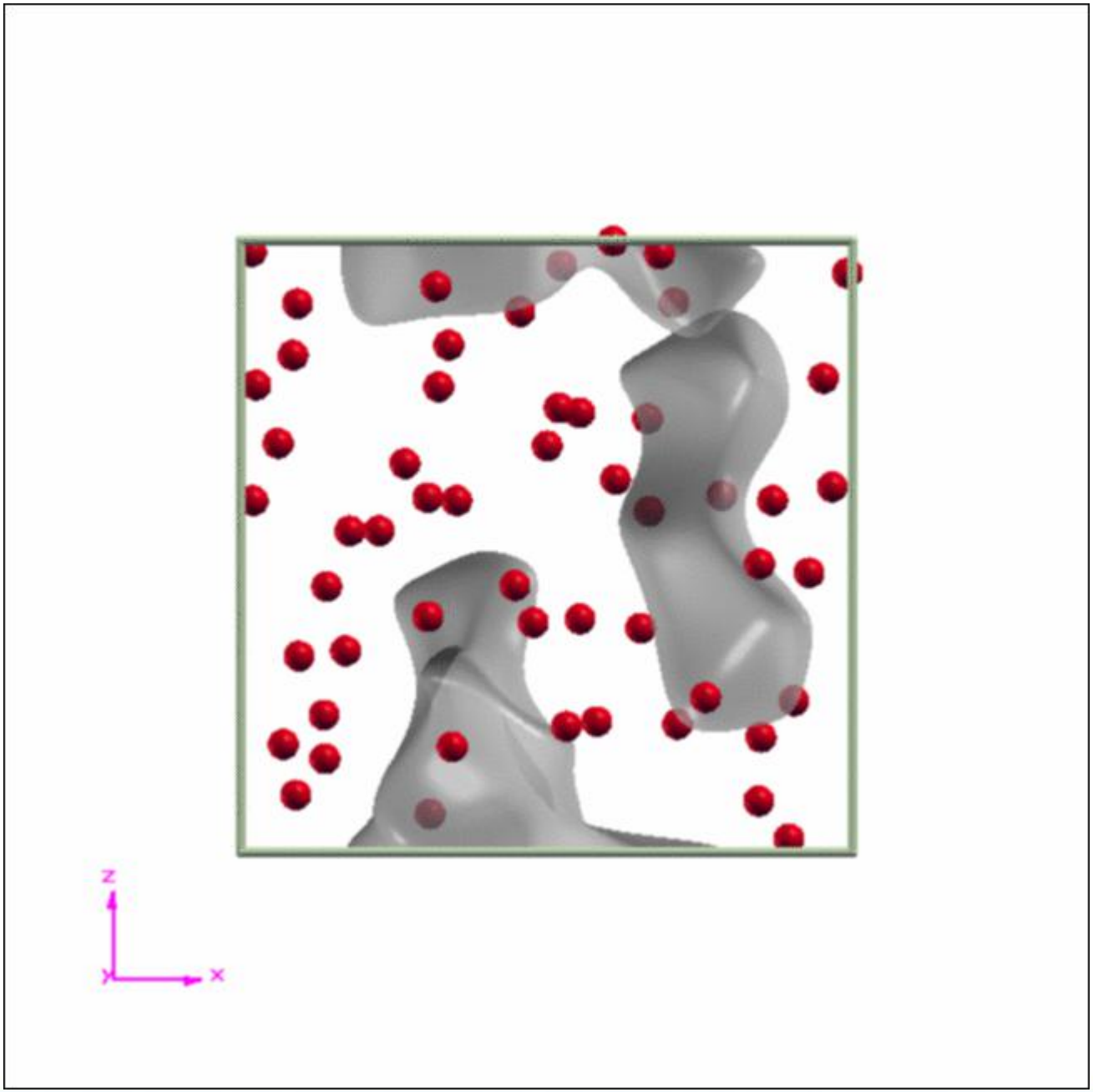

统计力学经典极限条件 $\lambda << d$ $n\lambda^3 << 1$

德布罗意平均热波长 $\lambda = \frac{h}{\sqrt{2\pi m k_B T}}$

分子间平均距离

Dyugaey [J. Low Temp. Phys. 78, 79 (1990)]:

① exchange of particles is negligible (Boltzmann statistics), but the quantum delocalization effects are still relevant

$$\lambda < d \quad or \quad \lambda \sim d$$

② exchange of particles is relevant and Bose-Einstein or Fermi-Dirac statistics should be applied

$$\lambda >> d$$

H atom:

1 eV

$$\lambda = \frac{h}{\sqrt{2\pi m k_B T}} = \frac{\sqrt{2\pi}}{\sqrt{1836 \times \frac{1}{27.21}}} a.u. \approx 0.305 a.u. = 0.16\dot{A}$$

1 g/cm^3

$$d = \sqrt[3]{\frac{m}{\rho}} = \sqrt[3]{\frac{1/6.02\times10^{23}\ g}{1.0 g/cm^3}} \approx 1.18\dot{A}$$

10 g/cm^3

$$d = \sqrt[3]{\frac{m}{\rho}} = \sqrt[3]{\frac{1/6.02\times10^{23}\ g}{10 g/cm^3}} \approx 0.55\dot{A}$$

Path integral molecular dynamics:

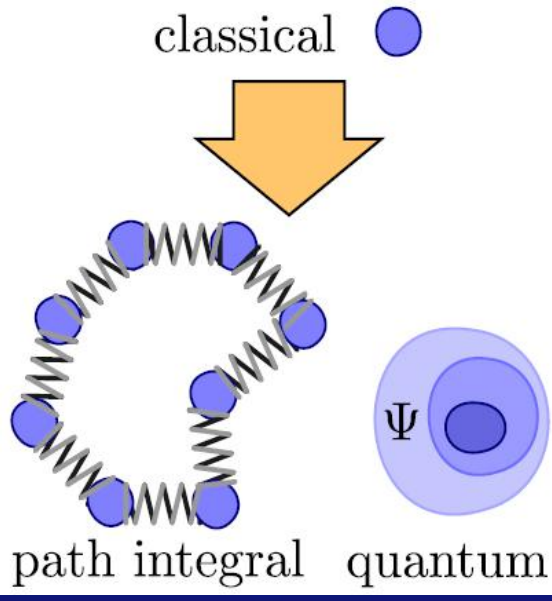

Nuclear quantum effects—path integral molecular dynamics

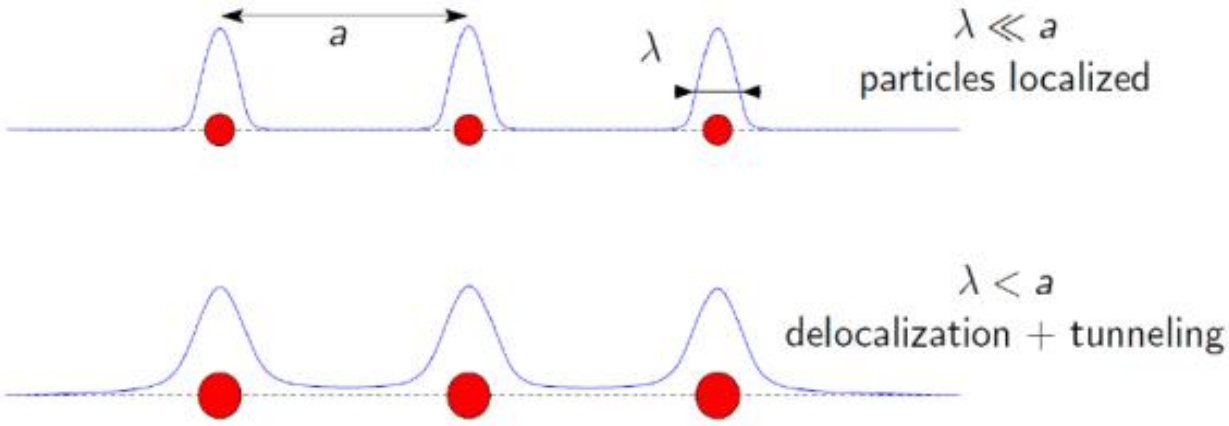

The *N*-particle quantum system is isomorphic to a *N* interacting ring polymers of length *P* with harmonic intrapolymeric forces.

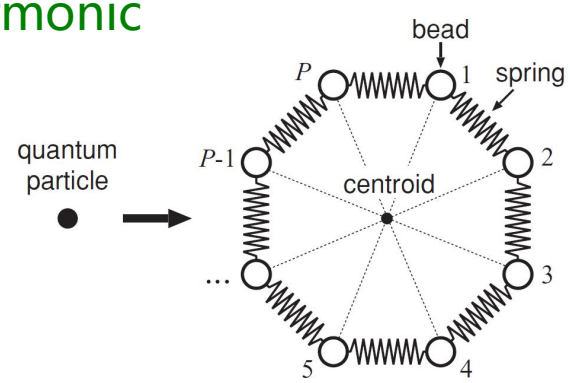

第一原理电子结构理论

第一原理路径积分分子动力学

Z. Phys. B 95, 143 (1994)

离子的量子效应

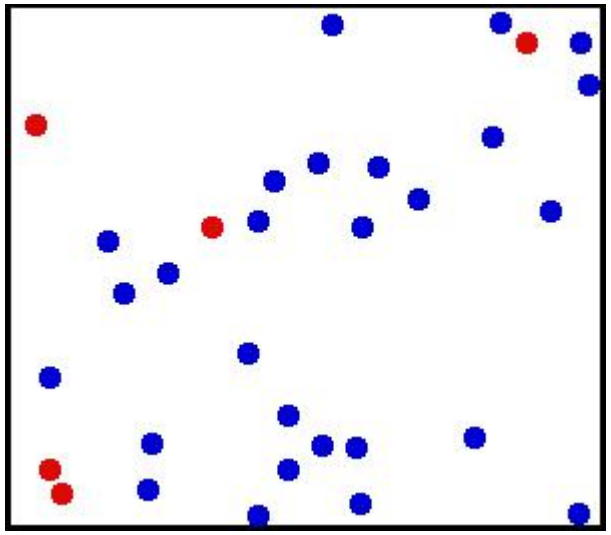

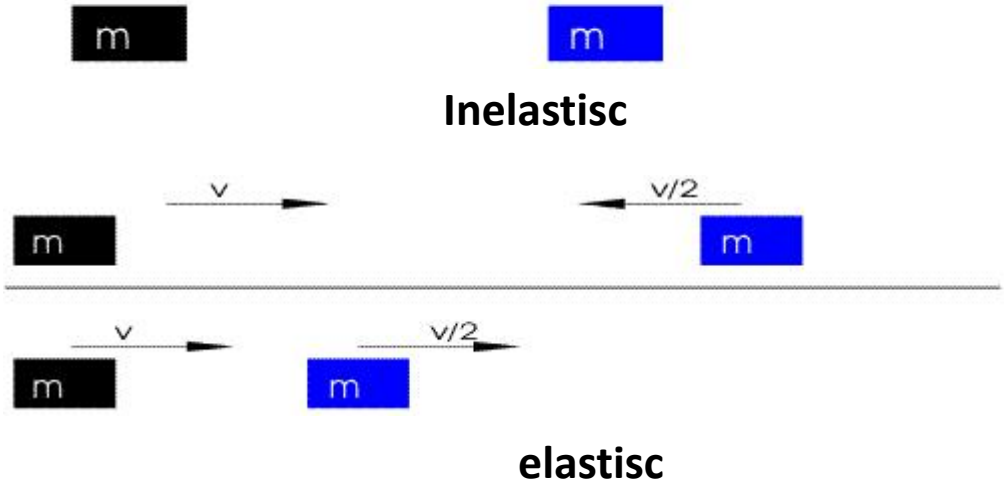
m
m
Inelastisc
v
v/2
m
m
v
v/2
m
m
elastisc

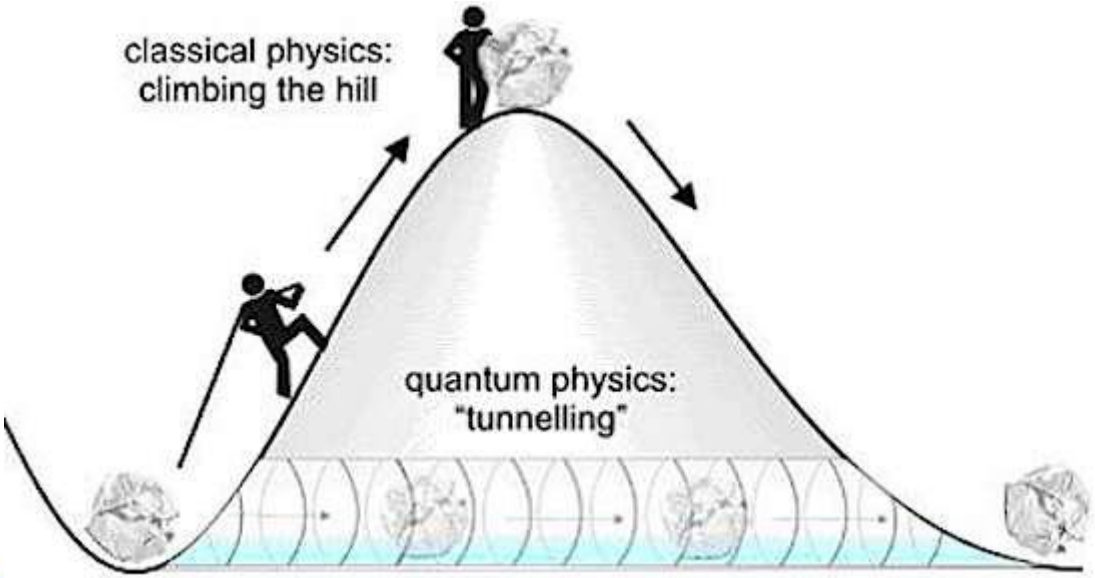
classical physics:
climbing the hill
quantum physics:
"tunnelling"

路径积分分子动力学方法

- 路径积分

$$K(x,t;x_0,t_0)=\sum_{x(t)} a\exp\left(\frac{i}{\hbar}I[x(t)]\right)=\int \exp\left(\frac{i}{\hbar}I[x(t)]\right)Dx(t)$$

$$I[x(t)]=\int_{t_0}^{t} L(x,\dot{x})dt$$

- 当 $I >> \hbar$ 时，使泛涵I [x (t)]取极值的路径 $x_c(t)$邻近的路径的贡献不可忽略

- 当二者可比拟时，必须考虑所有路径的贡献

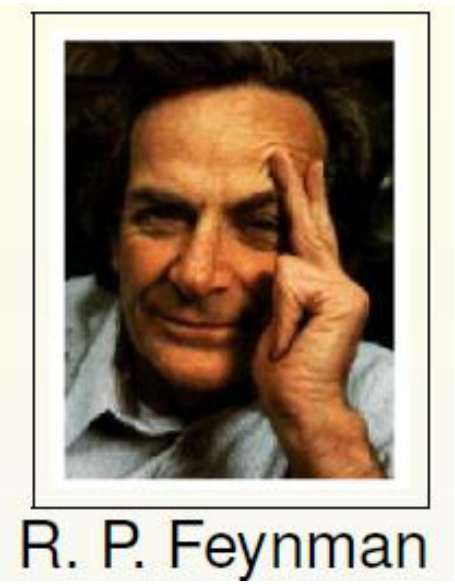
R. P. Feynman

路径积分分子动力学方法

处于热力学平衡状态的量子系统可以处于各种不同的能级，系统处于能量为 E_i 的状态的几率正比于 $\exp(-\beta E_i)$

$$P_i = \frac{1}{Z}\exp(-\beta E_i) \qquad \sum_i P_i = 1 \qquad \beta = 1/k_B T$$

$$Z = \sum_i \exp(-\beta E_i)$$

密度矩阵 $\rho(x_2, x_1) = \sum_i \phi_i(x_2)\phi_i^*(x_1)\exp(-\beta E_i) = \exp(-\beta H)$

配分函数 $Z = Tr(\rho) = \int \rho(x, x)dx$

路径积分分子动力学方法

密度矩阵 $\rho(x_2,x_1)=\sum_i \phi_i(x_2)\phi_i^*(x_1)\exp(-\beta E_i)$

传播函数 $K(x_2,t_2;x_1,t_1)=\sum_i \phi_i(x_2)\phi_i^*(x_1)\exp\left(-\frac{i}{\hbar}E_i(t_2-t_1)\right)$

$\rho(x_2,x_1)$ 可用 $K(x_2,t_2;x_1,t_1)$ 路径积分的方法计算

$t_2-t_1\to -i\beta\hbar$ $\qquad u=it$ $\qquad u_2=\hbar\beta, u_1=0$

$$\rho(x_2,x_1)=\int \exp\left\{-\frac{1}{\hbar}\int_0^{\beta\hbar}\left[\frac{m}{2}\dot{x}^2(u)+V(x)\right]du\right\}Dx(u)$$

$$Z=\int \rho(x,x)dx=\int dx_1\int_{x_1}^{x_1}\exp\left\{-\frac{1}{\hbar}\int_0^{\beta\hbar}\left[\frac{m}{2}\dot{x}^2(u)+V[x(u)]\right]du\right\}Dx(u)$$

路径积分分子动力学方法

$$Z=\int \rho(x,x)dx=\int dx_1\int_{x_1}^{x_1}\exp\left\{-\frac{1}{\hbar}\int_0^{\beta\hbar}\left[\frac{m}{2}\dot{x}^2(u)+V[x(u)]\right]du\right\}Dx(u)$$

u “时间” $\dot{x}=\frac{dx}{du}$ “速度” $\frac{m}{2}\dot{x}^2$ “动能”

离散化：

$$Z=\int \rho(x,x)\,dx=\int dx_1\left\langle x_1\left|e^{-\beta(T+U)}\right|x_1\right\rangle=\lim_{P\to\infty}\int dx_1\left\langle x_1\left|\Omega^P\right|x_1\right\rangle$$

$$\Omega=e^{-\frac{\beta}{2P}U}e^{-\frac{\beta}{P}T}e^{-\frac{\beta}{2P}U}$$

Trotter theorem: $e^{\alpha(A+B)}=\lim_{P\to\infty}\left[e^{\frac{\alpha}{2P}B}e^{\frac{\alpha}{P}A}e^{\frac{\alpha}{2P}B}\right]^P$

路径积分分子动力学方法

$$Z = \lim_{P\to\infty} \int dx_1 dx_2 \ldots dx_P \left\langle x_1 \left|\Omega\right| x_2 \right\rangle \left\langle x_2 \left|\Omega\right| x_3 \right\rangle \ldots \left\langle x_P \left|\Omega\right| x_1 \right\rangle$$

$$= \lim_{P\to\infty} \int \prod_{i=1}^{P} dx_i \left\langle x_i \left|\Omega\right| x_{i+1} \right\rangle \Big|_{x_{P+1}=x_1}$$

$$Z = \lim_{P\to\infty} N_p \int d\left\{R_I^{(1)}\right\} \cdots \int d\left\{R_I^{(P)}\right\} \exp\left[-\beta \sum_{s=1}^{P} \left\{ \sum_{I=1}^{N} \frac{1}{2} M_I \omega_p^2 \left(R_I^{(s)} - R_I^{(s+1)} \right)^2 + \frac{1}{P} E_0\left(\left\{ R_I \right\}^{(s)} \right) \right\} \right]$$

$$\omega_p^2 = P/\beta^2 \qquad R_I^{(P+1)} = R_I^{(P)}$$

$$Z = \lim_{P\to\infty} N \int d\left\{R\right\} \exp\left[-\beta \sum_{s=1}^{P} \left\{ \sum_{I=1}^{N} \frac{P_I^{(s)}}{2M_I'} + \frac{1}{2} M_I \omega_p^2 \left(R_I^{(s)} - R_I^{(s+1)} \right)^2 + \frac{1}{P} E_0\left(\left\{ R_I \right\}^{(s)} \right) \right\} \right]$$

$$L = \sum_{s=1}^{P} \left\{ \sum_{I=1}^{N} \frac{P_I^{(s)}}{2M_I'} + \frac{1}{2} M_I \omega_p^2 \left(R_I^{(s)} - R_I^{(s+1)} \right)^2 + \frac{1}{P} E_0\left(\left\{ R_I \right\}^{(s)} \right) \right\}$$

$$M_I' \ddot{R}_I^{(s)} = -\frac{1}{P} \frac{\partial E_0\left(\left\{ R_I \right\}^{(s)} \right)}{\partial R_I^{(s)}} - M_I \omega_p^2 \left(2R_I^{(s)} - R_I^{(s+1)} - R_I^{(s-1)} \right)$$

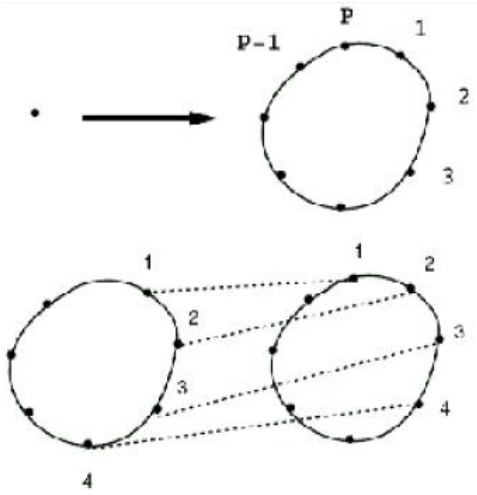

路径积分分子动力学方法

Primitive variables $\{R_I\}^{(s)}$ ⟶ Normal mode variables $\{y_I\}^{(s)}$

$$R_I^{(s)} = \sum_{k=1}^{P} a_I^{(k)} e^{2\pi i(s-1)(k-1)/P}$$

$$\left.\begin{aligned} y_I^{(1)} &= a_I^{(1)} \\ y_I^{(P)} &= a_I^{((P+2)/2)} \\ y_I^{(2s-2)} &= \mathrm{Re}(a_I^{(s)}) \\ y_I^{(2s-1)} &= \mathrm{Im}(a_I^{(s)}) \end{aligned}\right\} \quad y_I^{(s)} = \frac{1}{\sqrt{P}} \sum_{r=1}^{P} U_{sr} R_I^{(r)}$$

Centroid of the path $\quad y_I^{(1)} = R_I^c = \frac{1}{P} \sum_{r=1}^{P} R_I^{(r)}$

运动方程： $M_I'^{(s)} \ddot{y}_I^{(s)} = -\frac{1}{P} \frac{\partial E_0}{\partial y_I^{(s)}} - M_I^{(s)} \omega_p^2 y_I^{(s)}$

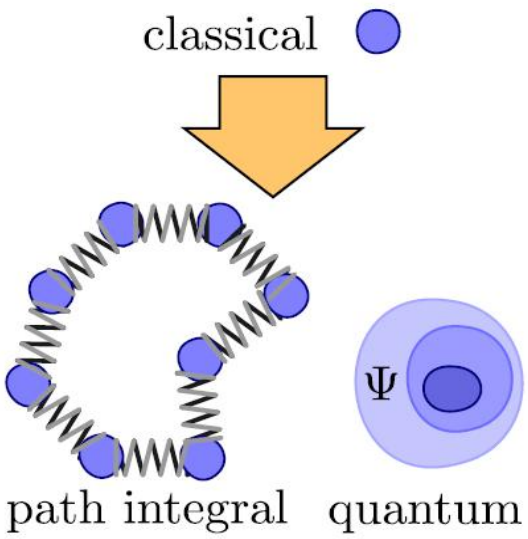

路径积分分子动力学方法

总能量：
$$E = -\frac{\partial}{\partial \beta} \ln Z = \lim_{P\to\infty} < \varepsilon_P >_{PI}$$

$$\varepsilon_P = \frac{3}{2} NPkT - \sum_{s=1}^{P} \sum_{I=1}^{N} \frac{1}{2} M_I \omega_p^2 \left(R_I^{(s)} - R_I^{(s+1)} \right)^2 + \frac{1}{P} \sum_{s=1}^{P} E_0 \left(\{ R_I \}^{(s)} \right)$$

压强：
$$P = -\frac{1}{\beta} \frac{\partial}{\partial V} \ln Z = \lim_{P\to\infty} < P_P >_{PI}$$

$$P_P = \frac{NP}{\beta V} - \frac{1}{3V} \sum_{s=1}^{P} \sum_{I=1}^{N} \left[M_I \omega_p^2 \left(R_I^{(s)} - R_I^{(s+1)} \right)^2 - \frac{1}{P} R_I^{(s)} \cdot \frac{\partial E_0}{\partial R_I^{(s)}} \right]$$

路径积分分子动力学方法

Centroid molecular dynamics (CMD)

Centroid trajectories of a quantum particle are generated by the semiclassical equation of motion

$$M_I \ddot{R}_I(t) = \left\langle F_I(R_1^C, \cdots, R_N^C) \right\rangle_{PI}$$

$$F_I(R_1^C, \cdots, R_N^C) = \sum_{s=1}^{P} f_I^{(s)}$$

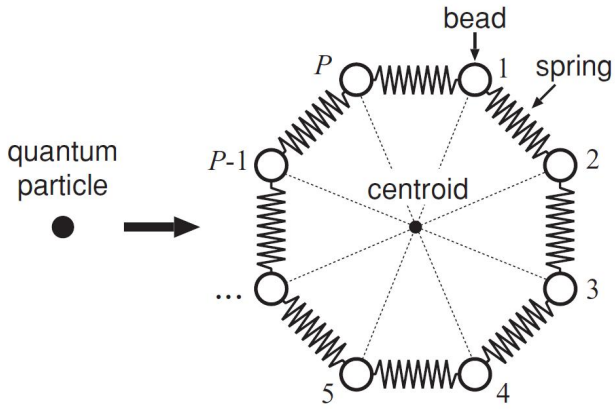

运动方程： $M_I'^{(1)} \ddot{y}_I^{(1)} = -\frac{1}{P}\frac{\partial E_0}{\partial y_I^{(1)}}$

$$y_I^{(1)} = R_I^c = \frac{1}{P}\sum_{r=1}^{P} R_I^{(r)}$$

$$M_I'^{(s)} \ddot{y}_I^{(s)} = -\frac{1}{P}\frac{\partial E_0}{\partial y_I^{(s)}} - M_I^{(s)} \omega_p^2 y_I^{(s)} \qquad s = 2, \cdots, P$$

绝热参数 γ

$$M_I'^{(1)} = M_I$$
$$M_I'^{(s)} = \gamma M_I^{(s)}$$

$0 < \gamma < 1$

J. Chem. Phys. 101, 6168 (1994);
Comput. Phys. Commun. 118, 166 (1999)

粒子量子隧穿的路径积分分子动力学

一维量子粒子势垒隧穿

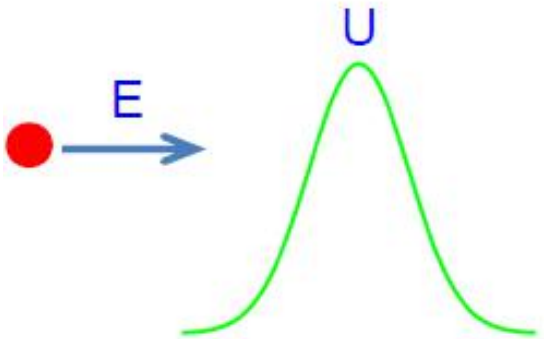

$$\omega_P = \sqrt{P} k_B T = \frac{2N}{g} \sqrt{P} E_0$$

$$\omega_P(t) = \frac{2N}{g} \sqrt{P} (aE(t) + bE_0)$$

参数a和b通过两个条件确定：

1. 当 $E(t) = E_0$ 时，$\omega_P = \frac{2N}{g} \sqrt{P} E_0$

2. 当 $E(t) = 0$ 时，ω_P 达到最小值，使得环形分子的均方回转直径等于德布罗意波长

$$a = 1 - (2R_{g0} / \lambda)^2 \qquad b = (2R_{g0} / \lambda)^2$$

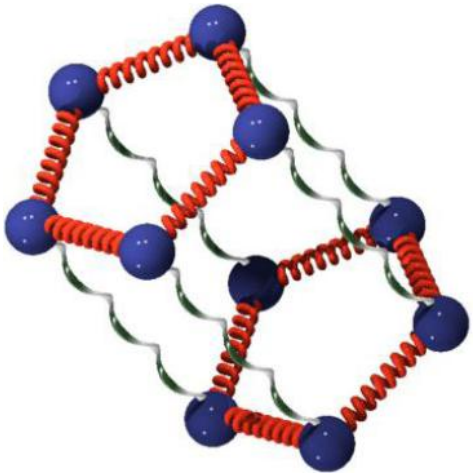

粒子量子隧穿的路径积分分子动力学

一维量子粒子势垒隧穿

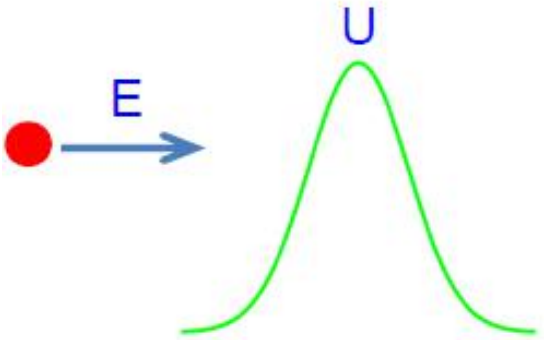

$$U(x) = U_0 \exp\left(-\frac{x^2}{a^2}\right)$$

$$U_0 = 5000K$$

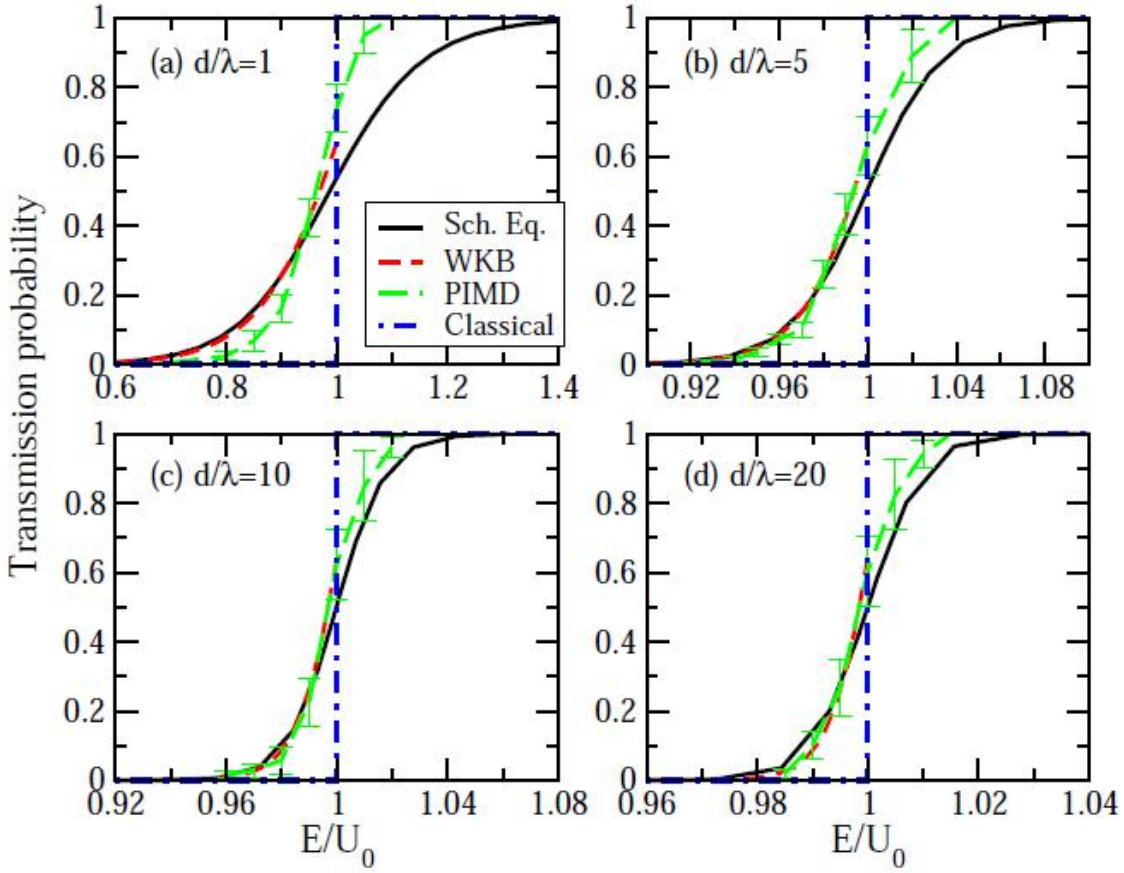

离子的量子隧穿效应

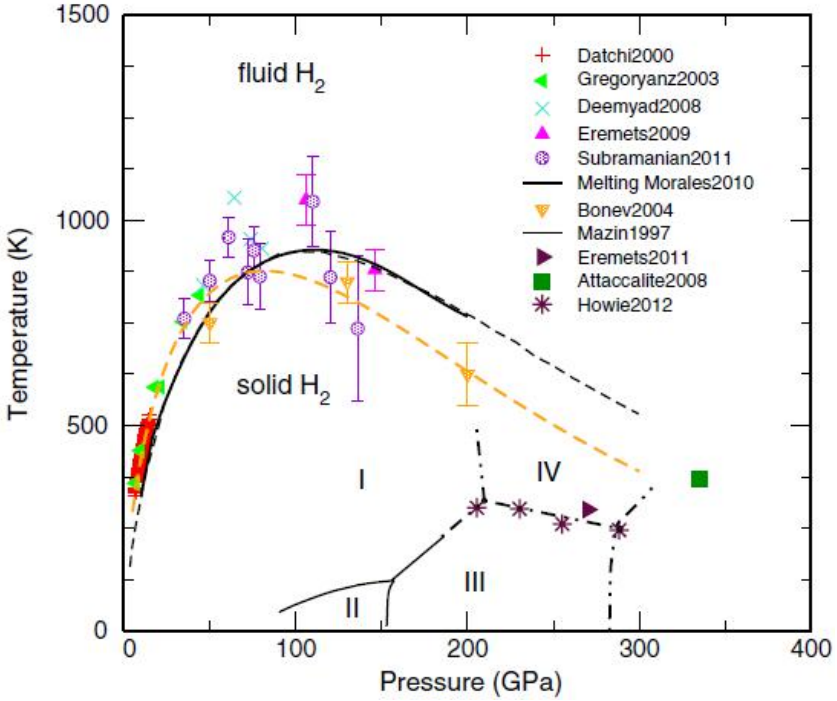

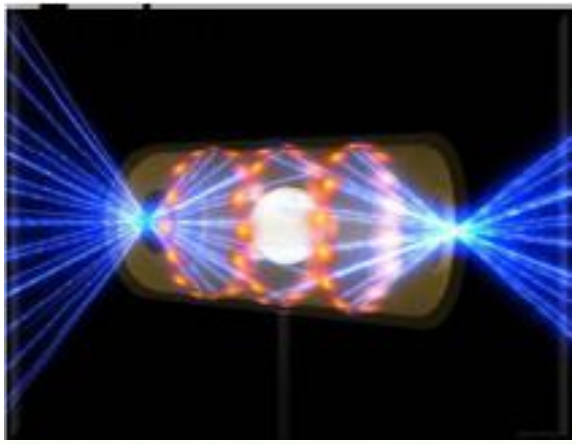

Rev. Mod. Phys. 84, 1607 (2012)

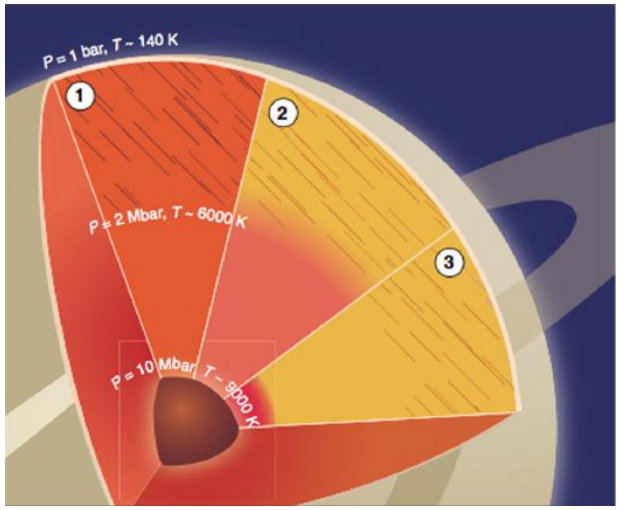

Saturn

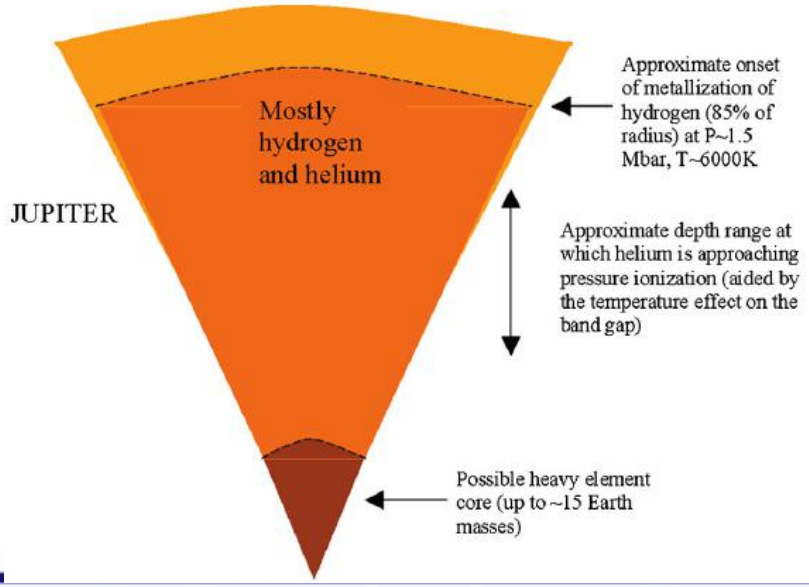

Computation details in MD simulations

- DFT with PBE exchange-correlation potential was used.
- Ultrasoft pseudopotential was used to describe the interaction between valence and core electrons.
- The plane-wave energy cutoff of 50 Ry was adopted with the charge-density cutoff of 400 Ry.
- Grimme scheme was used to treat van der Waals interaction.
- The cubic supercell includes 16 water molecules.
- All MD and PIMD simulations were performed with modified Quantum-ESPRESSO package.

Ice X

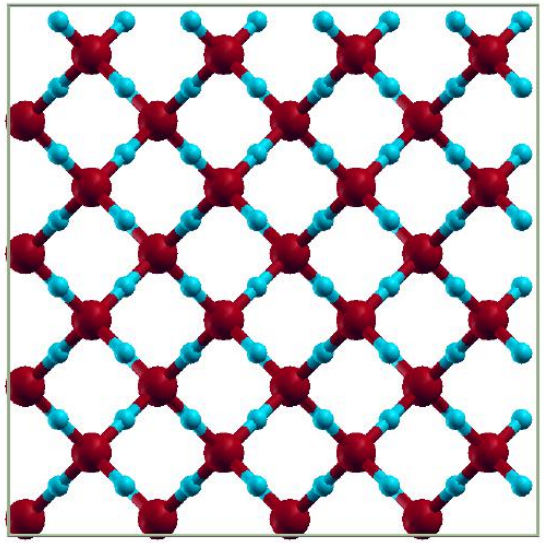

NQEs on phase transition of high-pressure ice

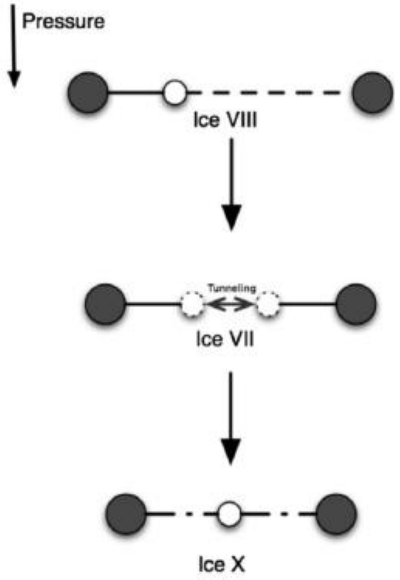

$$\delta = \mathrm{d(O_1H)\text{-}d(O_2H)}$$

34.5 GPa

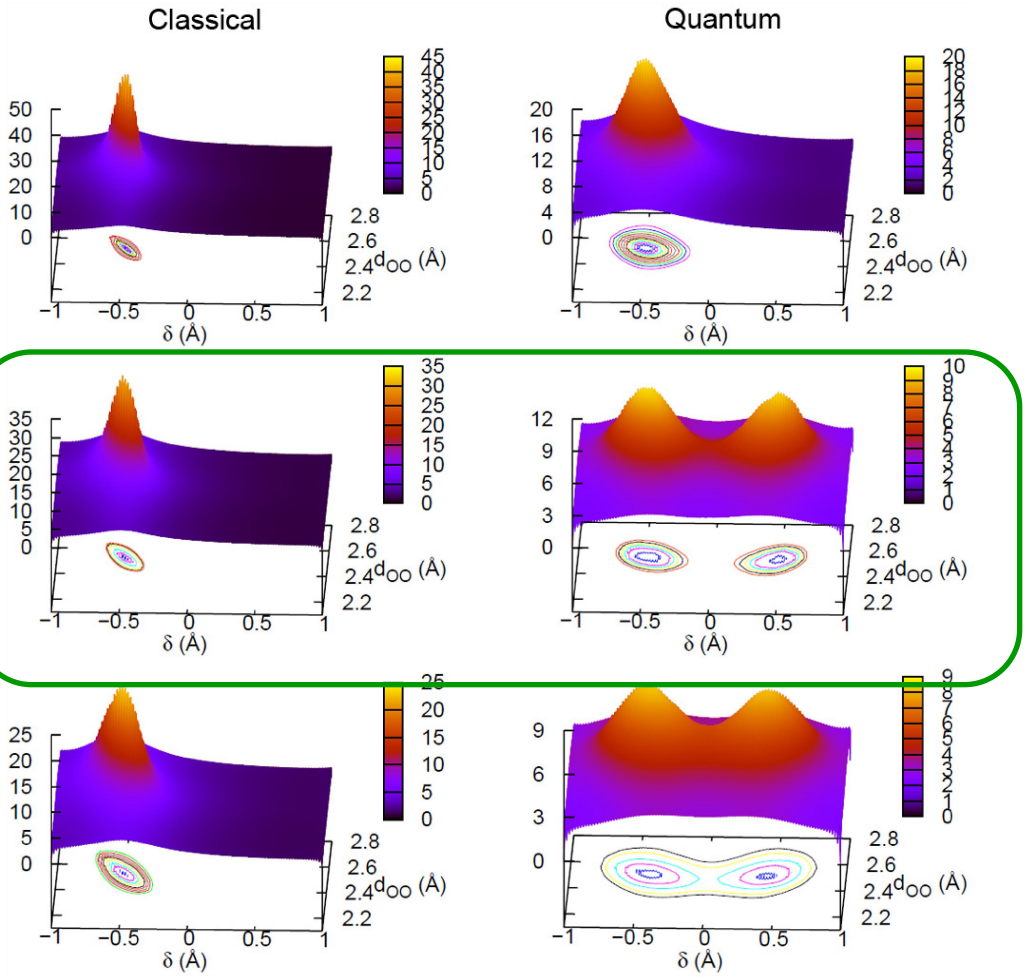

NQEs on phase transition of high-pressure ice

61.2 GPa

107.9 GPa

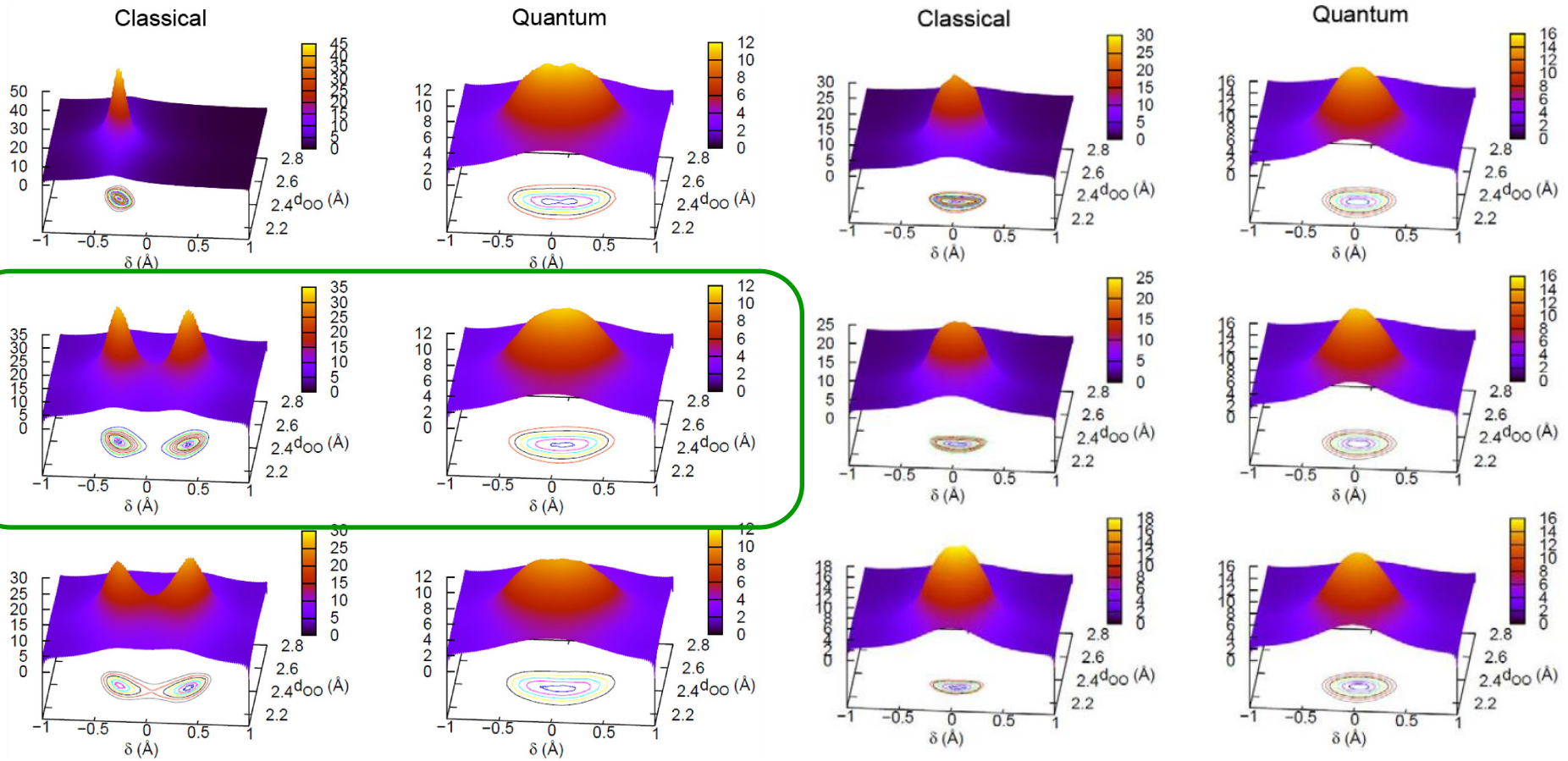

NQEs on phase transition of high-pressure ice

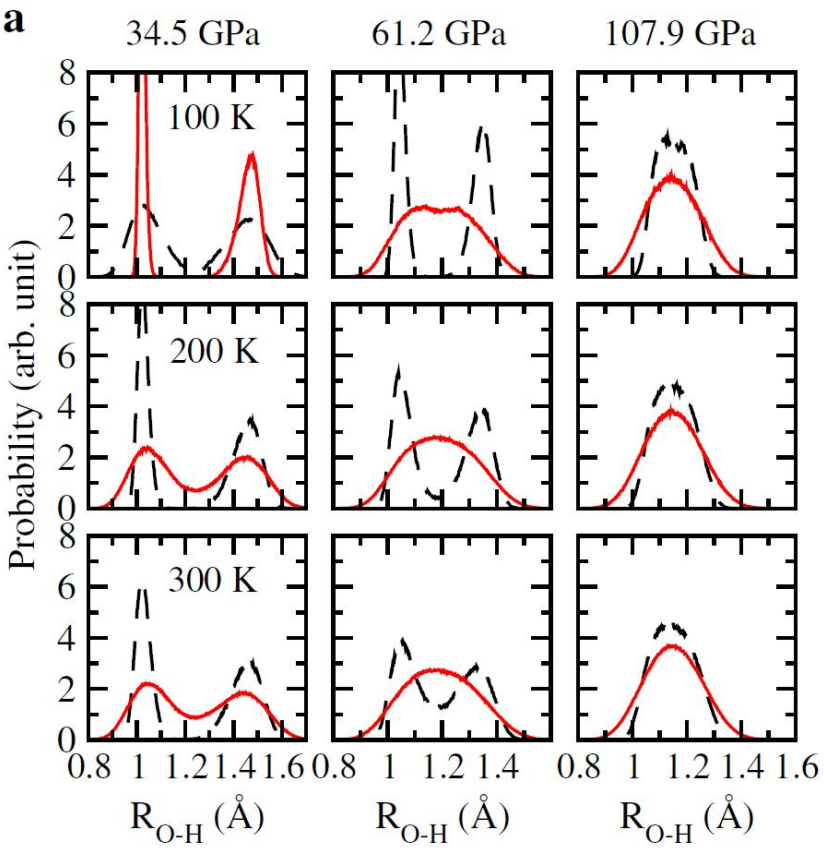

Distributions of the O-H bond lengths at different pressures and temperatures

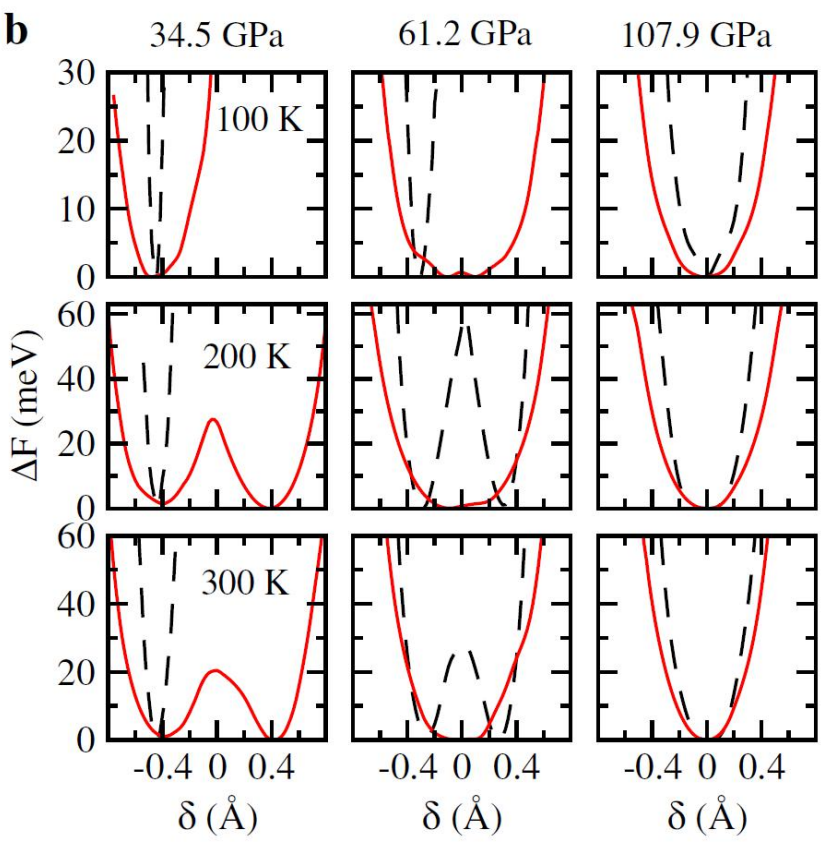

Free energy profiles of the protons along the two nearest neighbouring oxygen atoms obtained from quantum (solid lines) and classical (dashed lines) simulations.

Free energy profile: $\Delta F = -k_B T \ln[P(\delta)]$ $\delta = \mathrm{d(O_1H)\text{-}d(O_2H)}$

NQEs on phase transition of high-pressure ice

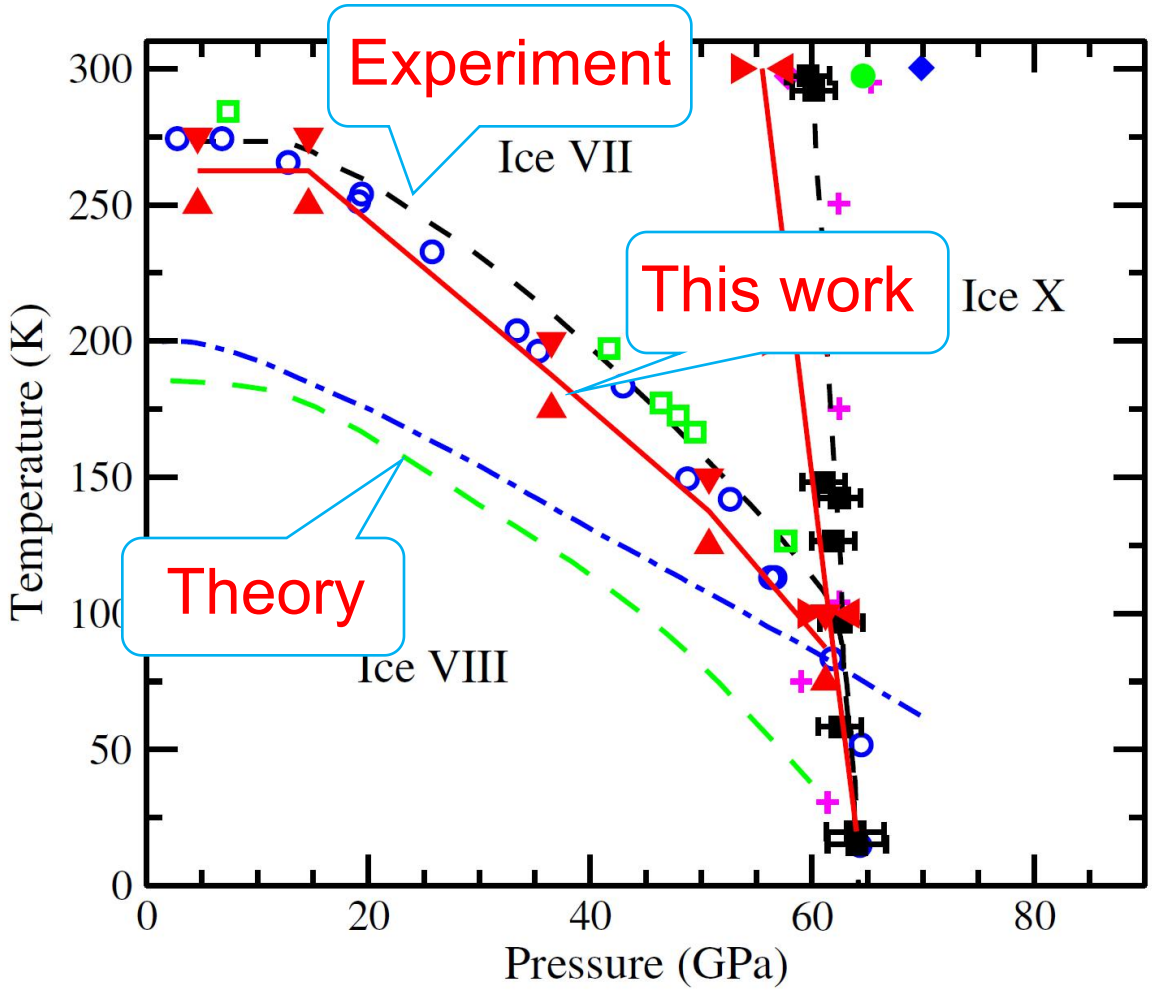

Theory: Chem. Phys. Lett. 499, 236 (2010);
Expt.: Phys. Rev. B 68, 014106 (2003)

K-edge x-ray absorption is an important probe of microscopic structure in high-pressure ice

- We use the full core hole approach to calculate the oxygen K-edge XAS of ice.
- DFT with PBE exchange-correlation potential
- We adopted a 4×4×4 k-points grid and a 90 Ry plane-wave energy cutoff to ensure the convergence.
- The calculated spectra were broadened using a Gaussian convolution of width 0.3 eV.
- The size of supercell including 16 water molecules is big enough for obtaining reliable oxygen K edge, as shown in the right figure.

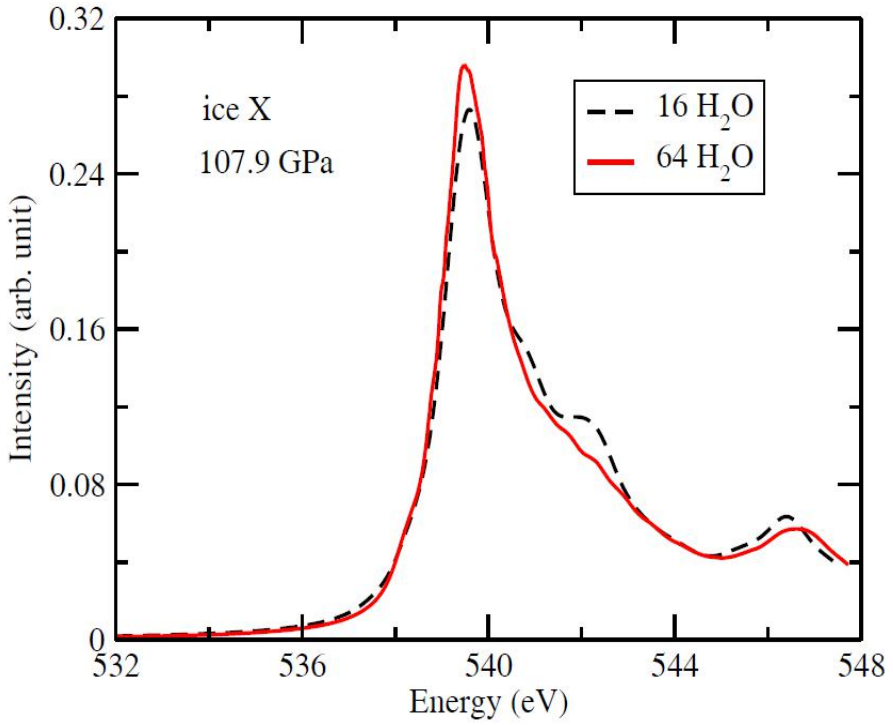

D. Kang et al. Scientific Reports 3, 3272 (2013)

高压冰的相变和K边X射线吸收谱

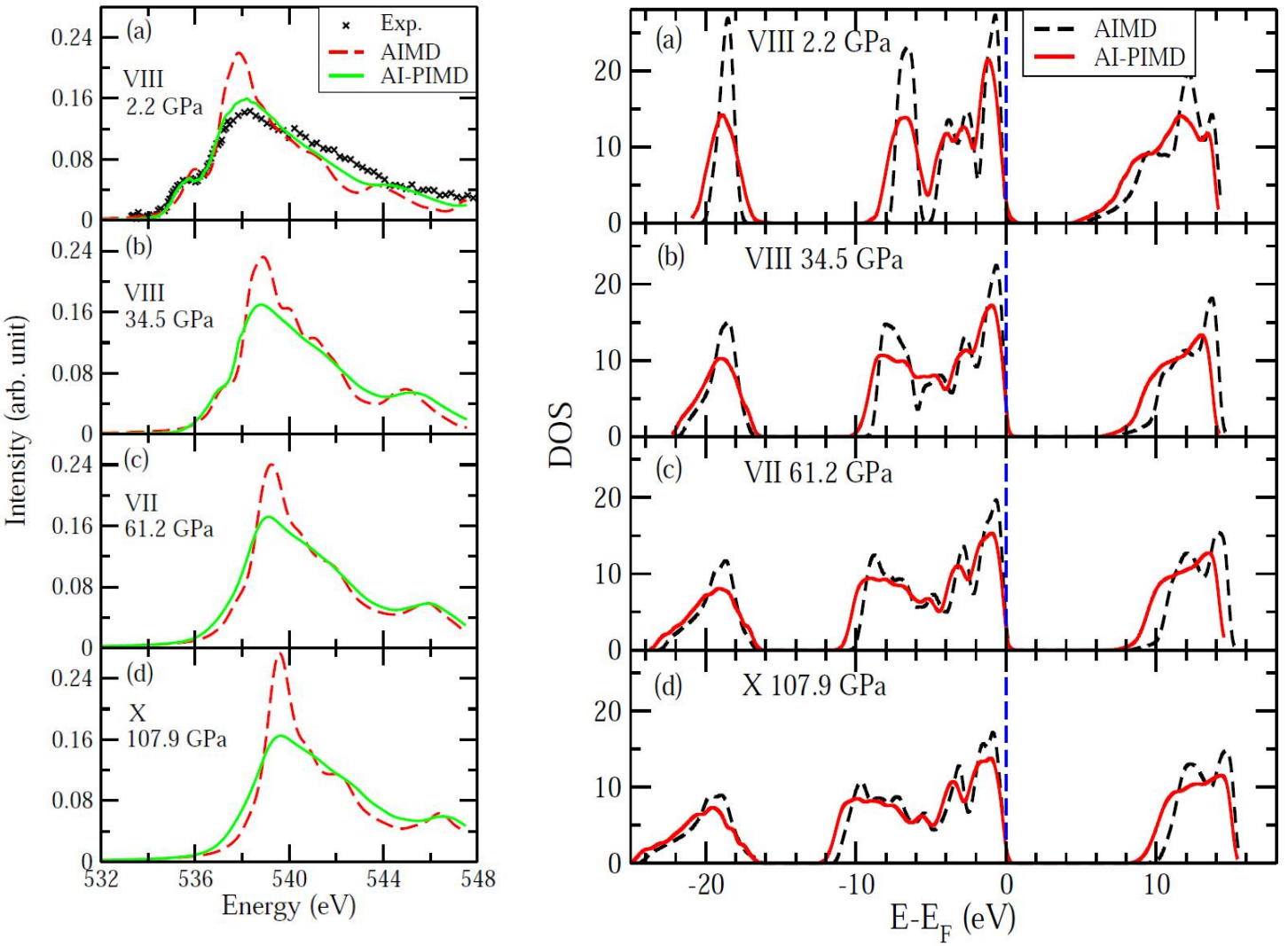

Exp.: J. Phys. Chem. B 114, 3804 (2010)

离子的量子隧穿效应

自扩散系数与粘滞系数

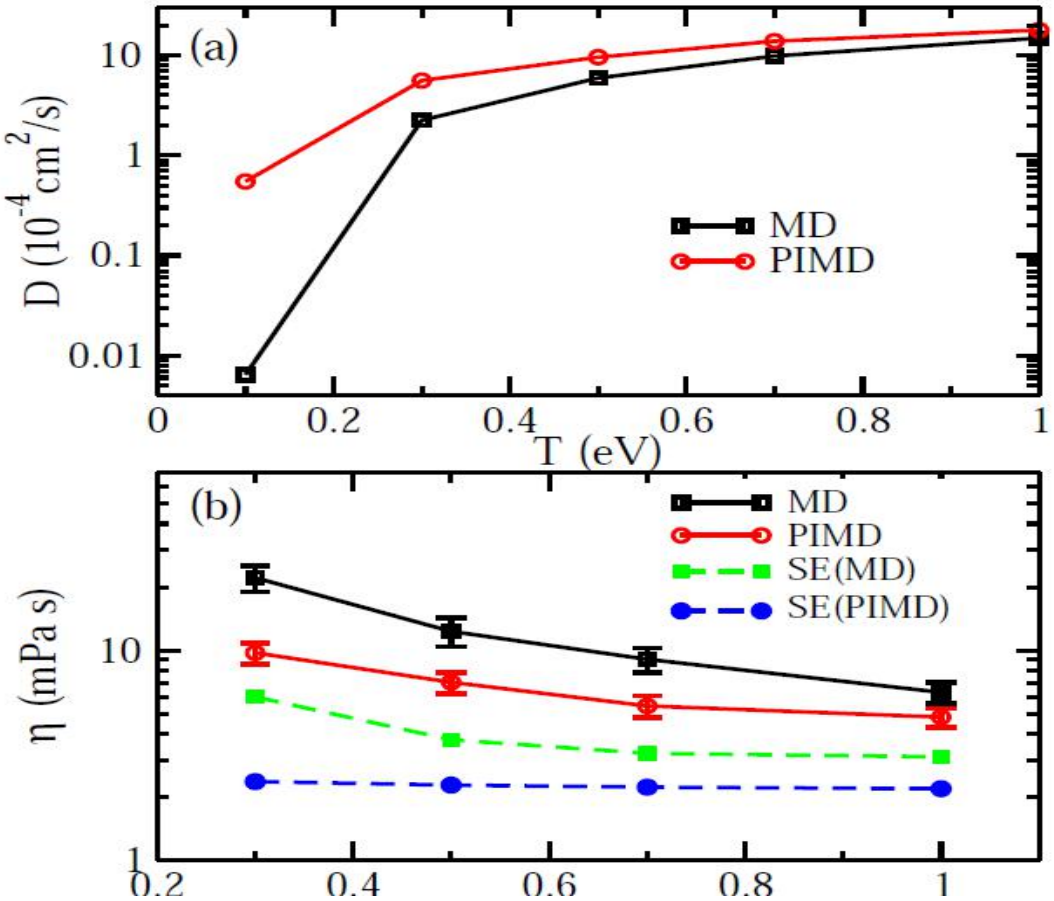

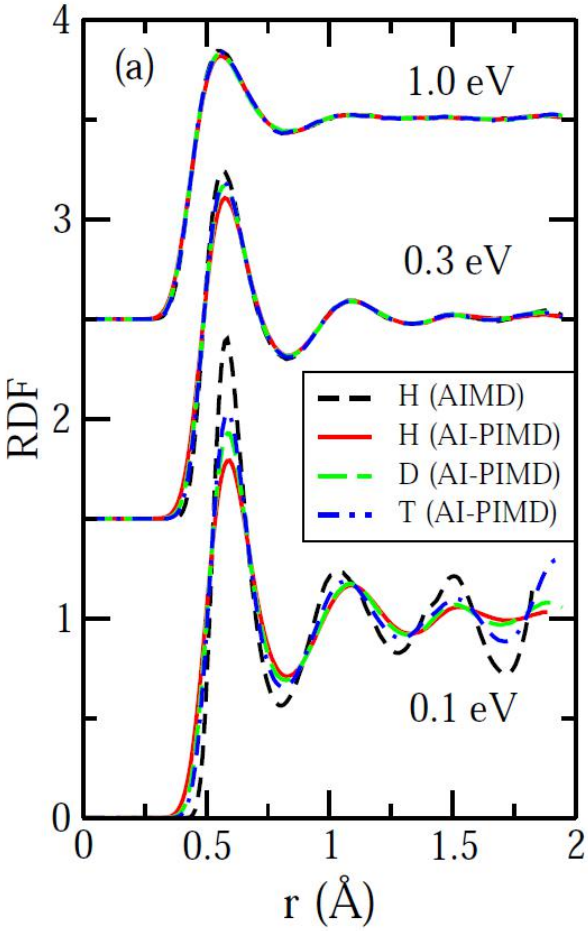

10 g/cm^3

Scientific Reports， 4: 5484 （2014）

Quantum effect of ions in dense matter

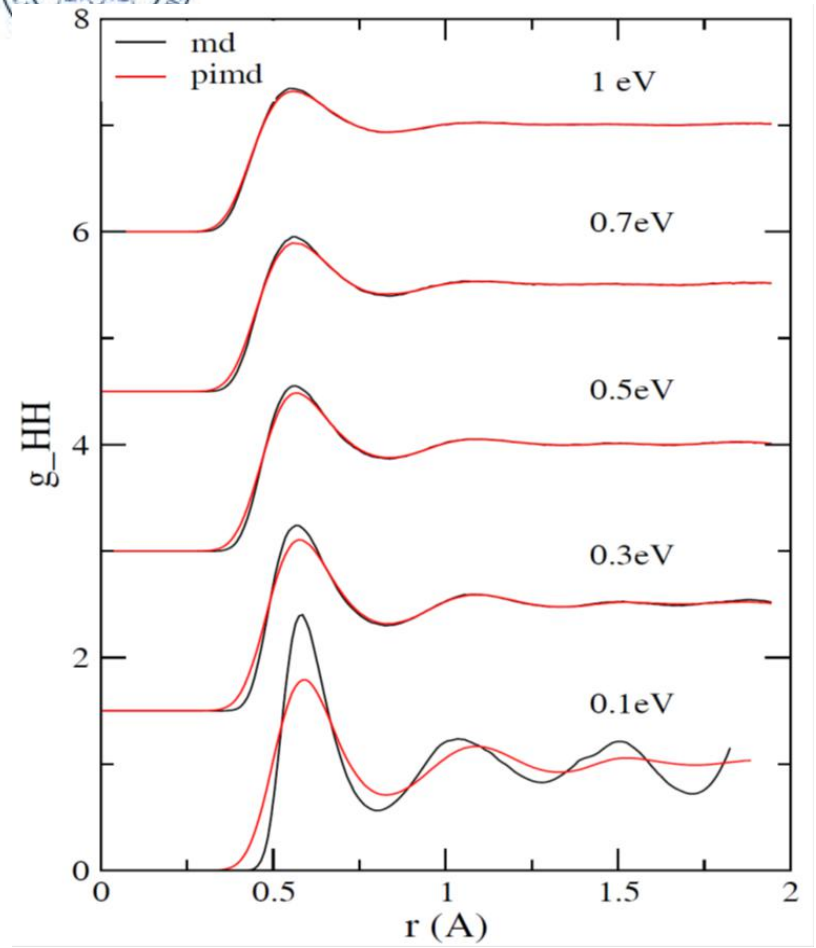

不同温度的10g/cm³氢的径向分布函数

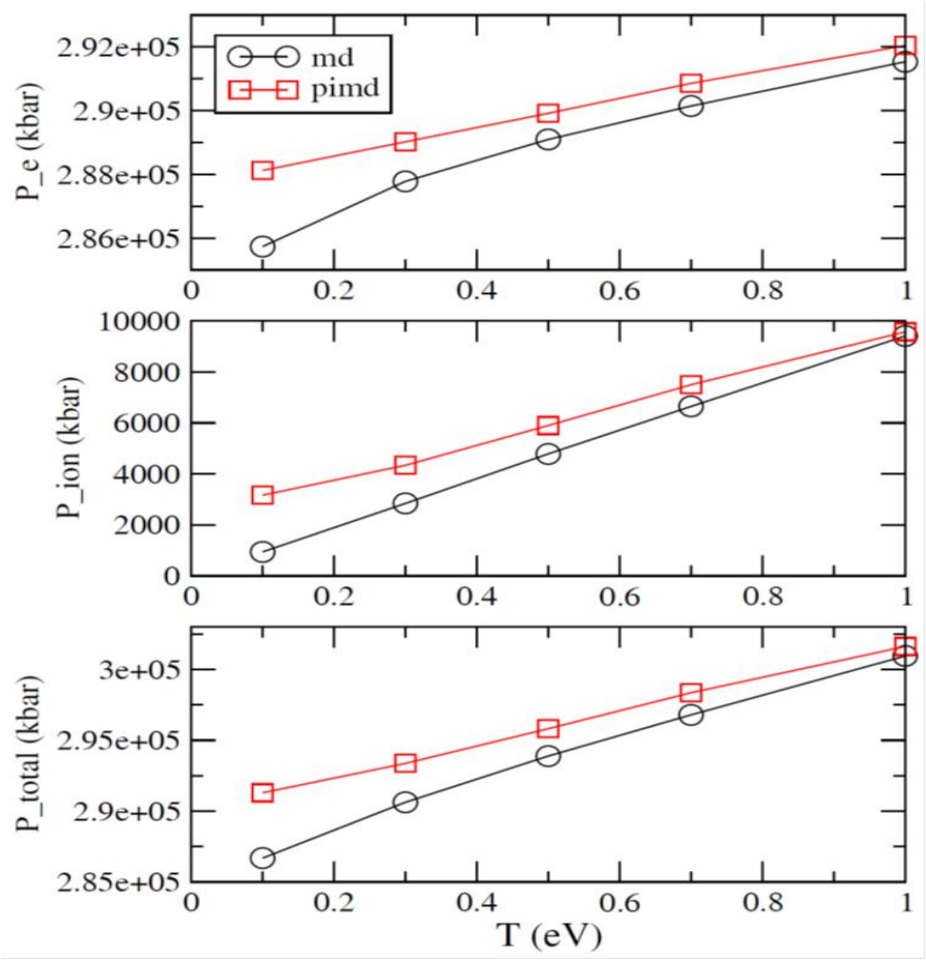

不同温度的10g/cm³氢的电子压强、离子压强、总压强

原子构型的演化

原子

团簇

大块固体

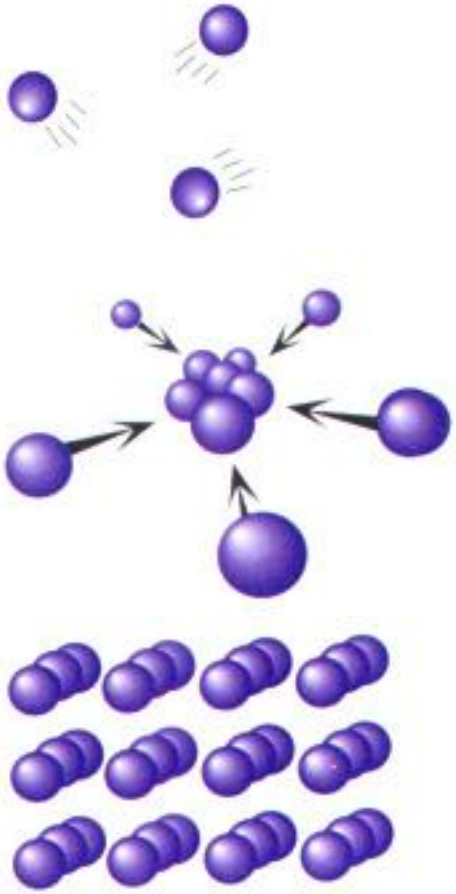

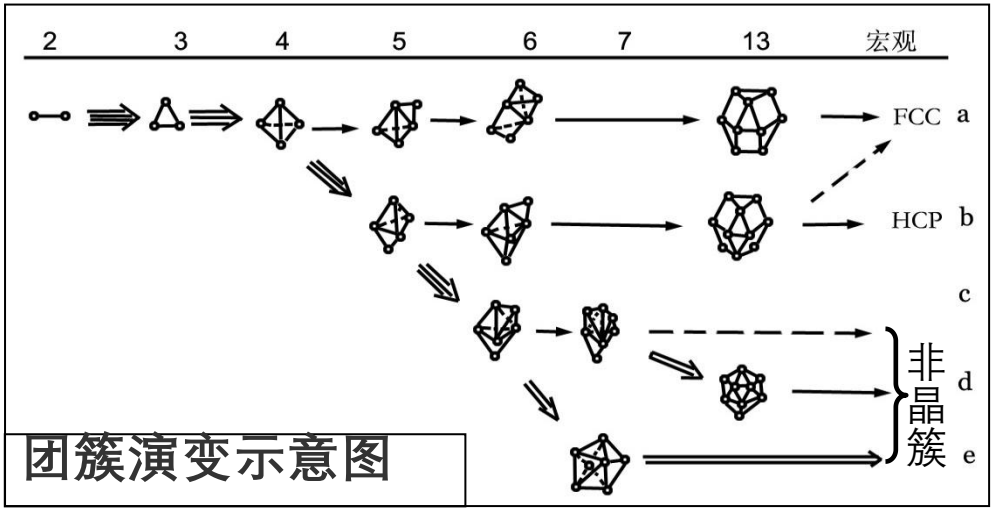

团簇演变示意图

原子团簇随尺寸的演变

电子结构的演化

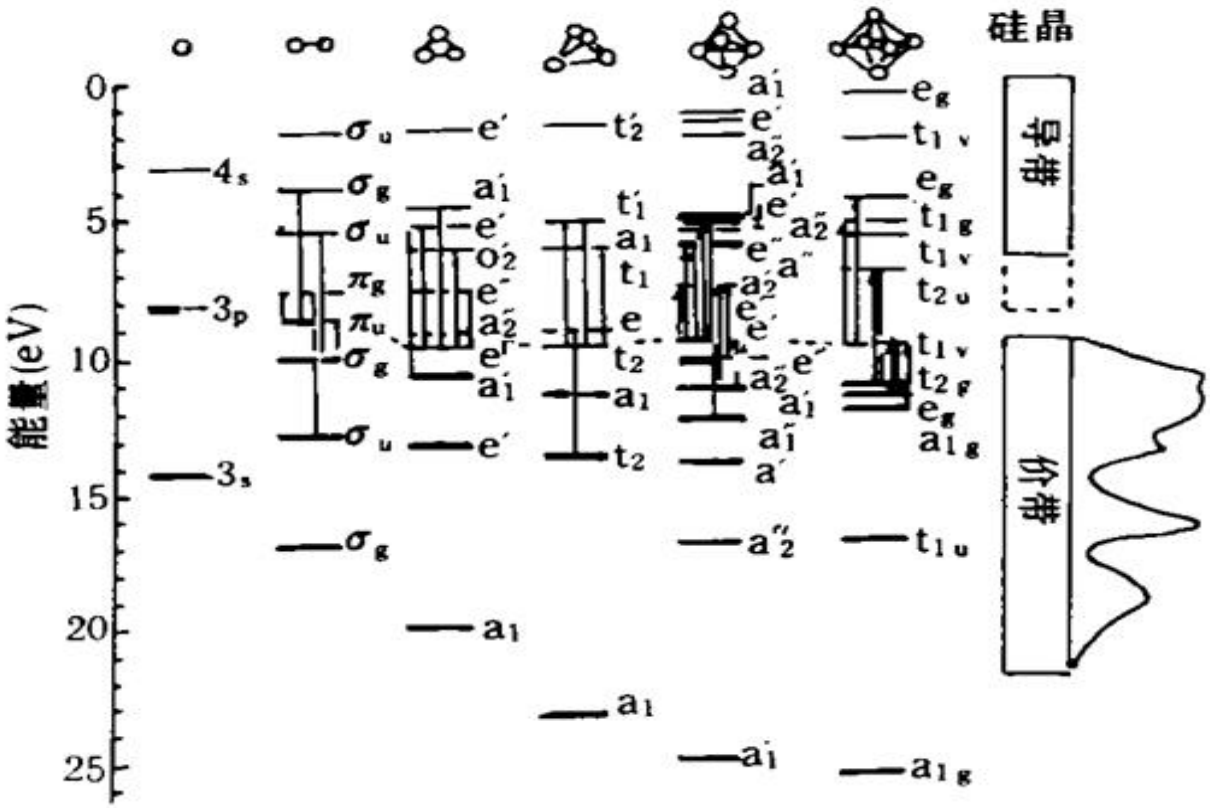

硅团簇的电子能级图。理论计算是采用黑格尔(Hückol)近似并取团簇有一定结构。

激光激发金团簇的电子激发模式

C_{60}

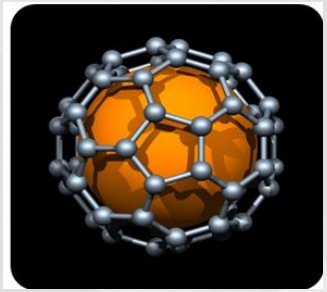

金团簇

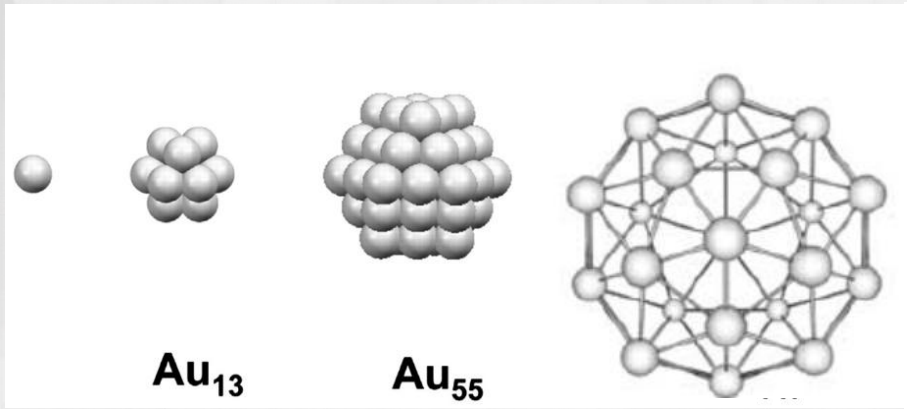

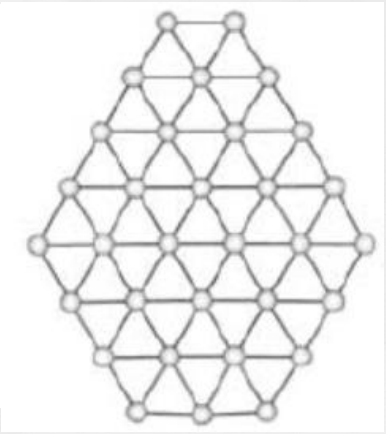

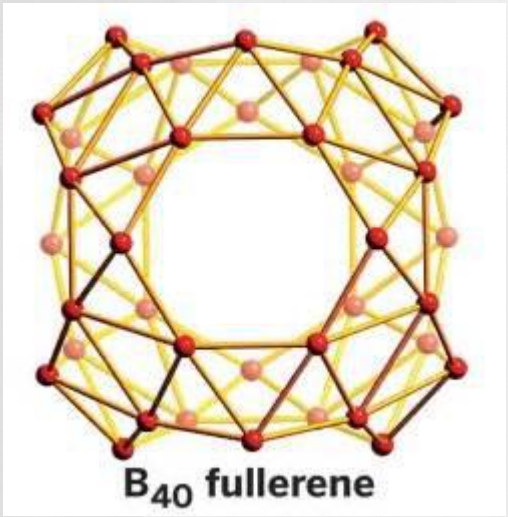

B_{40}

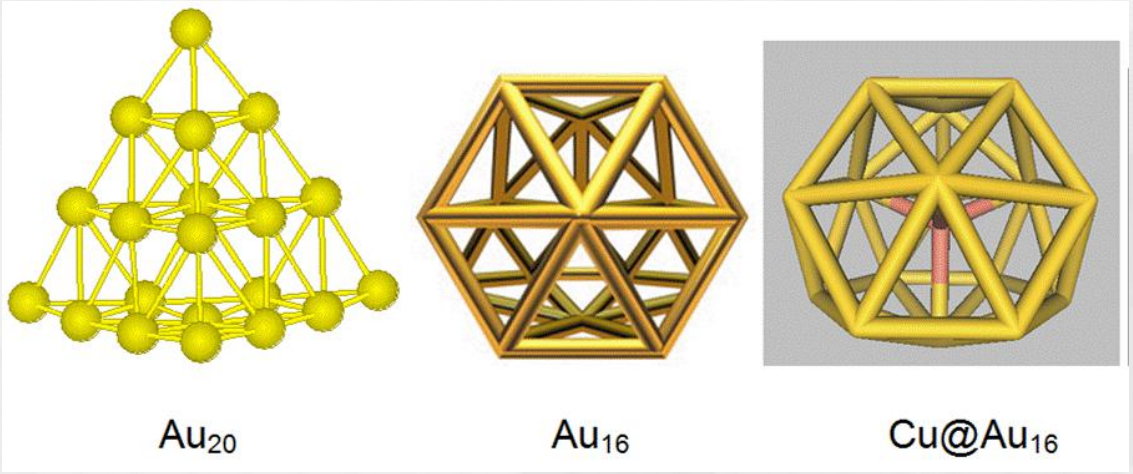

激光激发金团簇的电子激发模式

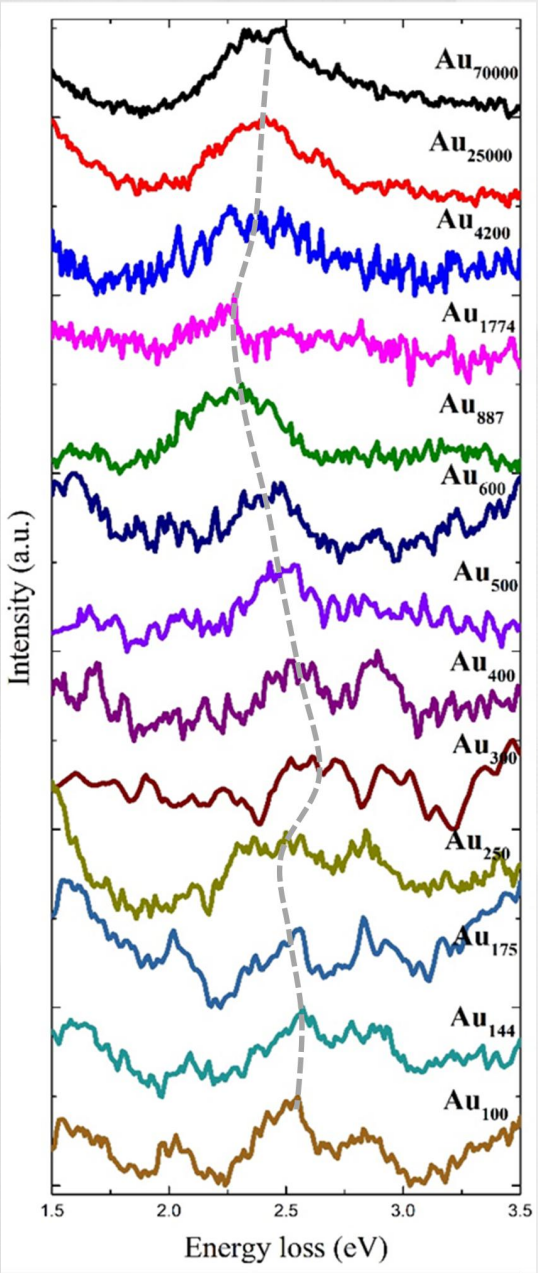

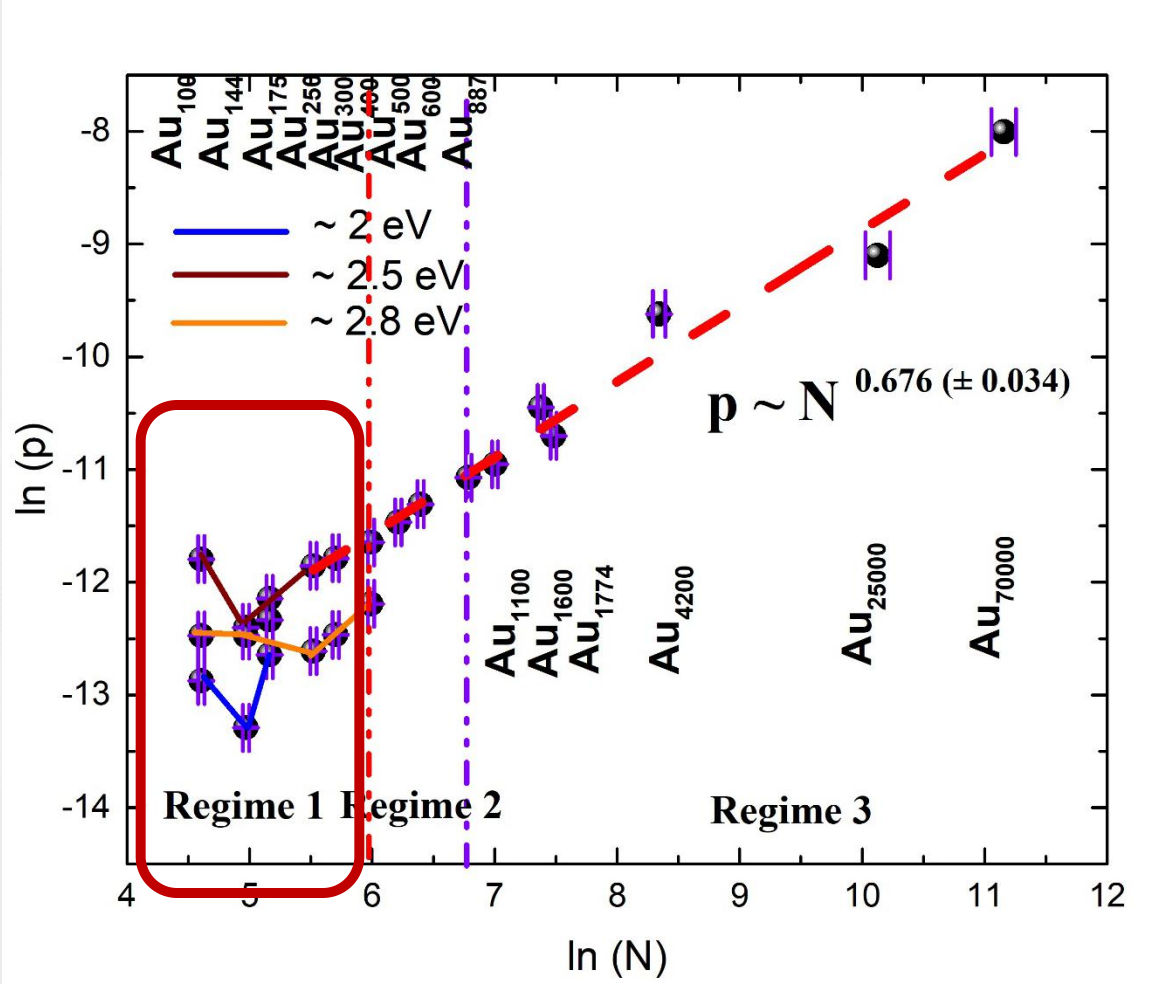

arXiv:2003.11191

Real time TD-DFT basis

- Time dependent Schrödinger Equation

$$i\frac{\partial\psi(\mathbf{r},t)}{\partial t} = \hat{H}(\mathbf{r},t)\psi(\mathbf{r},t)$$

- Time dependent wave function

$$\psi(\mathbf{r},t) = \sum_i c_i(t)\varphi_i(\mathbf{r},t)$$

- Time dependent spin orbitals

$$|\varphi_i(\mathbf{r},t)\rangle = \sum_\mu c_{\mu i}(t)\,|\chi_\mu(\mathbf{r})\rangle$$

激光激发金团簇的电子激发模式

含时密度泛函理论(TDDFT)考虑

$$H\left(t, R_j(t), n(t)\right)\psi_i(t) = \mathrm{i}\frac{\partial \psi_i(t)}{\partial t}$$

Au_{116}的能级计算

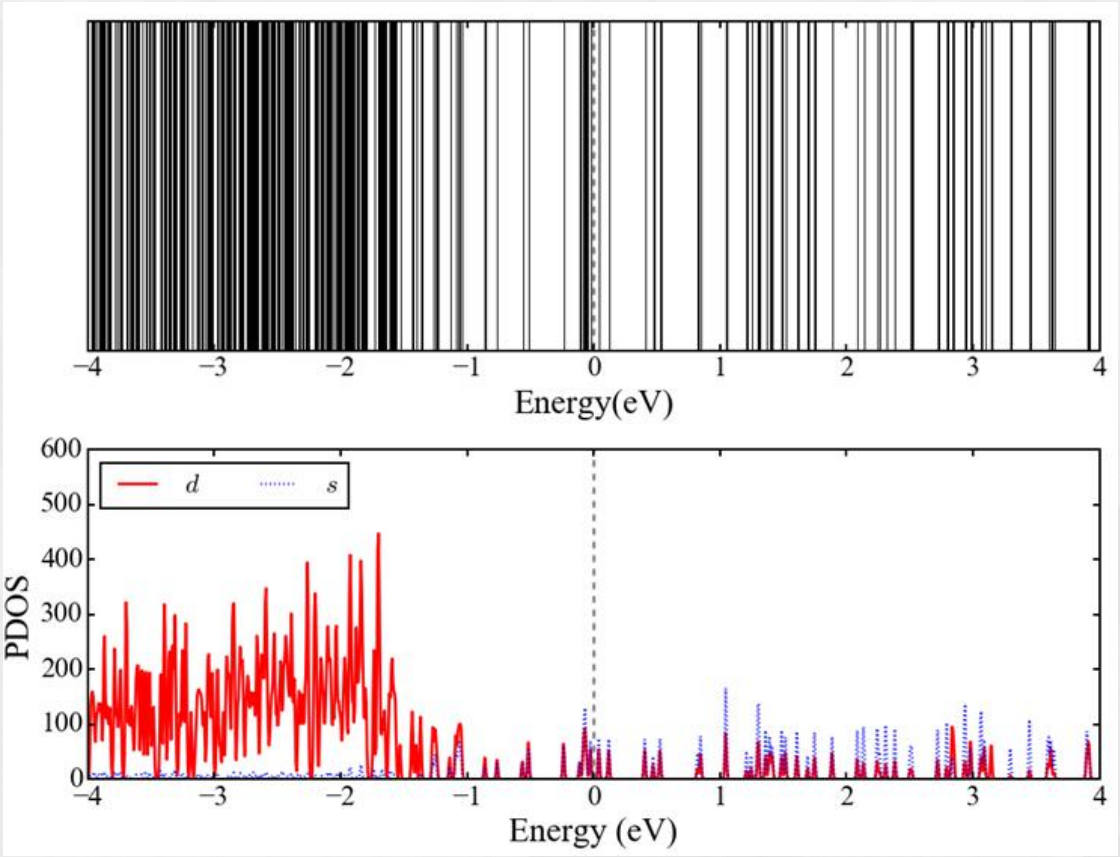

激光激发金团簇的电子激发模式

Au团簇的几何结构特点与吸收谱

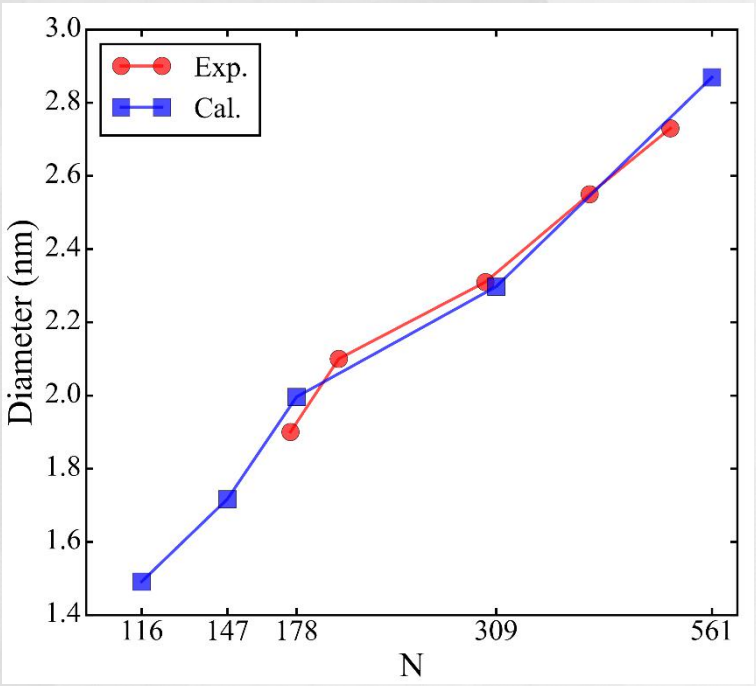

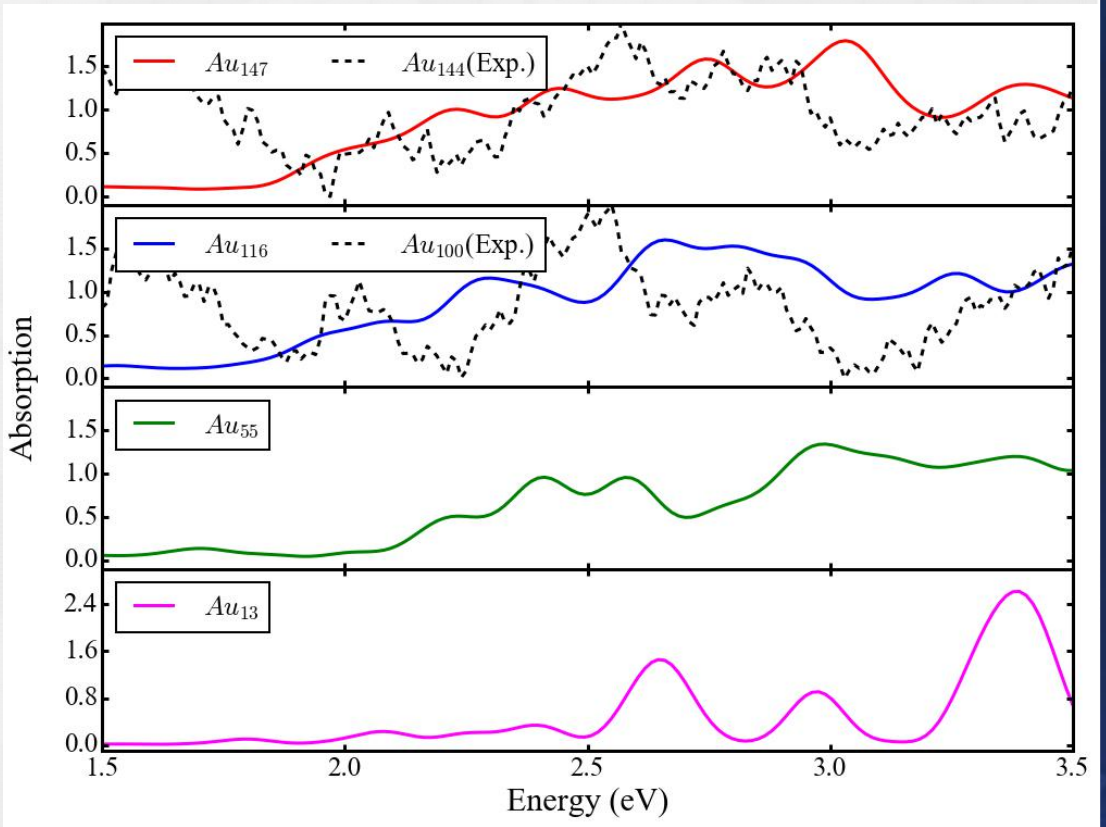

N	Bulk	561	309	147	55	13
d_{av}^{core}(Å)	2.935	2.910	2.900	2.894	2.863	2.831
d_{av}^{surf}(Å)	2.935	2.884	2.877	2.871	2.855	2.831

激光激发金团簇的电子激发模式

弱场下的电子电荷密度振荡

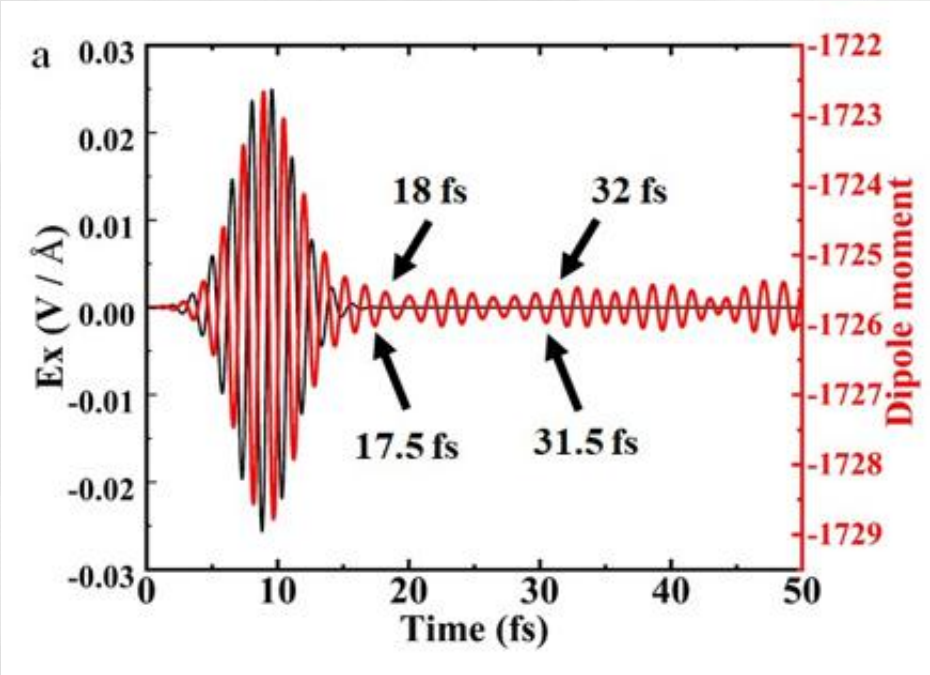

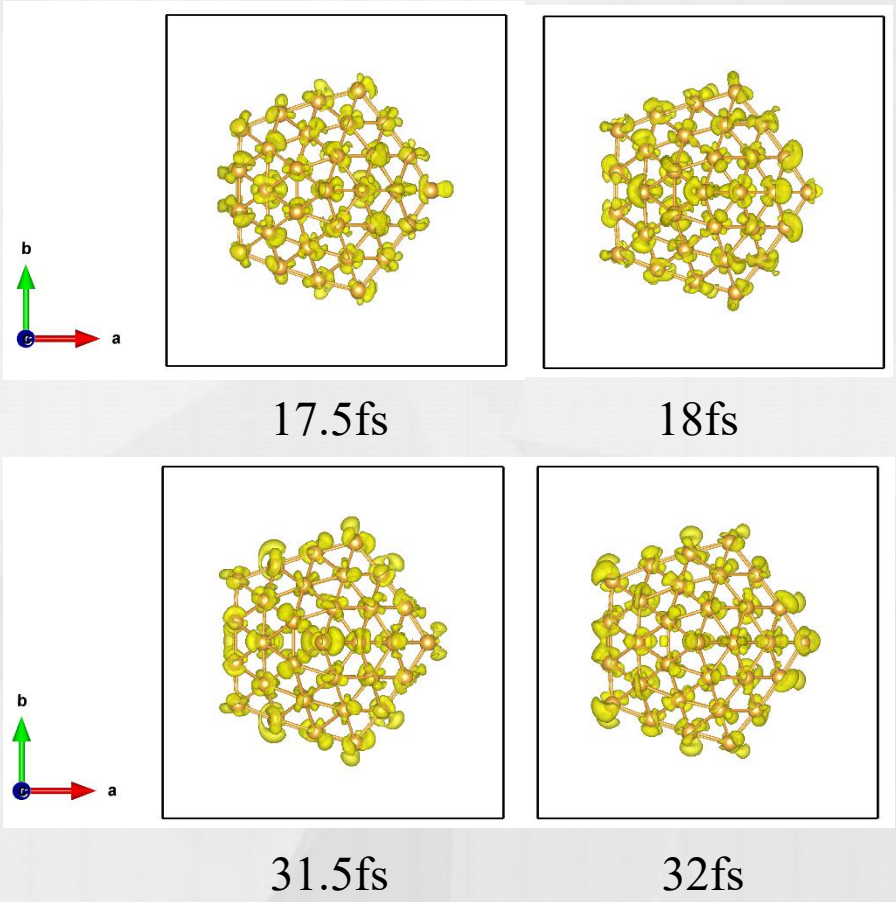

激光激发金团簇的电子激发模式

判断激发是单电子还是集体激发

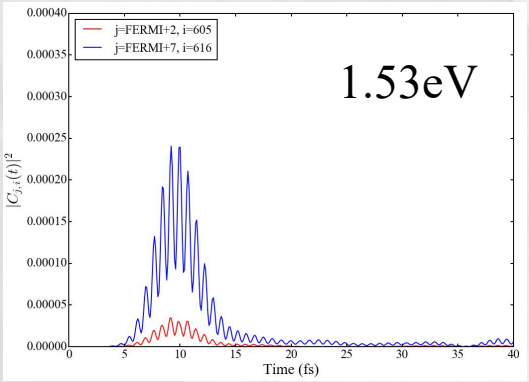

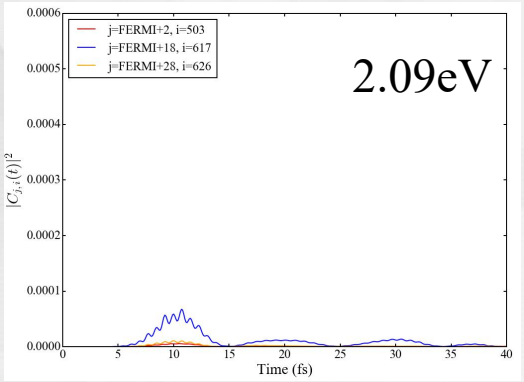

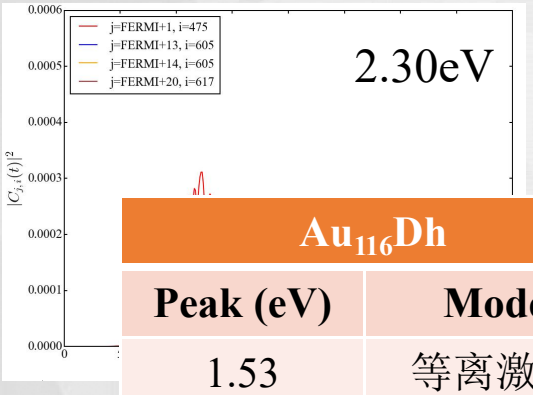

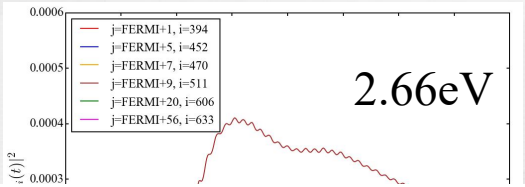

从电子占据来看，与之有关认定其为单电子能级模式。仅1.53eV呈现等离激元振荡的行为，其他类似单电子。

单电子能级引起的类plasmon

$Au_{116}Dh$		$Au_{55}Dh$		$Au_{13}Dh$	
Peak (eV)	Mode	Peak (eV)	Mode	Peak (eV)	Mode
1.53	等离激元	1.708	等离激元	1.791	等离激元
2.09	单电子激发	2.232	单电子激发	2.101	等离激元
2.30	单电子激发	2.411	单电子激发	2.384	等离激元
2.66	单电子激发	2.577	单电子激发	2.652	单电子激发
		2.990	单电子激发	2.976	单电子激发

激光激发金团簇的电子激发模式

场强增强引起Au团簇激发模式转变

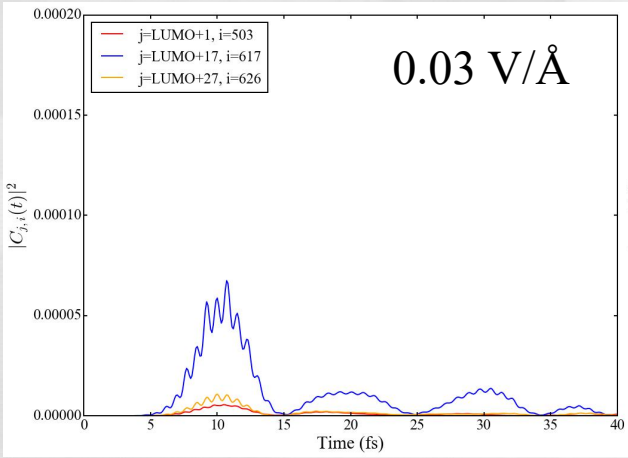

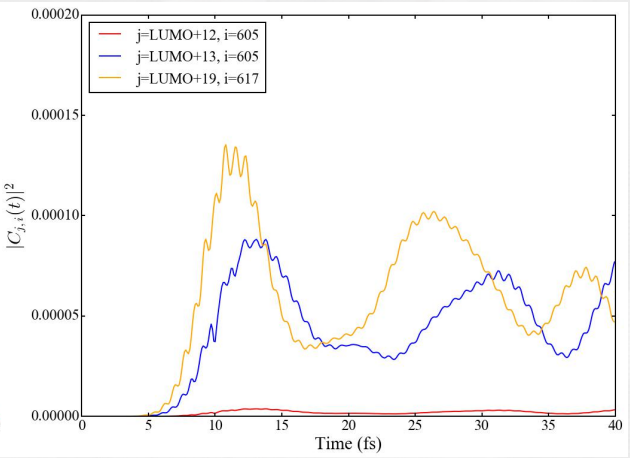

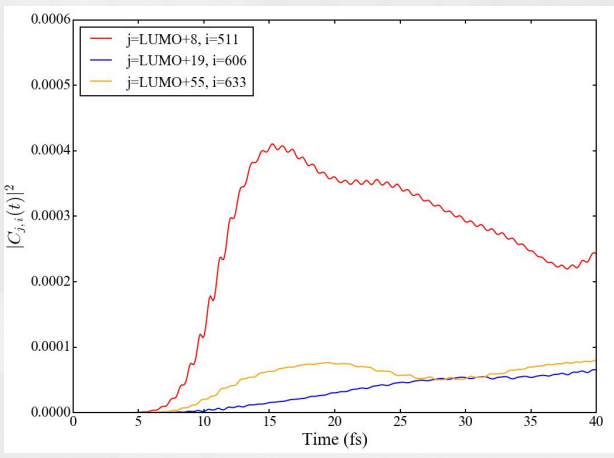

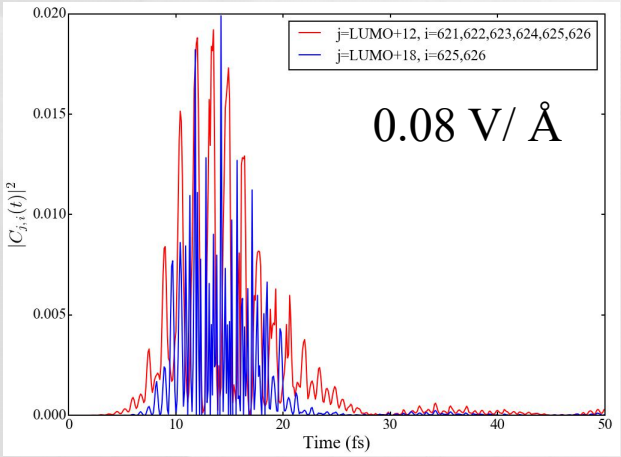

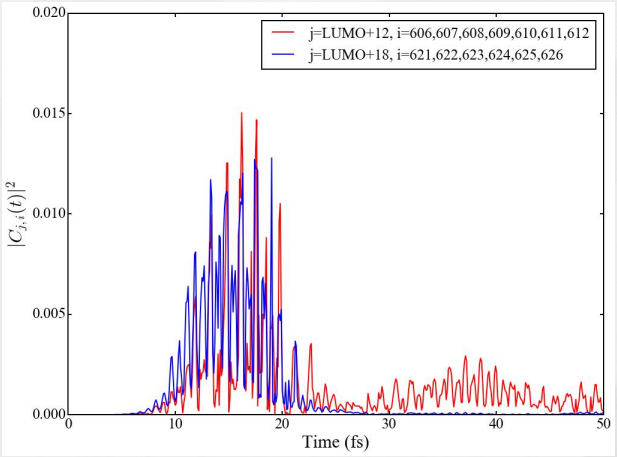

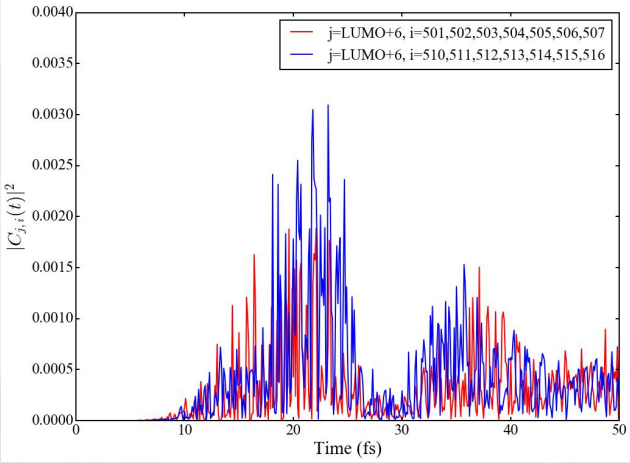

E_{abs}≈ 2.09eV

E_{abs}≈ 2.30eV

E_{abs}≈ 2.66eV

激光产生温稠密物质动态演化

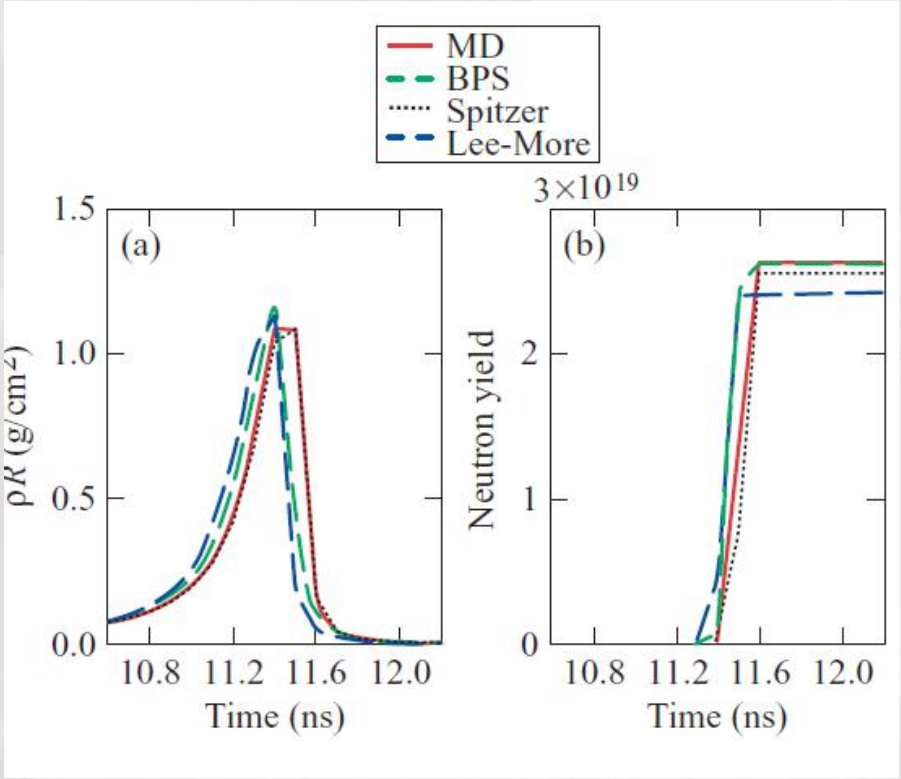

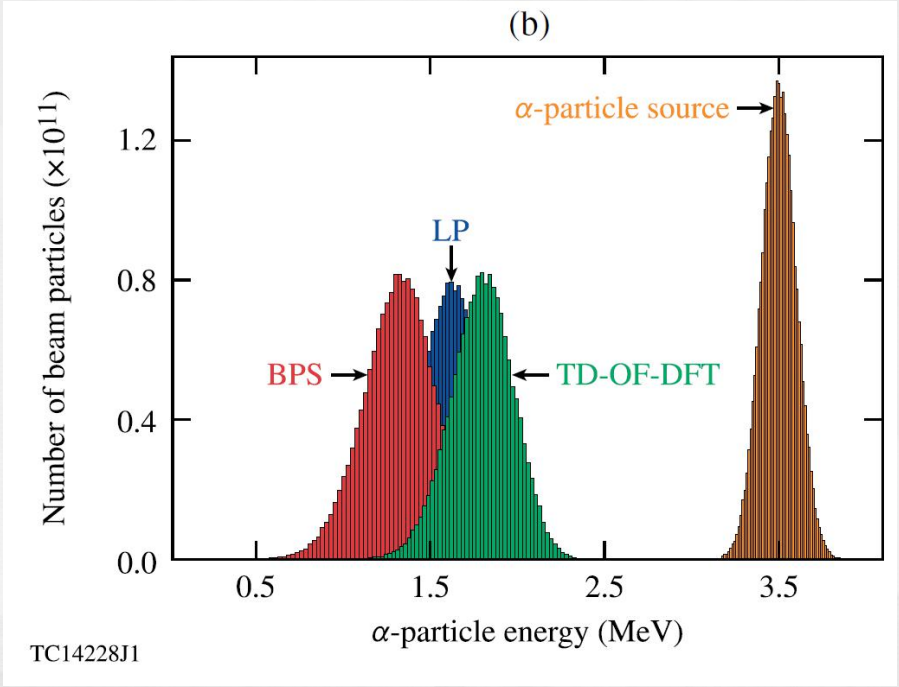

流体模拟表明，是否考虑电子动力学对激光和带电粒子能量沉积效率的影响达到50%

S. Hu, Phys. Rev. E 84, 016408 (2011)
Collins et al. Phys. Rev. Lett. 121, 145001 (2018)

激光激发金团簇的电子激发模式

场强增强会导致单电子激发转变为集体激发

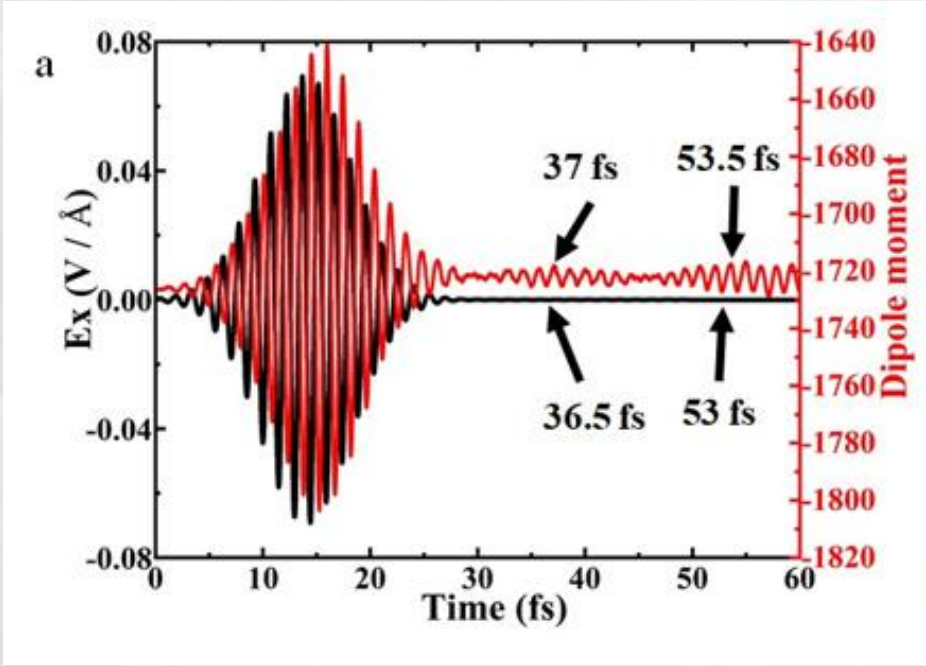

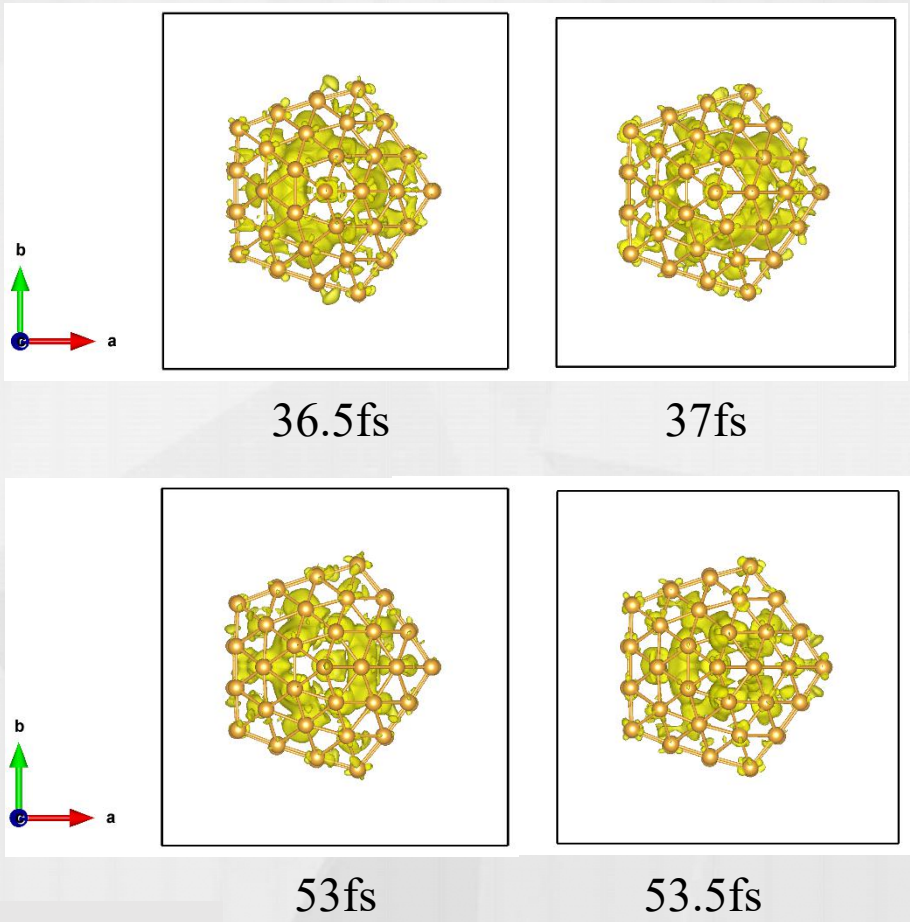

arXiv:2003.11191 (2020)

Accepted by National Science Review

激光产生温稠密物质动态演化

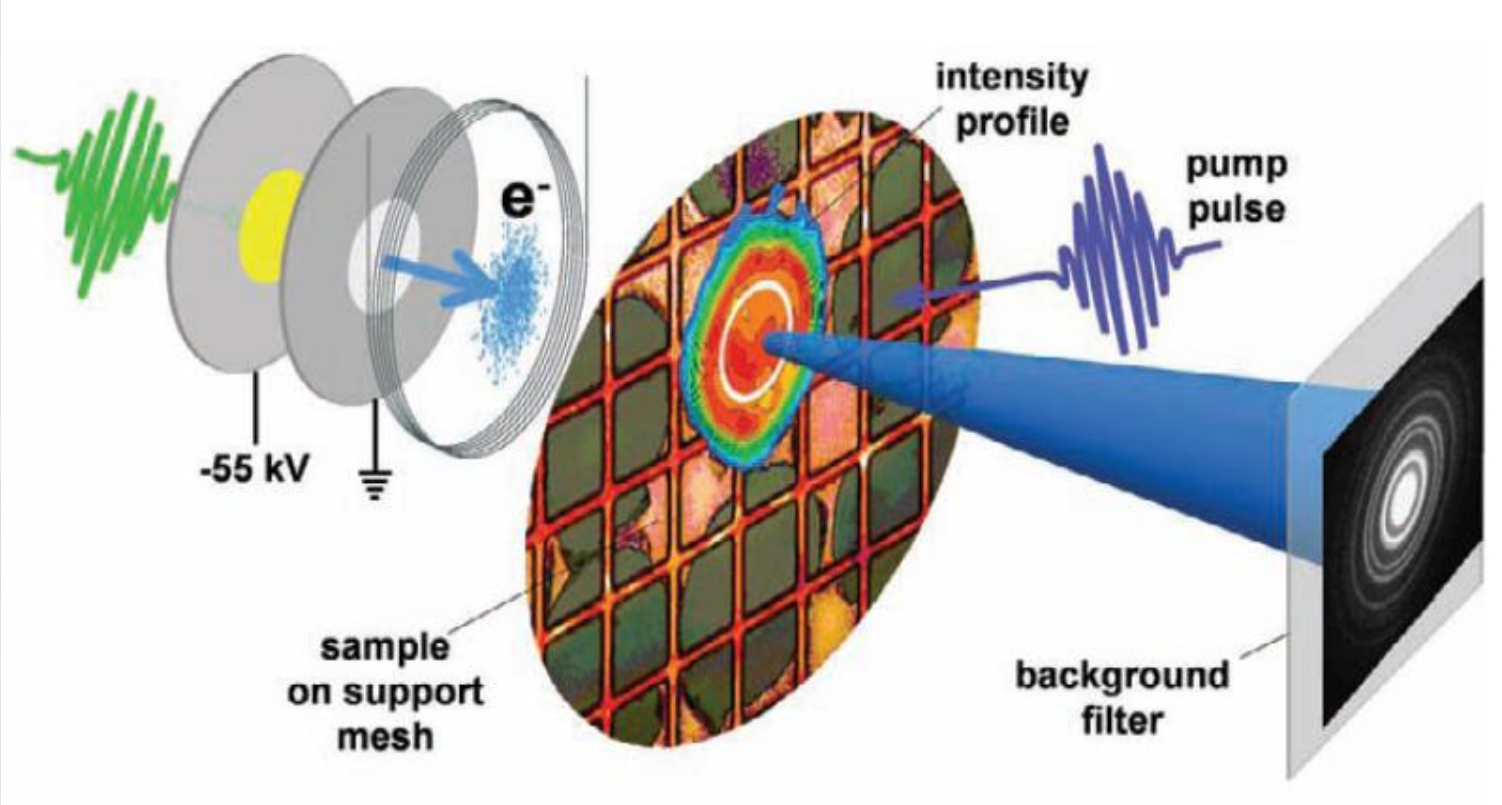

Laser induced the formation of warm dense matter:

Non-equilibrium process

Ultrafast dynamics

Ernstorfer et al. Science 323, 1033-1037 (2009)

康冬冬、戴佳钰*等. 强激光与粒子束 32: 092006 (2020)

Kinetics model：

Temperature relaxation rate: Laudau-Spitzer theory

$$\nu_{ei} = \frac{8\sqrt{2\pi} n_i e^4 Z^2}{3mM} \left(\frac{k_B T_e}{m} + \frac{k_B T_i}{M}\right)^{-3/2} ln\Lambda,$$

binary collisions, weakly coupled, dilute gases

Coulomb logarithm $ln\Lambda$

Lenard-Balescu (LB) (A. Lenard, Ann. Phys. (N.Y.) 10, 390 (1960).)

Brown, Preston, and Singleton (BPS) (L. S. Brown, D. L. Preston, and R. L. Singleton, Phys. Rev. E 86, 016406 (2012).)

Gericke, Murillo, and Schlanges (GMS) (D. O. Gericke, M. S. Murillo, and M. Schlanges, Phys. Rev. E 65, 036418 (2002).)

……

The general physics is to determine the cross sections

激光产生温稠密物质动态演化

Molecular dynamics can also simulate the cross section

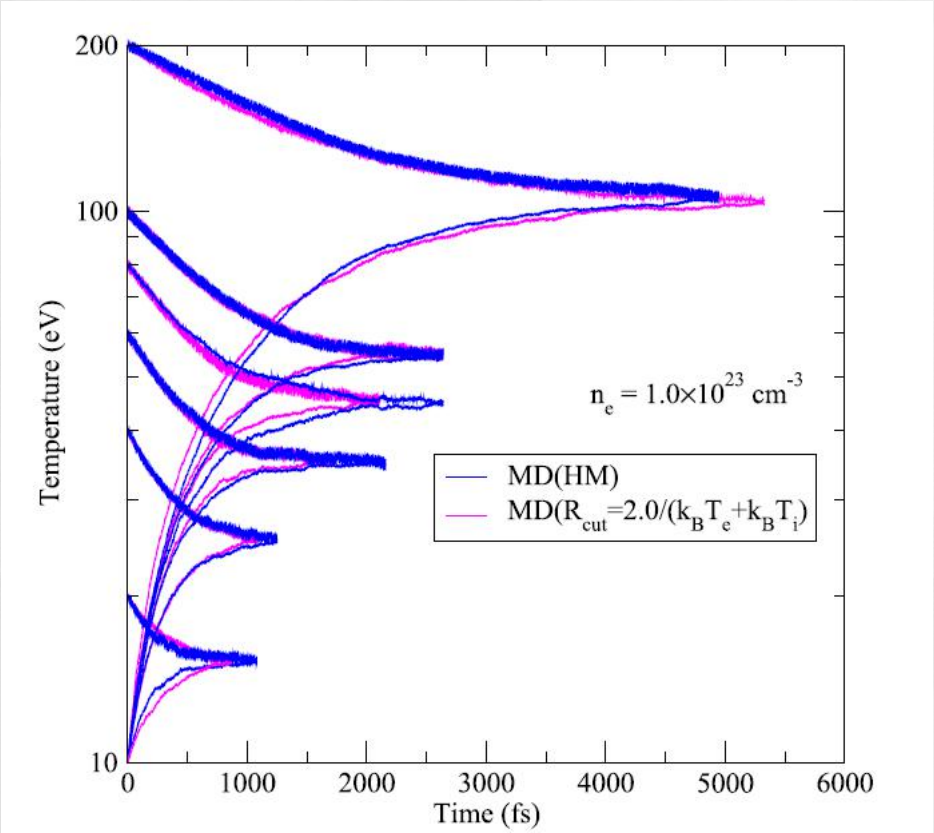

High Energy Density Physics 13 (2014) 34–39

Quantum statistical potential (QSP)

$$V_{ab}(r) = \frac{Z_a Z_b e^2}{r}\left[1 - \exp(-2\pi/\Lambda_{ab})\right] + k_B T \ln 2\exp\left(-4\pi r^2 \Big/ \left(\Lambda_{ab}^2 \ln 2\right)\right)\delta_{ae}\delta_{be}$$

Classical MD：

1. Ion is treated as positive point charge
2. Electron is treated as negative point charge

Difficulties：

1. How to describe ionization and recombination
2. Coulomb Catastrophe
3. Quantum Scattering/cross sections

Quantum dynamics

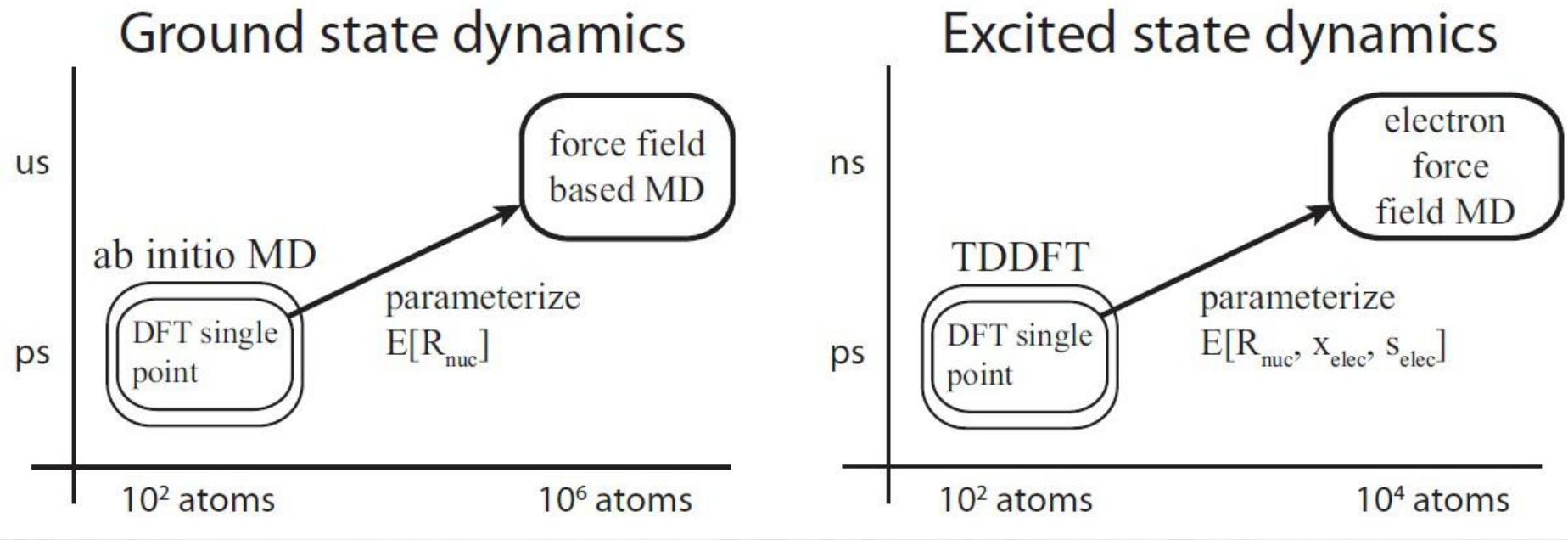

- **Non-Born-Oppenheimer**
- Real dynamics and Large-scale simulation

Electron force field (eFF) MD

Difficulties：

1. How to describe ionization and recombination
2. Coulomb Catastrophe
3. Quantum Scattering/cross sections

激光产生温稠密物质动态演化

eFF can be viewed as an development of wave packet molecular dynamics considering electronic quantum effects and can describe non-adiabatic dynamics.

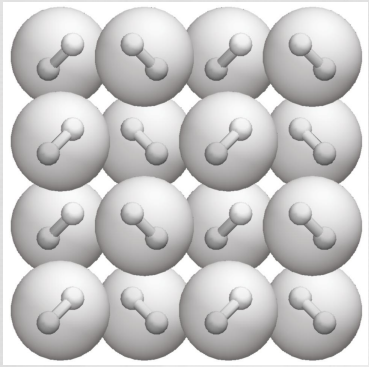

Assumption:

- Electrons are treated as Gaussian wave packets
- Ions are treated as charged points
- **The collisions between electrons and ions are included naturelly**

Gaussian wave packets: $\psi(\vec{r}) = (\frac{2}{\pi s^2})^{3/4} \exp[-(\frac{1}{s^2} - \frac{2p_s}{s}\frac{i}{\hbar})(\vec{r}-\vec{x})^2]\exp[\frac{i}{\hbar}\vec{p}_x \cdot \vec{r}]$

Equation of motion:

$$\dot{\vec{p}}_x = -\nabla_x V \qquad \dot{\vec{x}} = \dot{\vec{p}}_x / m_e$$

$$\dot{p}_s = -\partial V / \partial s \qquad \dot{s} = (3m_e / 4)^{-1} p_s$$

$$\dot{\vec{p}}_R = -\nabla_R V \qquad \dot{\vec{R}} = \vec{p}_R / m_{nuc}$$

Electron Force Field method

Energy：

$$E = E_{eke} + E_{nuc\cdot nuc} + E_{nuc\cdot elec} + E_{elec\cdot elec} + E_{Pauli}$$
$$+ \sum_i \frac{1}{2} m_e \left|\dot{x}_i\right|^2 + \frac{1}{2}\left(\frac{3}{4} m_e\right)\dot{s}_i^{\,2} + \sum_j \frac{1}{2} m_{ion} \left|\dot{x}_j\right|^2$$

In which：

$$E_{ke} = \sum_i \int \psi_i^* \left(-\frac{\hbar^2}{2m_e}\Delta\right)\psi_i dV = \sum_i \frac{\hbar^2}{m_e}\frac{3}{2}\frac{1}{s_i^{\,2}}$$

$$E_{nuc\cdot nuc} = \frac{1}{4\pi\varepsilon_0}\sum_{i<j}\frac{Z_i Z_j}{R_{ij}}$$

$$E_{nuc\cdot elec} = -\sum_{i,j} Z_i \int \frac{\left|\psi_j\right|^2}{R_{ij}} dV = -\frac{1}{4\pi\varepsilon_0}\sum_{i,j}\frac{Z_i}{R_{ij}}\,\mathrm{Erf}\left(\frac{\sqrt{2}R_{ij}}{s_i}\right)$$

$$E_{elec\cdot elec} = \sum_{i<j}\int \frac{\left|\psi_i\right|^2\left|\psi_j\right|^2}{x_{ij}} dV = \frac{1}{4\pi\varepsilon_0}\sum_{i<j}\frac{1}{x_{ij}}\,\mathrm{Erf}\left(\frac{\sqrt{2}x_{ij}}{\sqrt{s_i^2 + s_j^2}}\right)$$

$$E_{Pauli} = \sum_{\sigma_i=\sigma_j} E\left(\uparrow\uparrow\right)_{ij} + \sum_{\sigma_i\neq\sigma_j} E\left(\uparrow\downarrow\right)_{ij}$$

Electron Force Field method

$$E_{Pauli} = \sum_{\sigma_i=\sigma_j} E(\uparrow\uparrow)_{ij} + \sum_{\sigma_i\neq\sigma_j} E(\uparrow\downarrow)_{ij}$$

$$\Psi_{Slater} = \frac{1}{\sqrt{2-2S^2}}(\phi_1(r_1)\phi_2(r_2) - \phi_2(r_1)\phi_1(r_2))$$

$$\Psi_{Hartree} = \phi_1(r_1)\phi_2(r_2)$$

$$E_u = \langle \Psi_{Slater} | -\frac{1}{2}\nabla^2 | \Psi_{Slater} \rangle - \langle \Psi_{\text{Hartree}} | -\frac{1}{2}\nabla^2 | \Psi_{\text{Hartree}} \rangle$$

$$= \frac{S^2}{1-S^2}(t_{11} + t_{12} - \frac{2t_{12}}{S})$$

$$\Psi_{\text{VB}} = \frac{1}{\sqrt{2+2S^2}}(\phi_1(r_1)\phi_2(r_2) + \phi_2(r_1)\phi_1(r_2))$$

$$\Psi_{Hartree} = \phi_1(r_1)\phi_2(r_2)$$

$$E_g = \langle \Psi_{\text{VB}} | -\frac{1}{2}\nabla^2 | \Psi_{\text{VB}} \rangle - \langle \Psi_{\text{Hartree}} | -\frac{1}{2}\nabla^2 | \Psi_{\text{Hartree}} \rangle$$

$$= \frac{S^2}{1+S^2}(t_{11} + t_{12} - \frac{2t_{12}}{S})$$

$$E(\uparrow\uparrow) = E_u - (1+\rho)E_g$$

$$E(\uparrow\downarrow) = \rho E_g$$

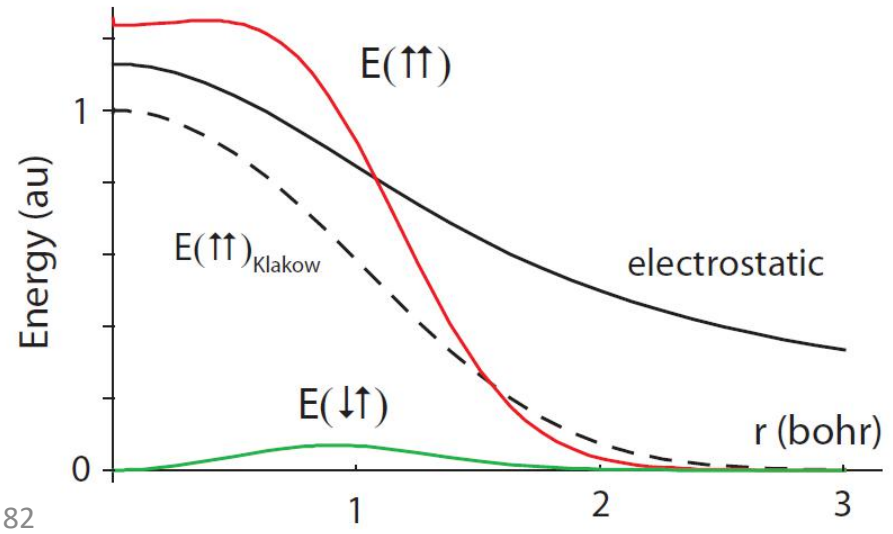

激光产生温稠密物质动态演化

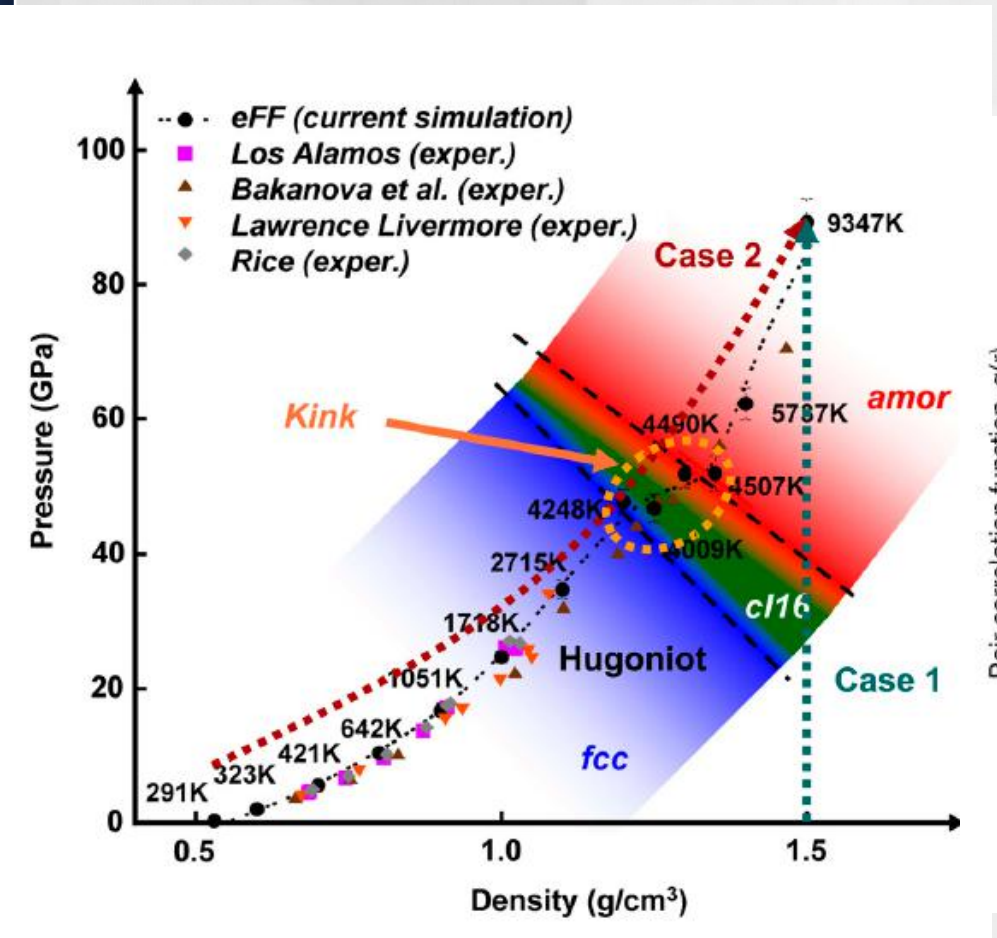

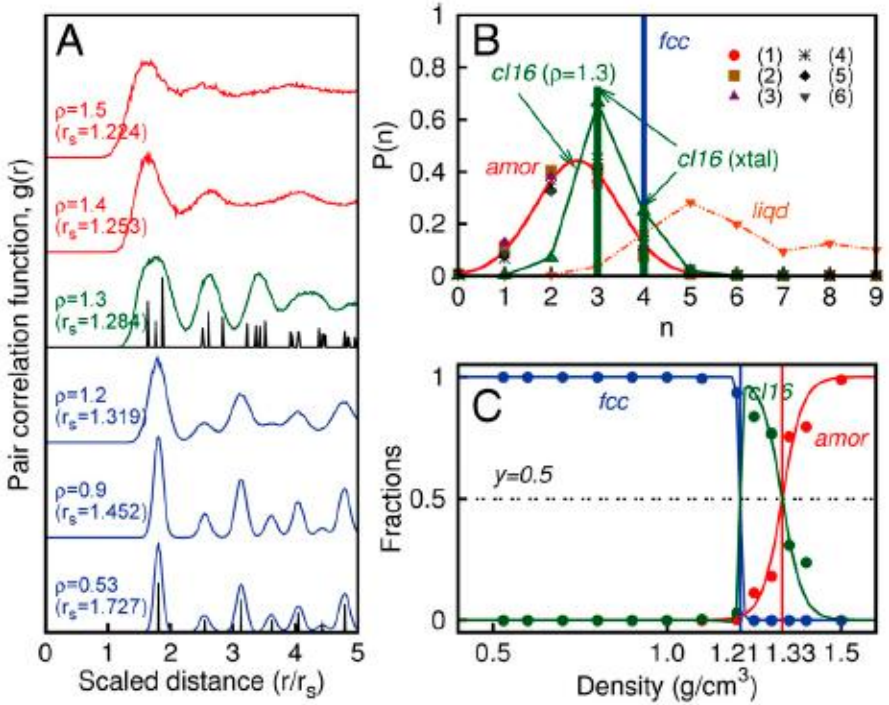

PNAS(2010)

激光产生温稠密物质动态演化

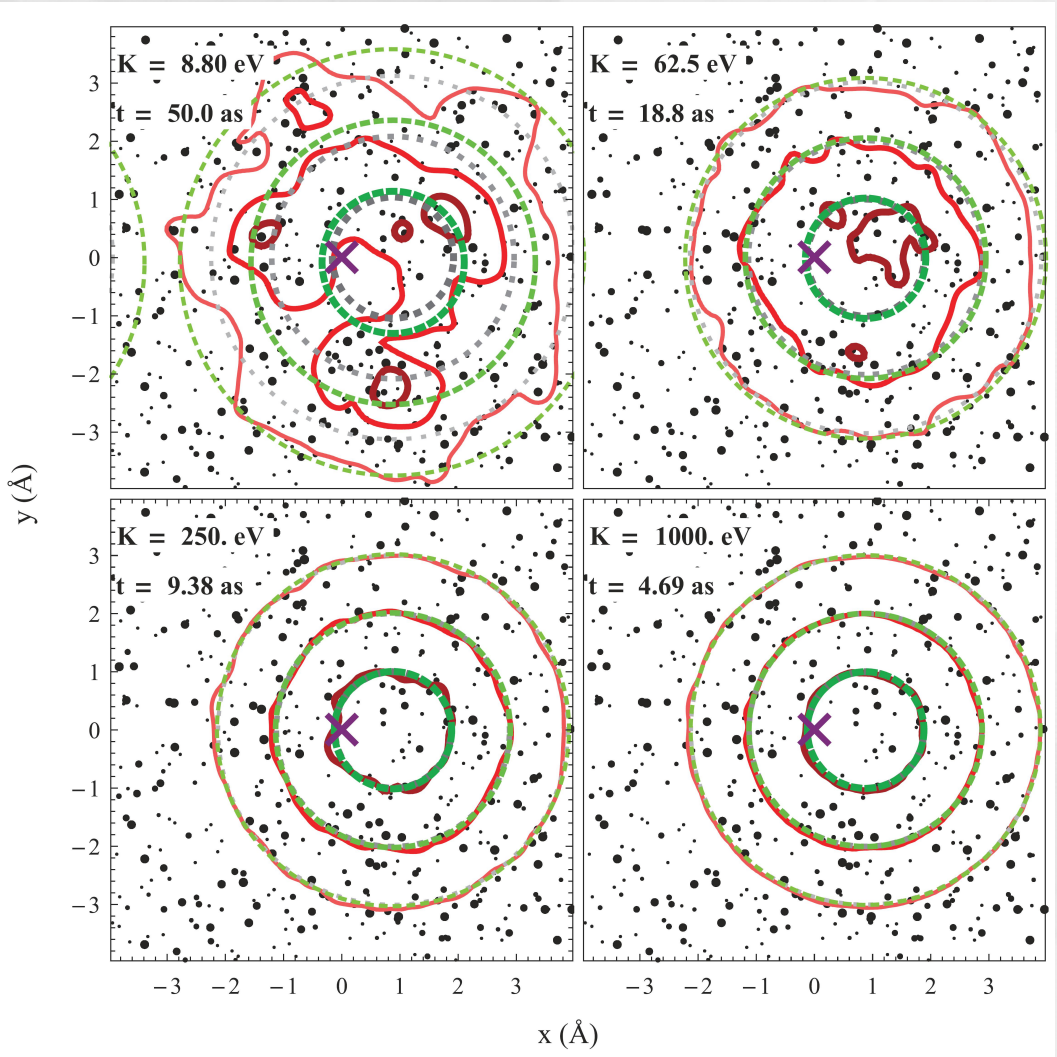

温度越高波包越弥散

?

温度越高电子分布越局域

Grabowski et al. Phys. Rev. E 87, 063104 (2013)

Ma and Dai et al. Phys. Plasma. 25, 012707 (2018)*

激光产生温稠密物质动态演化

Improved eFF with a boundary limitation at high temperature : Constrianed eFF (CEFF)

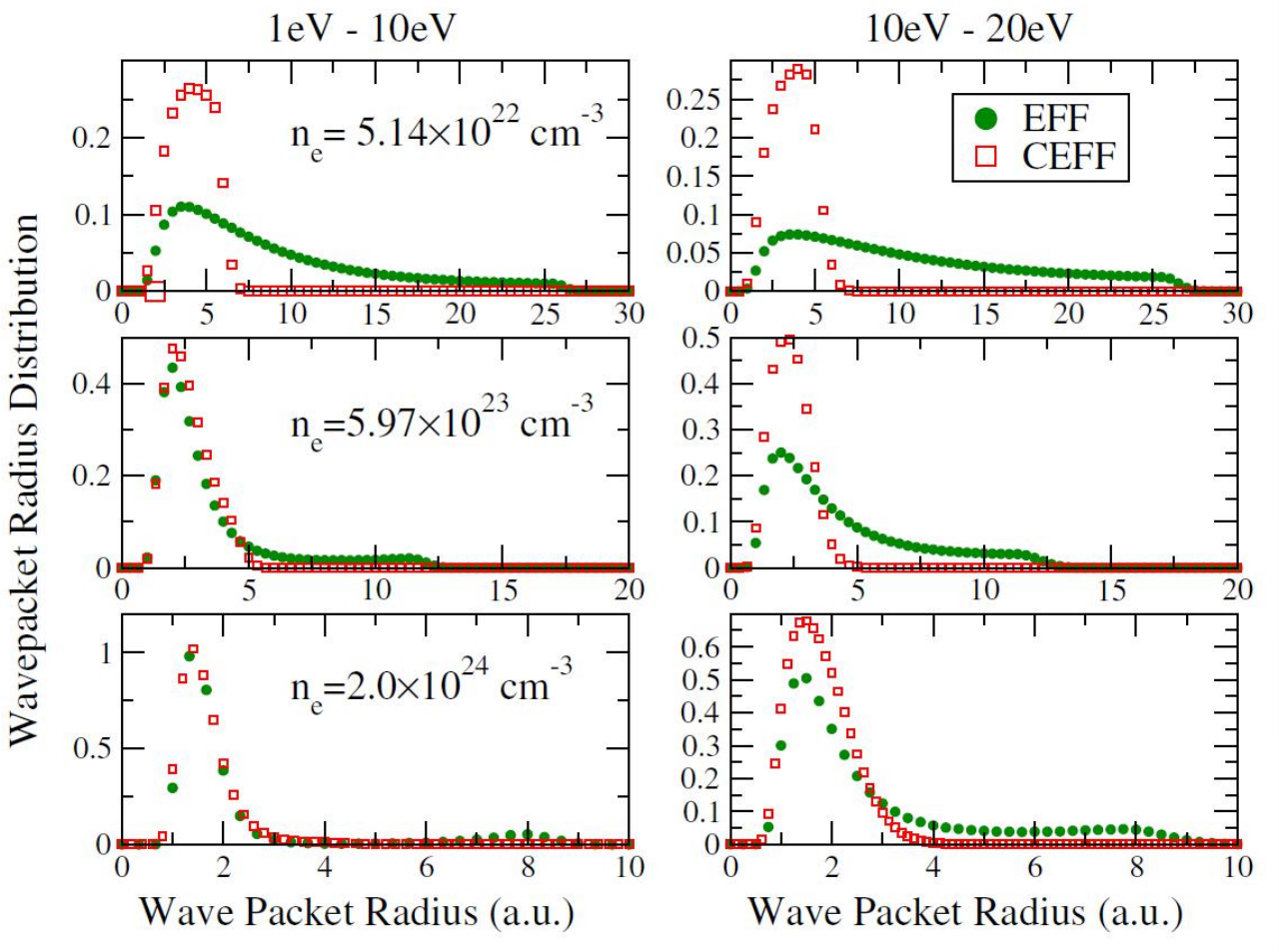

Boundary of the wavepackets= $\sqrt{k_B T_e / 4\pi e^2 n_e}$ + $Ze^2/k_B T_e$

Screening effect

R_c classical distance

激光产生温稠密物质动态演化

Relaxation time:
HM: 757 fs
eFF: 2041 fs

Relaxation time:
HM: 212 fs
eFF: 597 fs

Relaxation time:
HM: 132 fs
eFF: 403 fs

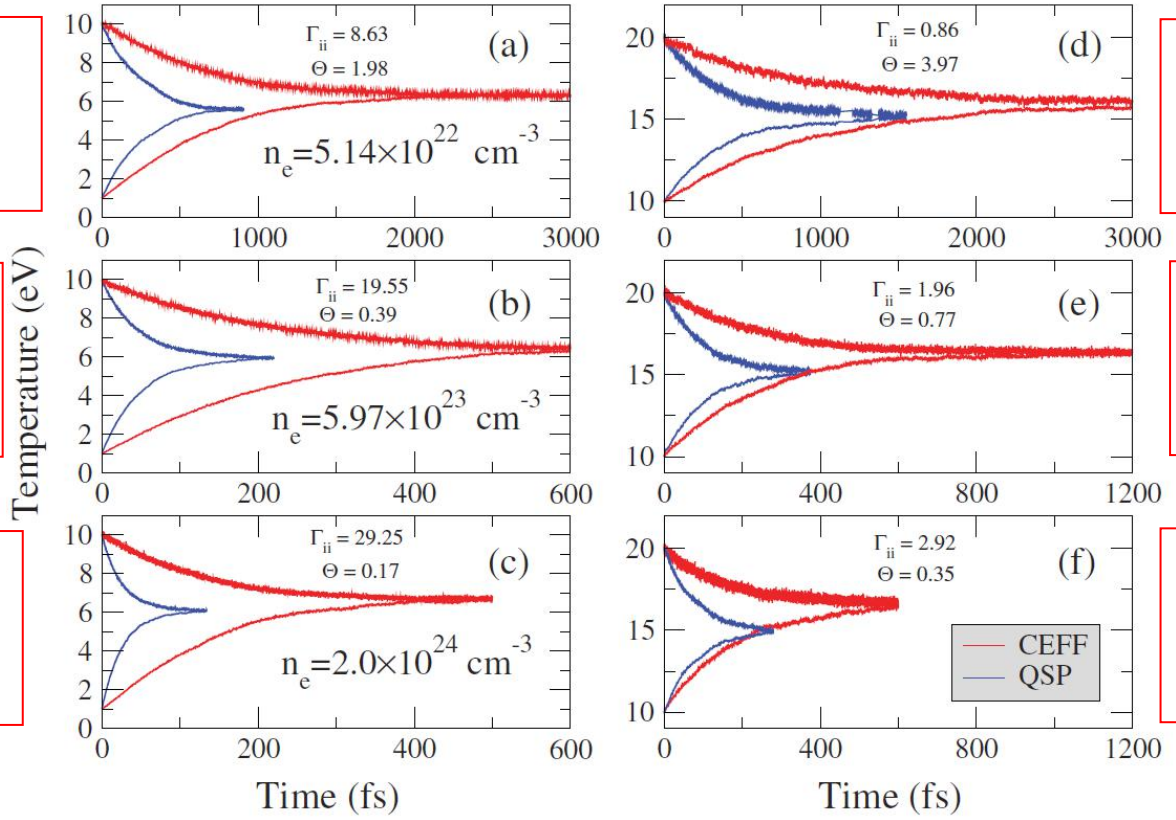

Relaxation time:
HM: 1522 fs
eFF: 3071 fs

Relaxation time:
HM: 366 fs
eFF: 845 fs

Relaxation time:
HM: 248 fs
eFF: 591 fs

CEFF results are in good agreement with the recent results of LCLS experiments at Stanford.

进一步的流体计算表明，激光效率沉积将差别200%以上

激光产生温稠密物质动态演化

◆ Coulomb logarithm

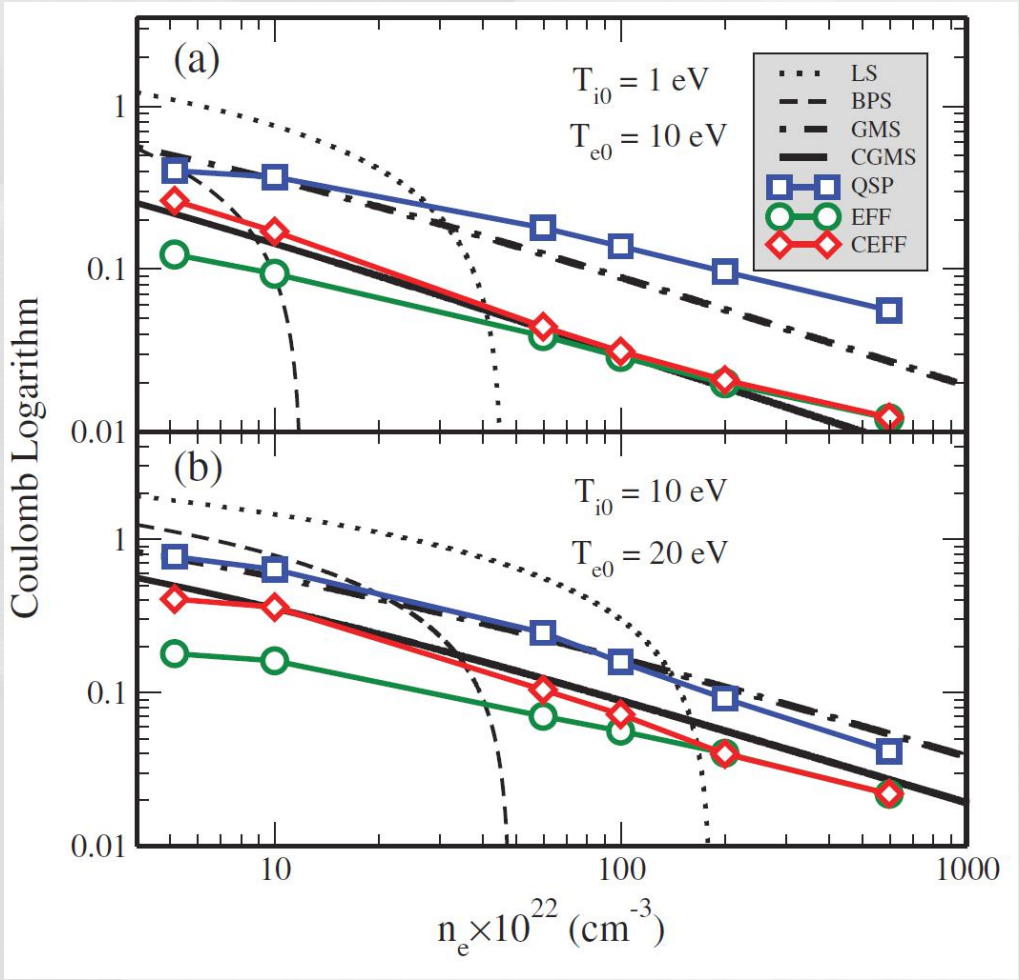

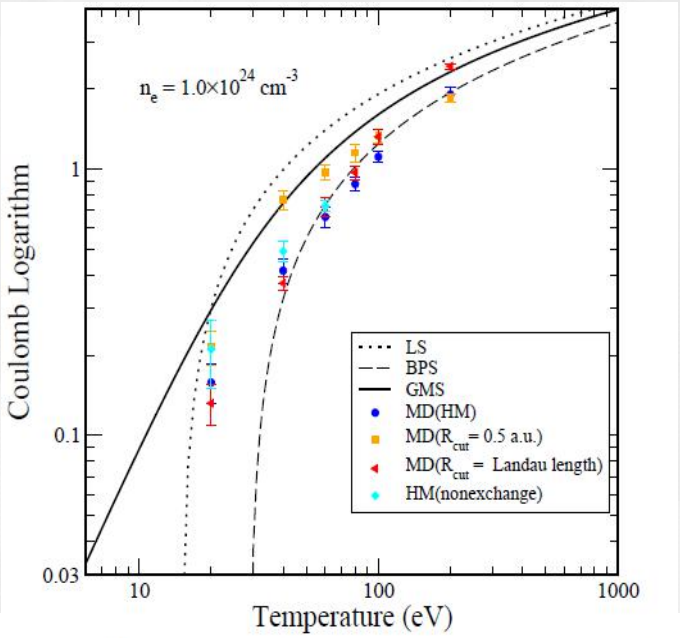

$$L_{GMS} = \frac{1}{2} ln(1 + [\lambda_D^2 + R_i^2]/[\Lambda^2/8\pi + b_c^2])$$

$$b_c = Ze^2 / k_B T_e$$

Coupled GMS (CGMS)

$$b_c = 2Ze^2 / (k_B T_e + k_B T_i)$$

Ma, Dai, Zhao* and Yuan. Phys. Rev. Lett. 122: 015001 (2019)*

Zeng and Dai. Sci. China Phys. Mech. Astron. 63, 263011 (2020)*

87

Carbon allotropes: Graphite and diamond

- Thermodynamics: graphite is stable and diamond is metastable
- This is a very high energy barrier between them ~3.5 eV

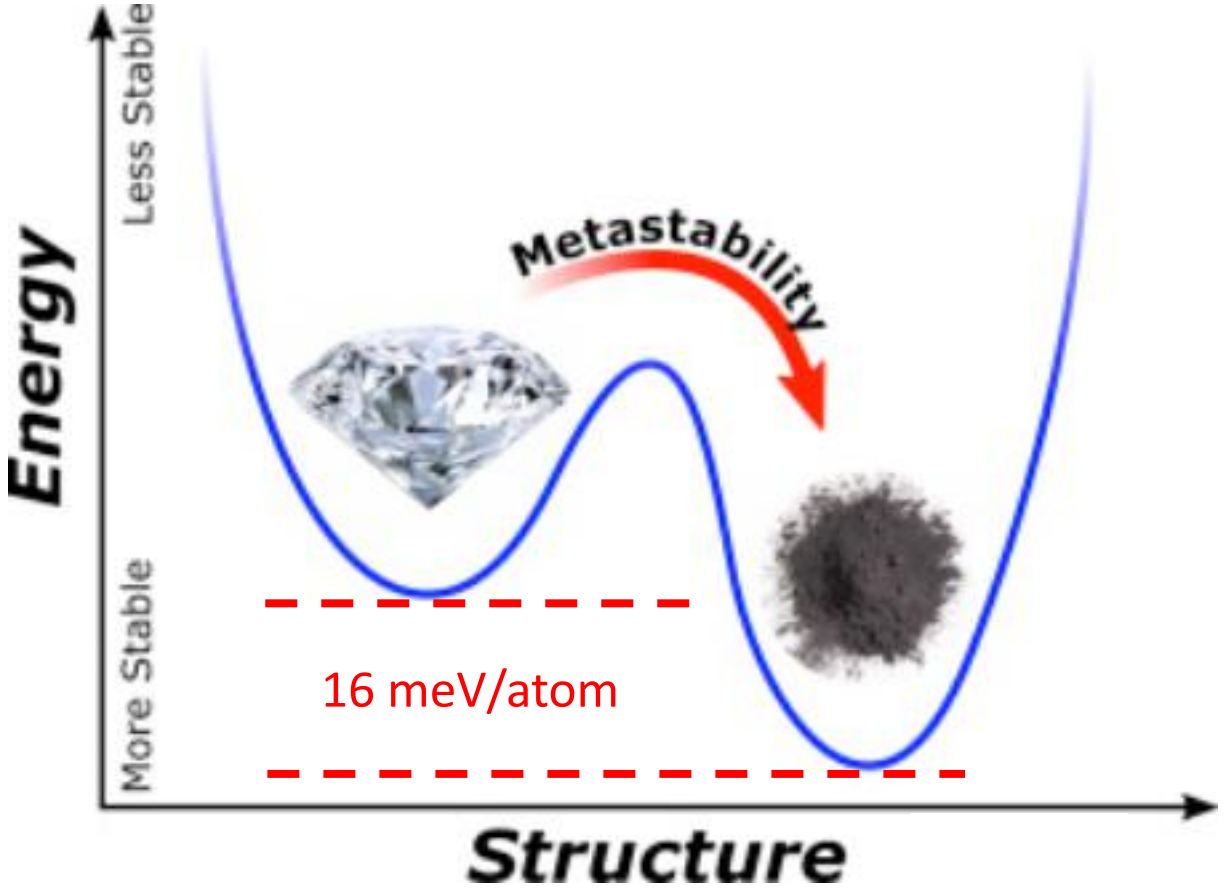

Solid-to-solid structural phase transition

- It requires ultra high pressure (~50 GPa) and temperature (~3000 K) to turn graphite into diamond
- Diamond can transforms to graphite by heating it up to 1500 K

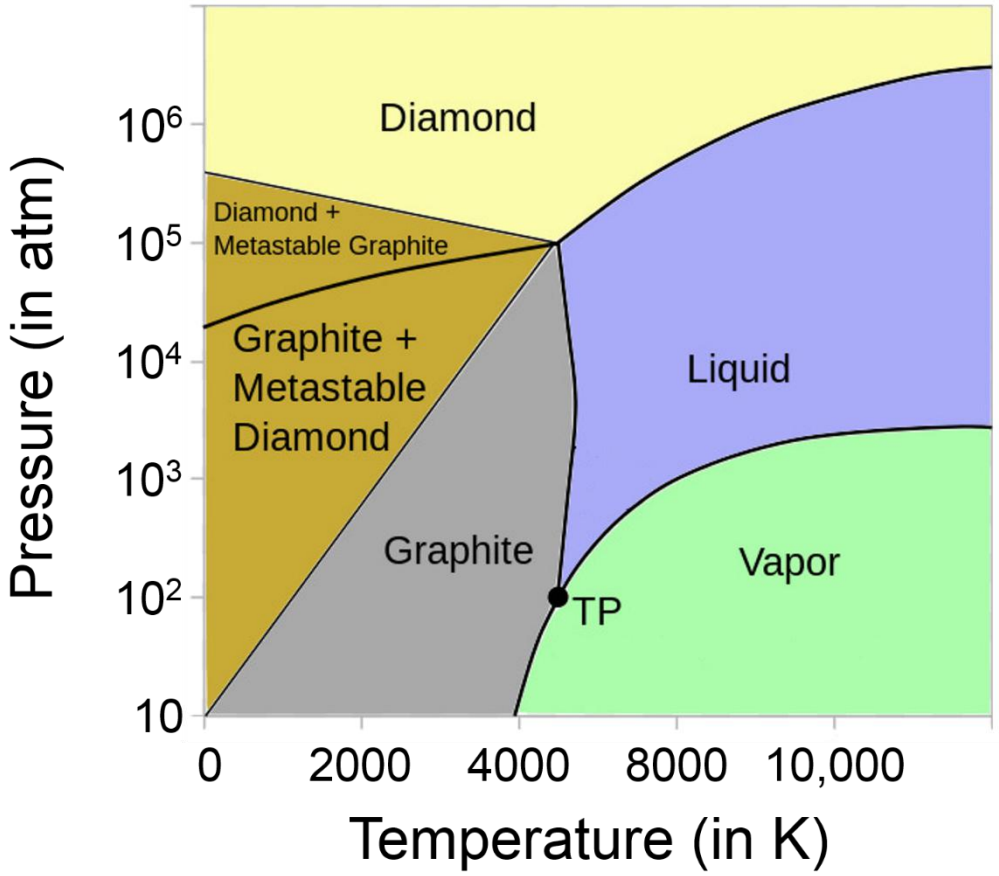

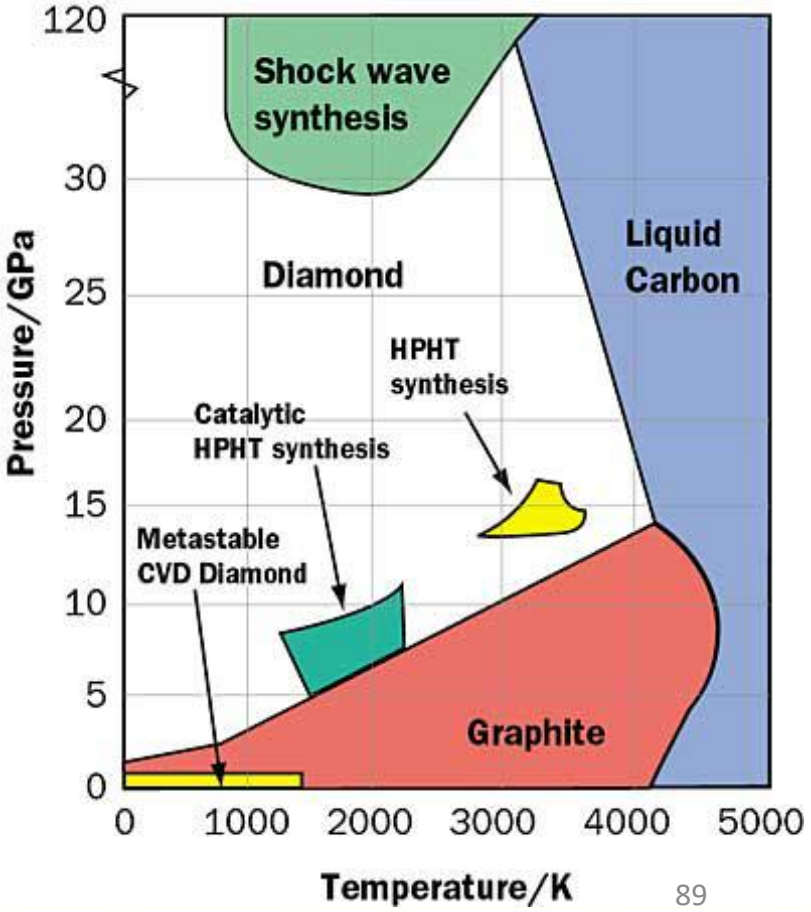

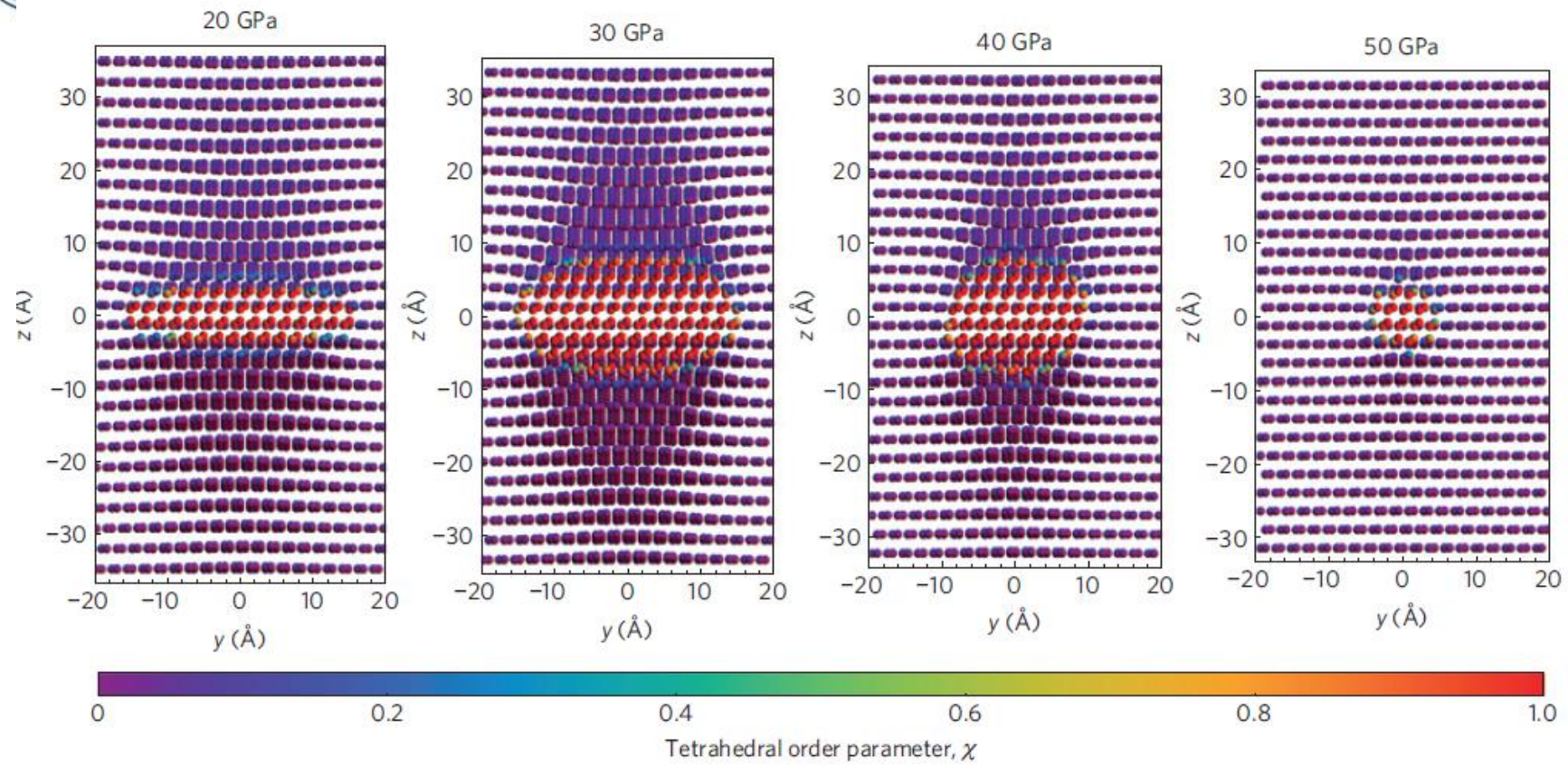

Nucleation mechanism for the direct graphite-to-diamond phase transition

nature materials

Graphene: a new paradigm in quantum materials

"Schrödinger fermions"

Electron metal

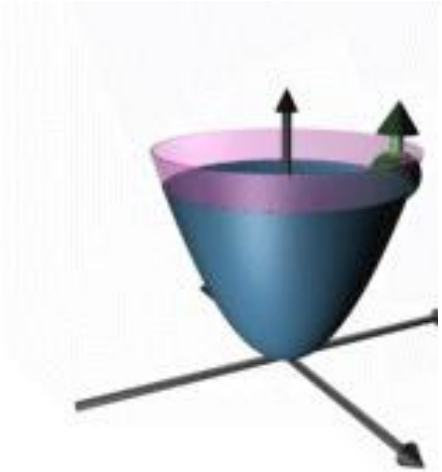

Hole metal

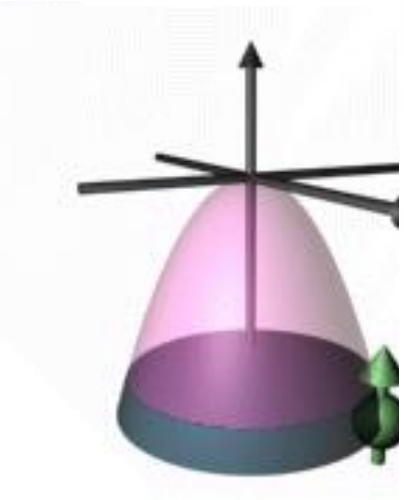

$$\hat{H} = \hat{p}^2/2m^*$$

massless Dirac fermions

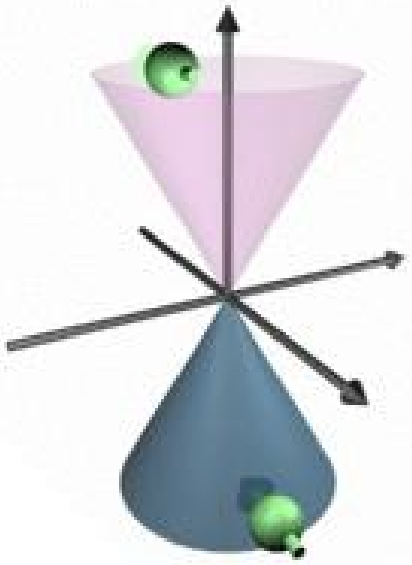

$$\hat{H} = v_F \vec{\sigma} \cdot \hat{p}$$

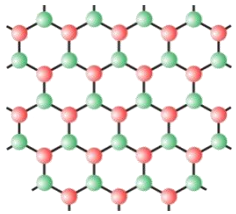

monolayer graphene

massive chiral fermions

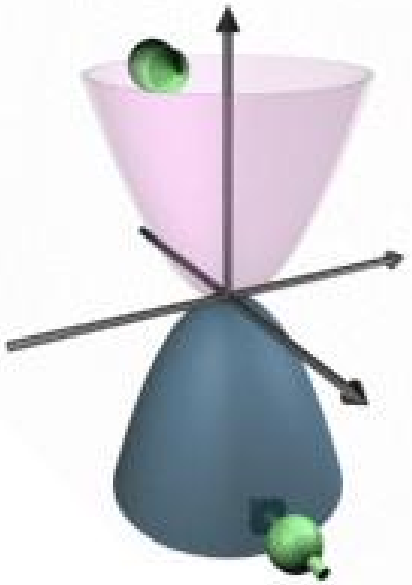

$$\hat{H} = \vec{\sigma} \cdot \hat{p}^2/2m^*$$

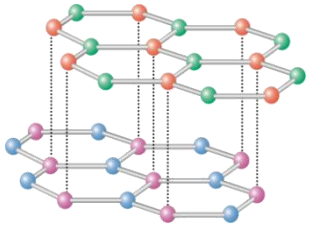

bilayer graphene

Trilayer graphene: ABA and ABC stacking

- TLG has two stable structures: ABA Bernal & ABC rhombohedral
- Only a hexagon slip in the most top graphene layer
- ABA is a semimetal, while ABC a gate-tunable semiconductor

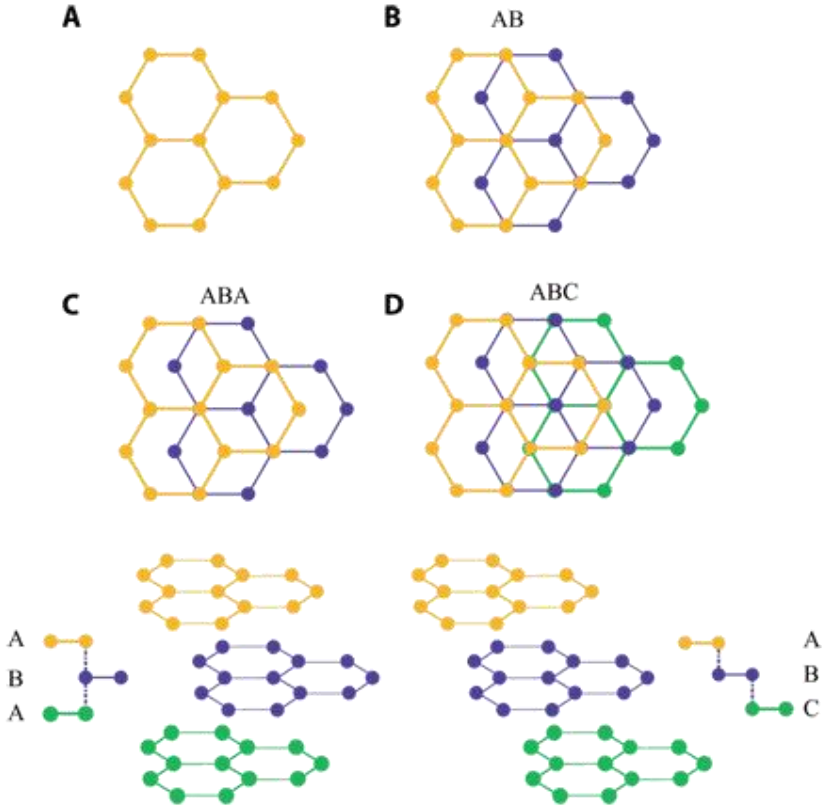

Y. Shan et al, *Science Advances* (2018)

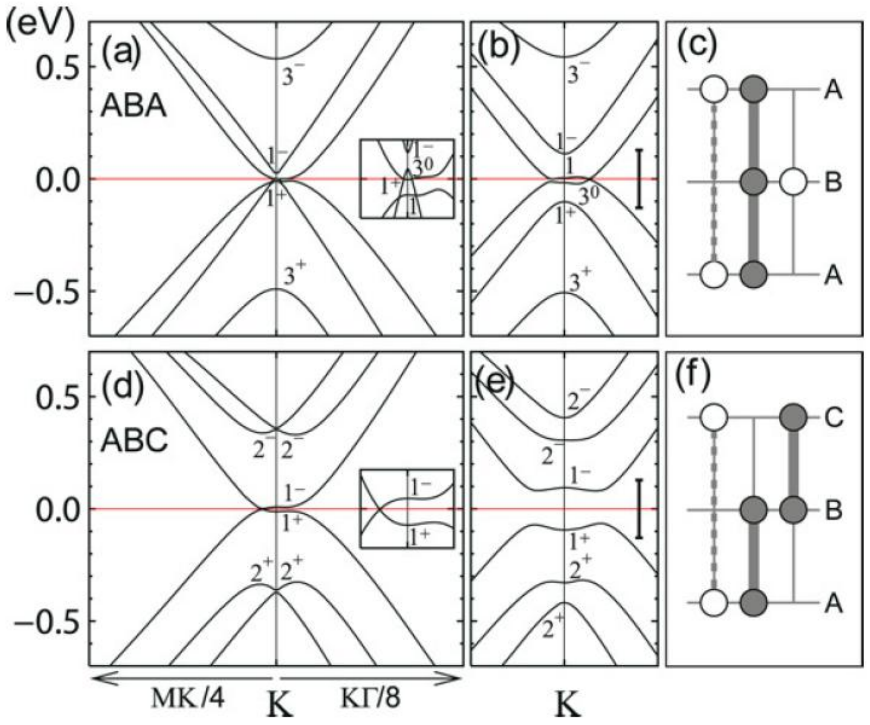

M. Aoki . *Solid state communications* (2007)

激光诱导物质结构相变

- Ultrafast pulse laser also can trigger the structure transition
- Thermal mechanism: equilibrium, slow, irreversible…
- Pump mechanism: non-equilibrium, fast, reversible…

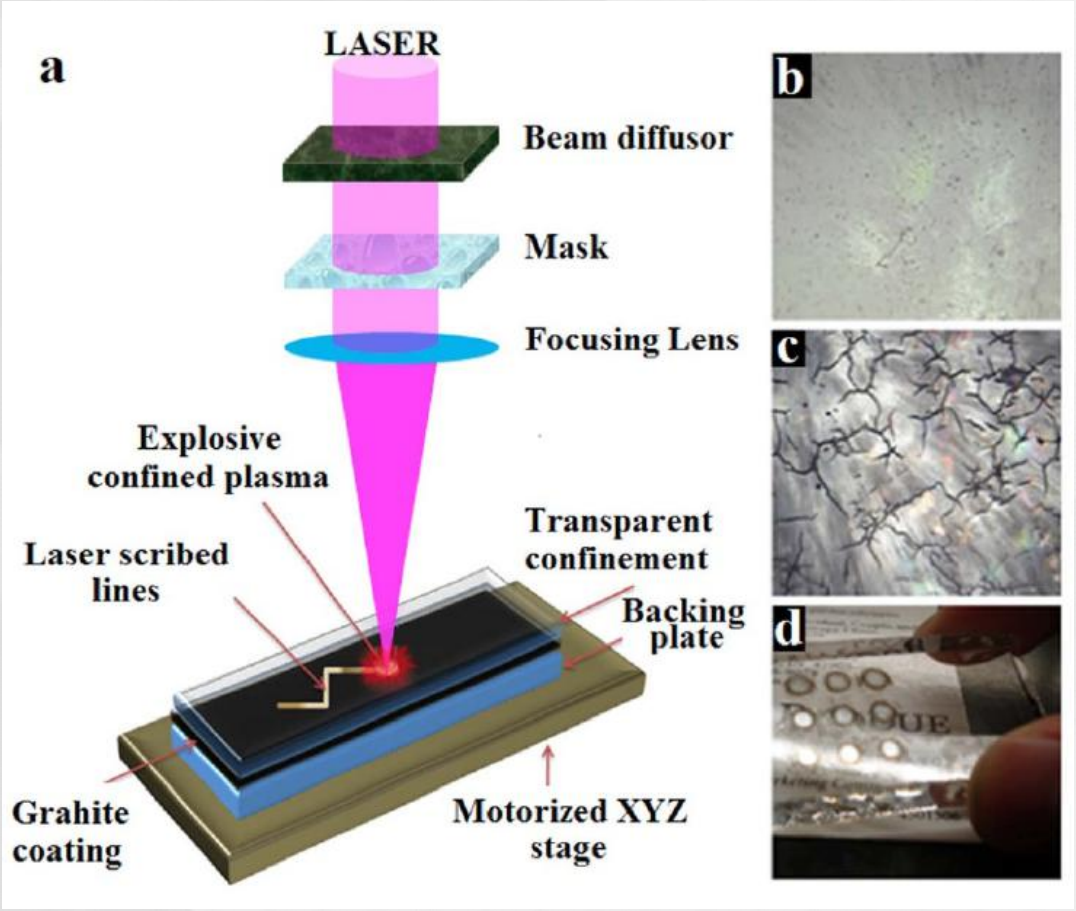

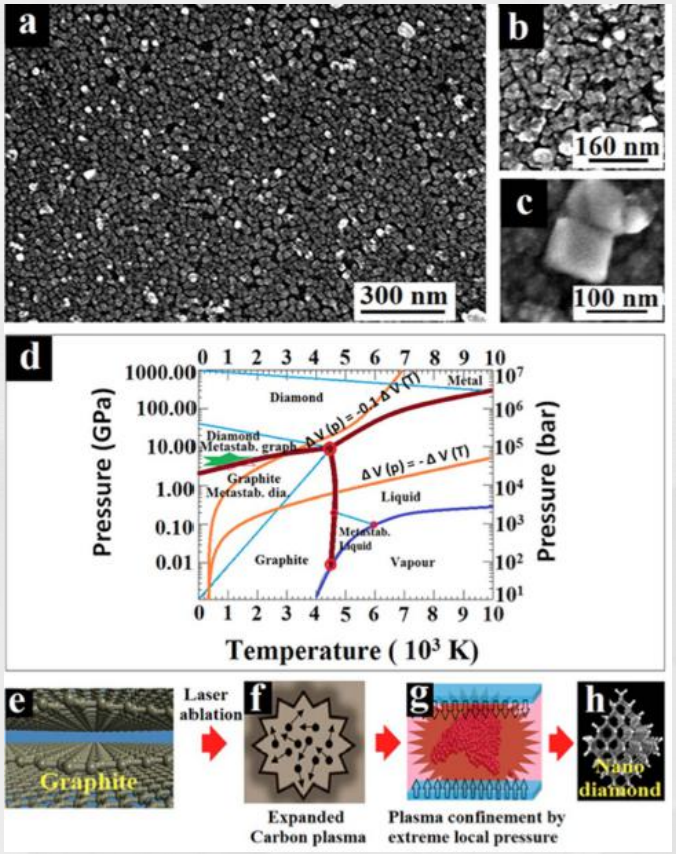

Nian et al, *Scientific reports* (2014)

激光诱导物质结构相变

- Thermodynamics: ABC is metastable compared with ABA
- Light-induced ABC to ABA transformation
- Energy difference is determined by experiments and calculations

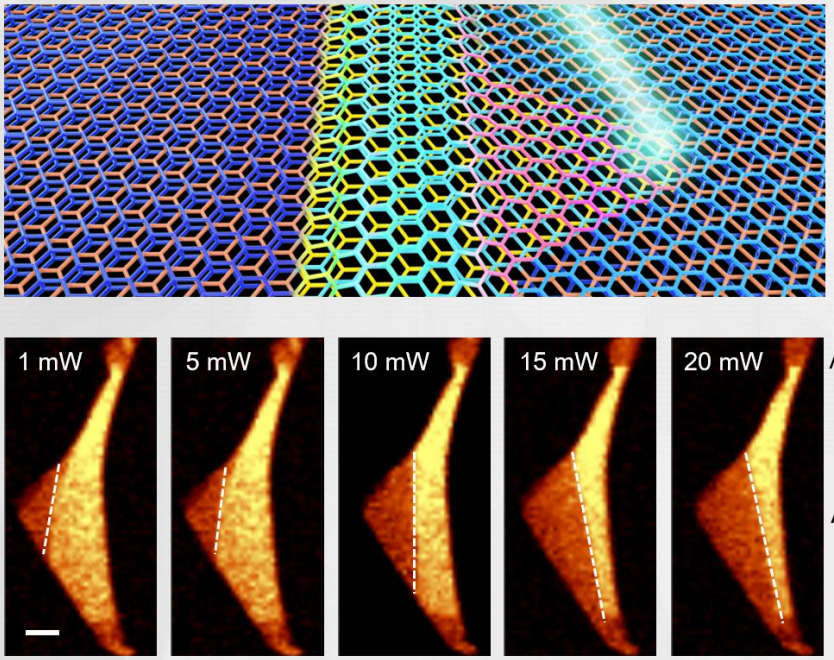

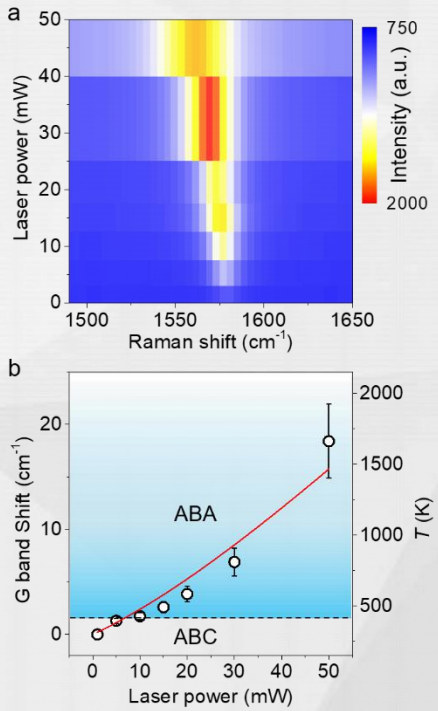

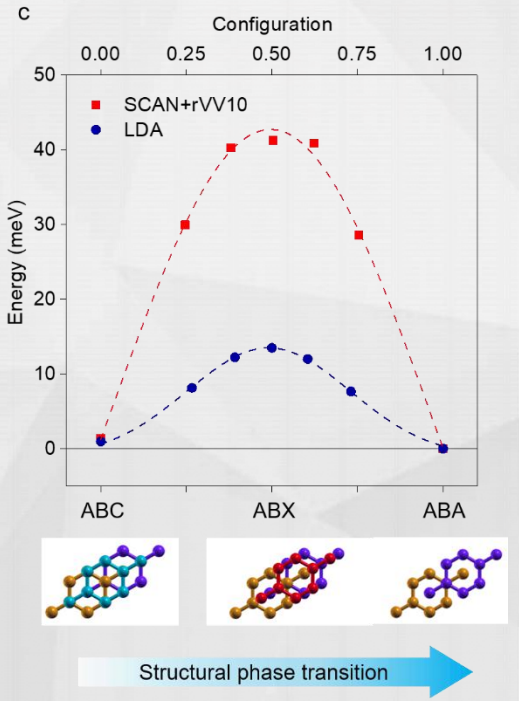

Zhang, Zhu and Dai* et al. Light: Science & Applications 9:174 (2020).*

Electron-ion energy exchange

- CEFF is limited in time and size scale

❖ Two-Temperature Model coupled Molecular Dynamics (**TTM-MD**, Duffy *et.al* , Norman *et.al*)

$$C_e \frac{\partial T_e}{\partial t} = -g_{ei}(T_e - T_i) + S(r,t)$$

$$m_i \frac{\partial v_i}{\partial t} = F_i(t) - \gamma_i v_i + \tilde{F}(t)$$

Laser energy: $$S(t) = \frac{\rho \Delta \epsilon}{\tau_0 \sqrt{\pi}} \exp\left[-\left(\frac{t - t_0}{\tau_0}\right)^2\right]$$

[1]Duffy and Rutherford J Phys: Condens Matter, 2006, 19(1): 016207
[2]Norman et al. Contrib Plasma Phys 2013, 53(2): 129-139

Electron-ion energy exchange

- Simulation cell

MD part： 73a*100a*100a （30nm Au foil， 2,920,000 atoms, FCC)

FE part： 84*1*1 (1-dimension electron temperature field)

- Timesteps： 1fs (MD) ,1as (FE)

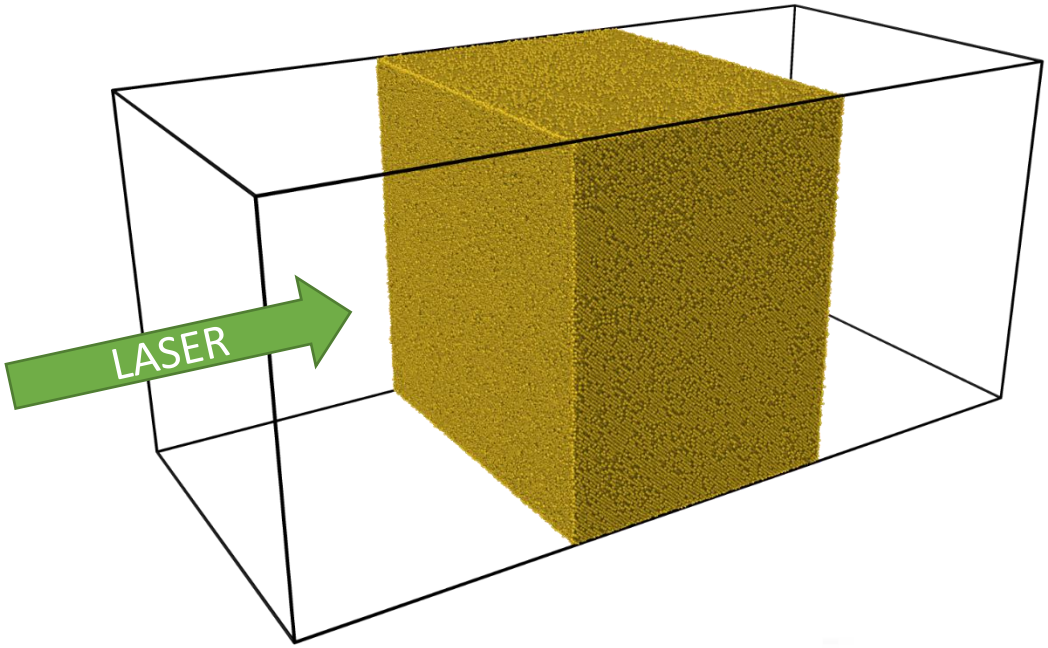

Electron-ion energy exchange

Dynamic Process of ultrafast laser heating(0.2MJ/kg,45fs)

1. Laser energy deposition and electron-phonon energy exchange

- Highly non-equilibrium state
- Uniform heating (ballistic transport of electrons is considered)

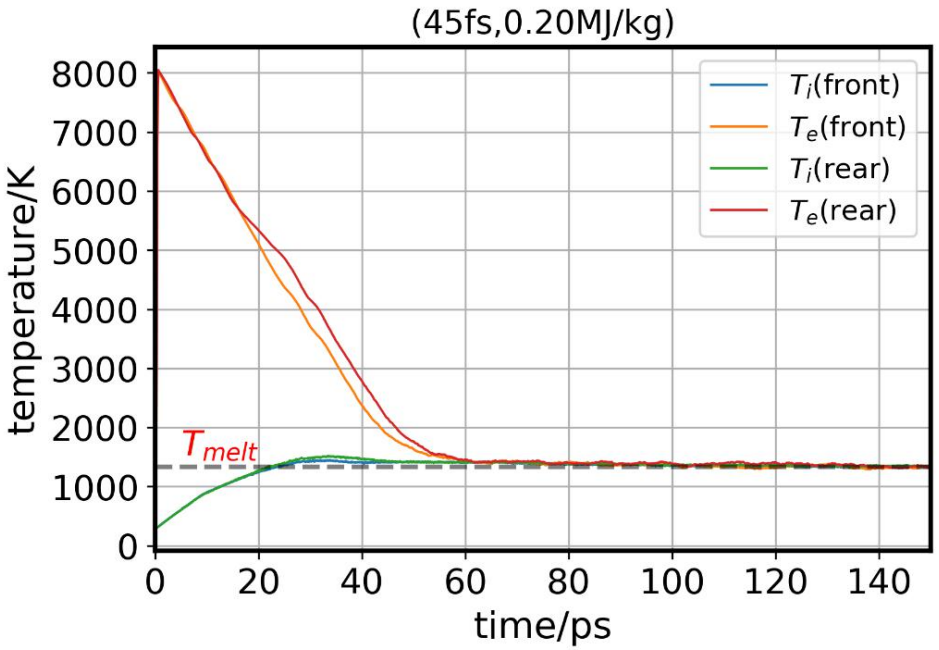

Electron-ion energy exchange

Dynamic Process of ultrafast laser heating(0.2MJ/kg,45fs)

2. Lattice thermal response

- Partial stress confinement
- Periodic oscillation of pressure (propagation of stress wave)

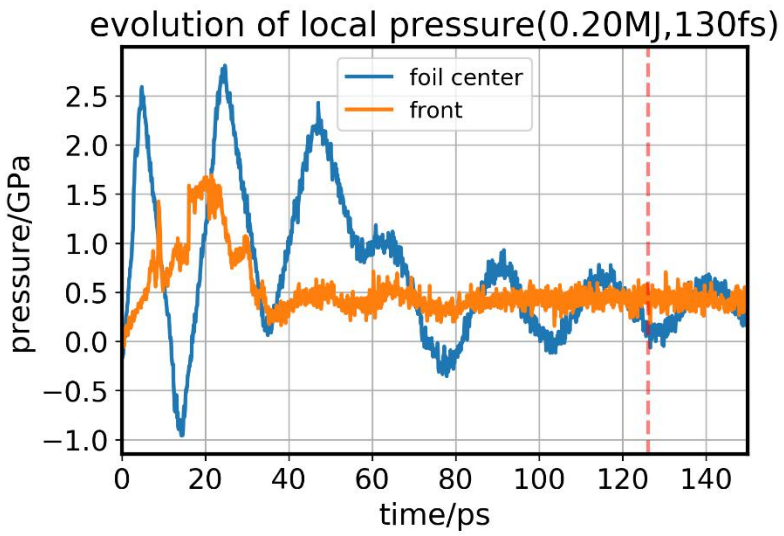

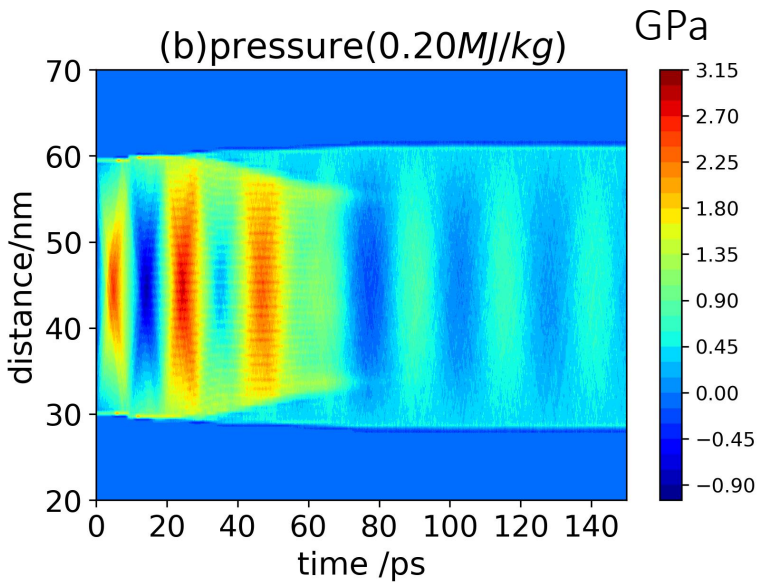

Electron-ion energy exchange

Dynamic Process of ultrafast laser heating (0.2MJ/kg,45fs)

3. Melting mechanism

- **Heterogeneous melting** $(10^2 \sim 10^3 ps)$**: propagation of melting front from free surface**
- **Homogeneous melting** $(\sim 10^1 ps)$ **: nucleation and growth of liquid regions inside foil**

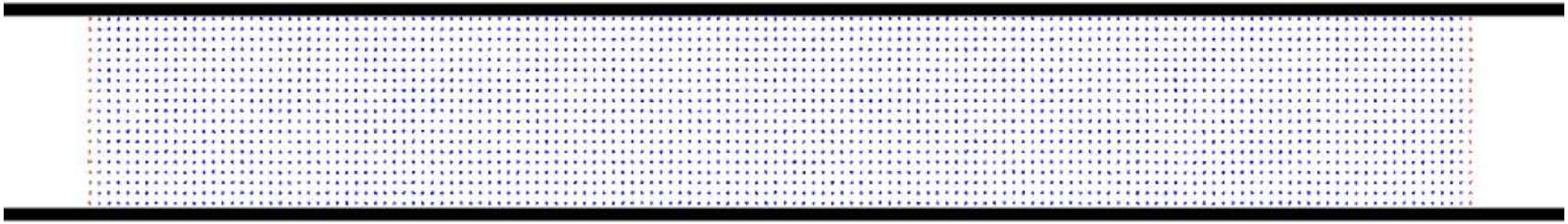

Electron-ion energy exchange

Complete melting time (45fs, 35nm Au foil)

4. Complete melting time

- A threshold (0.19MJ/kg) is found to identify two different regimes
- Indicated a shorter melting time than measurements from Mo Science, 360: 1451 (2018).
-

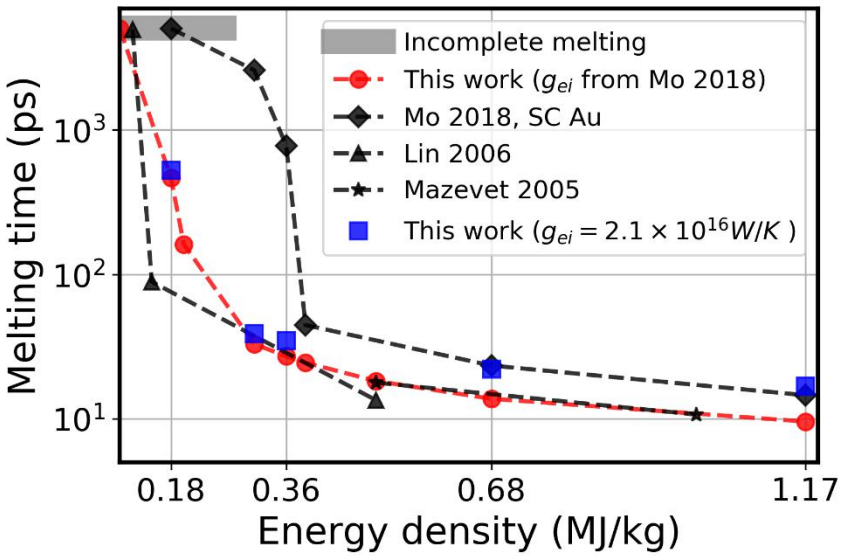

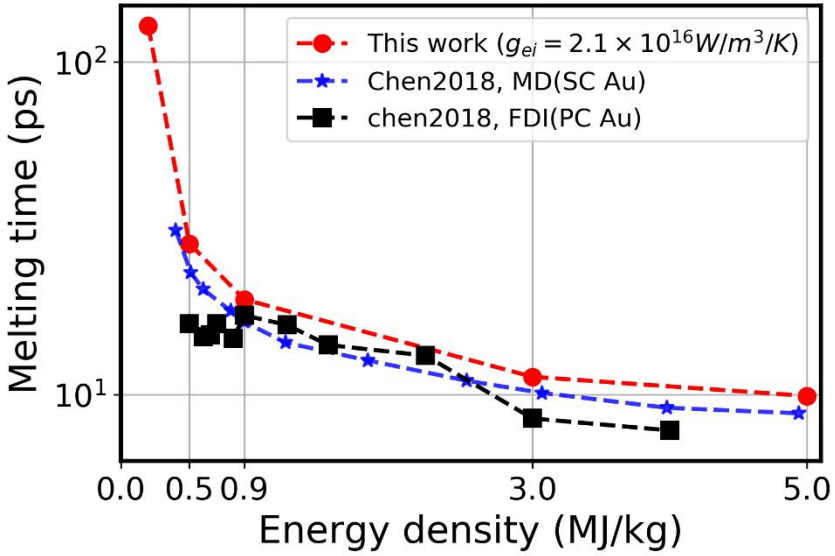

[1] Chen, Mo, Soulard, et al. Physical Review Letters,2018, 121(7): 075002
[2] Mo M, Chen Z, Li R, et al. Science, 2018, 360(6396): 1451–1455

Zeng and Dai. Sci. China Phys. Mech. Astron. (https://doi.org/10.1007/s11433-019-1466-2)*

激光诱导物质结构相变

冲击波加载
爆炸、轻气炮、电磁驱动、激光等

状态测量
速度干涉仪VISAR
获取冲击波波形

结构诊断
原位X射线衍射装置及电镜观察

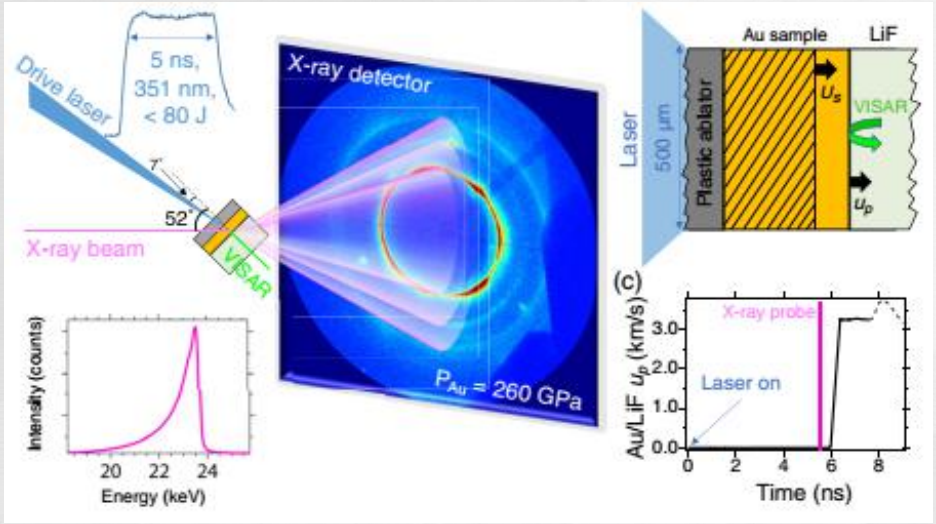

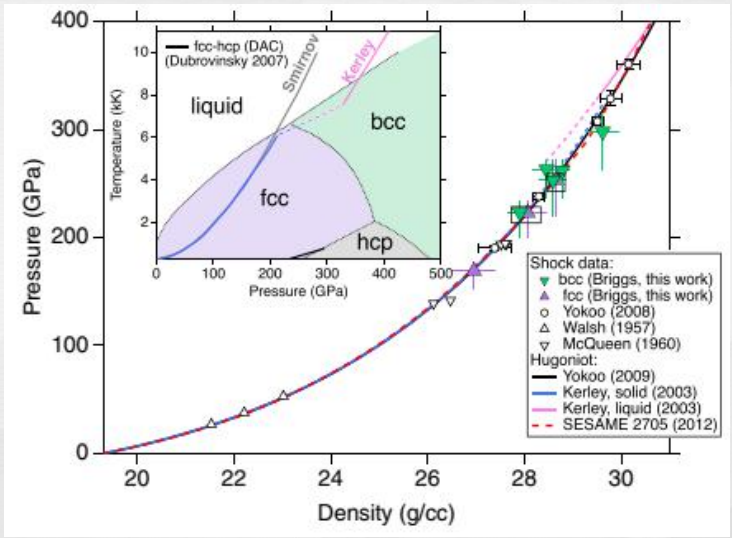

R. Briggs et al. PRL 123 045701 (2019); S. M. Sharma et al. PRL 123 045702 (2019)

√ 精确的状态方程，结构相变点的初步探测

x 技术门槛高、成本昂贵

x 缺乏微观结构高精度诊断及动力学过程观测

Shock-compressed states

Hugoniot Relation

$$E - E_0 = (P + P_0)(1/\rho_0 - 1/\rho)/2$$

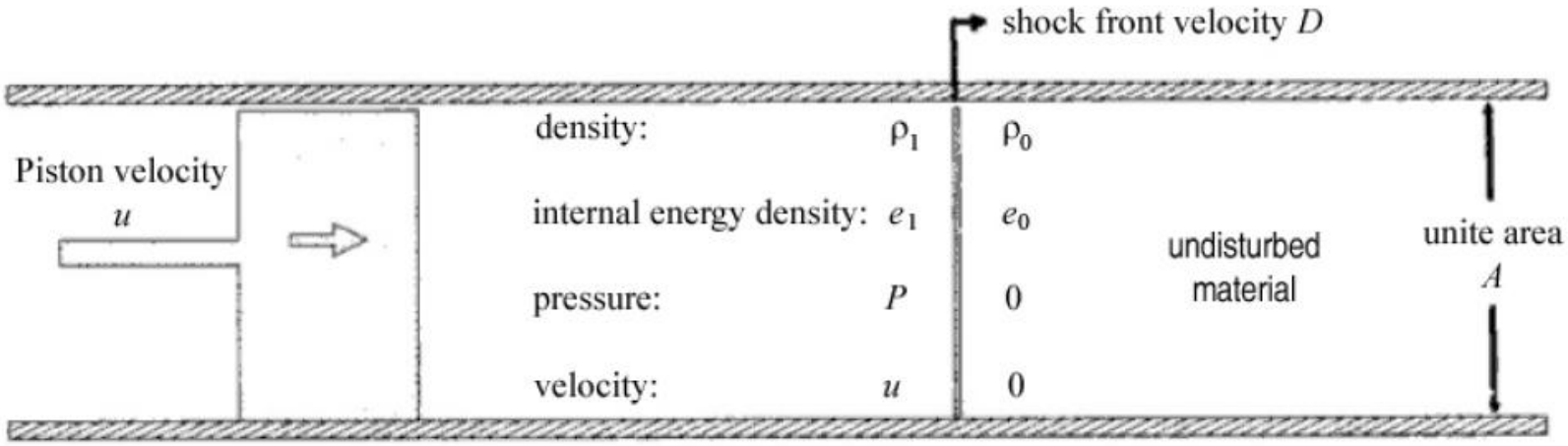

Figure 1. Constant velocity piston-generated shock transition from state 0 to state 1.

冲击压缩理论研究方法

DFT calculations

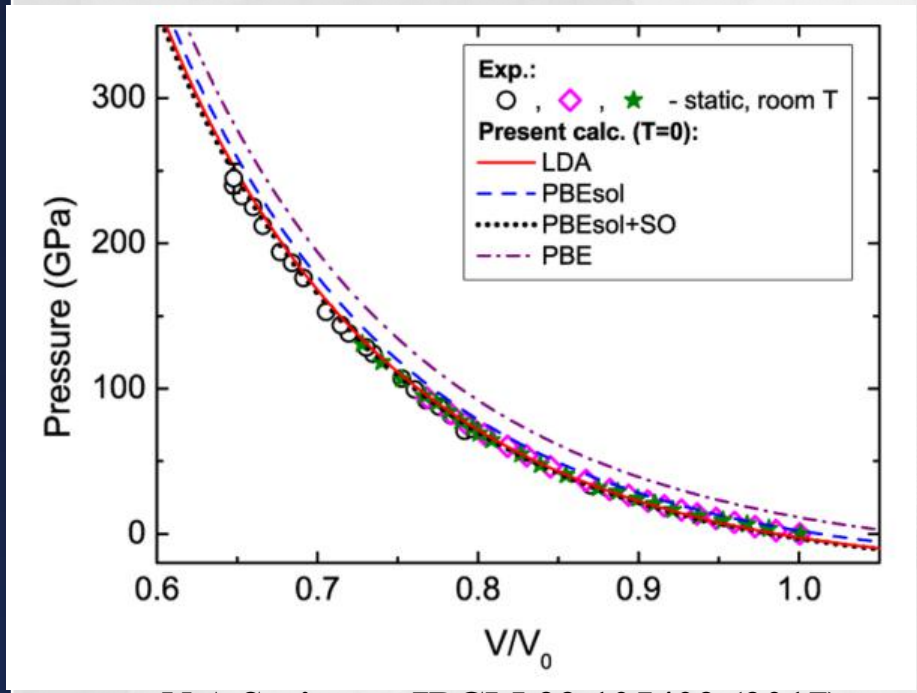

N A Smirnov JPCM 29 105402 (2017)

√ 计算精确，状态方程预测准
x 体系小，计算量大
x 静态计算

MD simulations

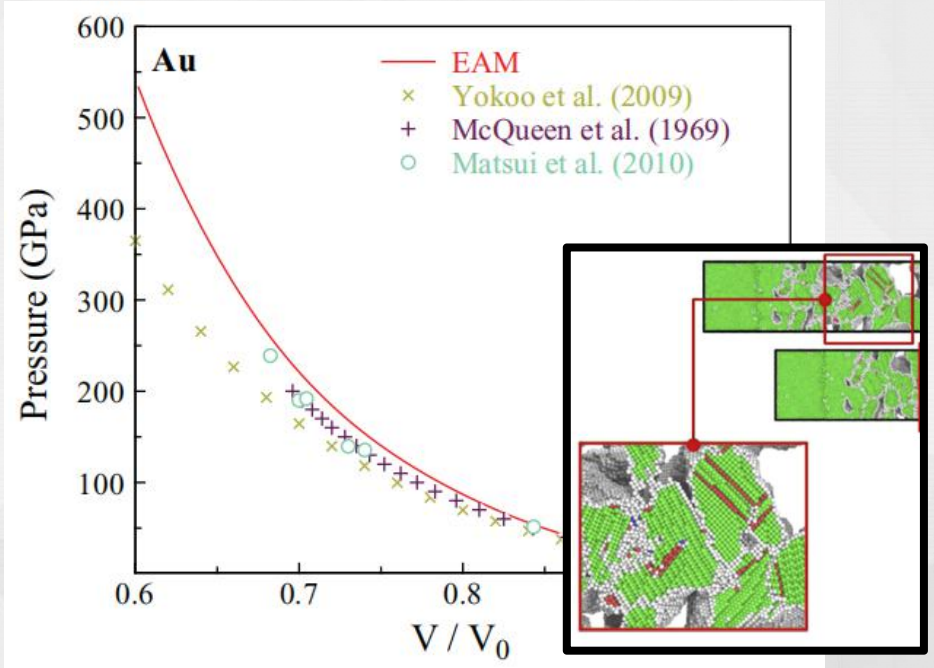

H. W. Sheng PRB 83 134118 (2011)

x 依赖势函数（宽温度宽密度）
√ 体系大，效率高
√ 动态过程，微观结构

激光drive冲击压缩金 FCC→BCC 相变

exp. by Briggs

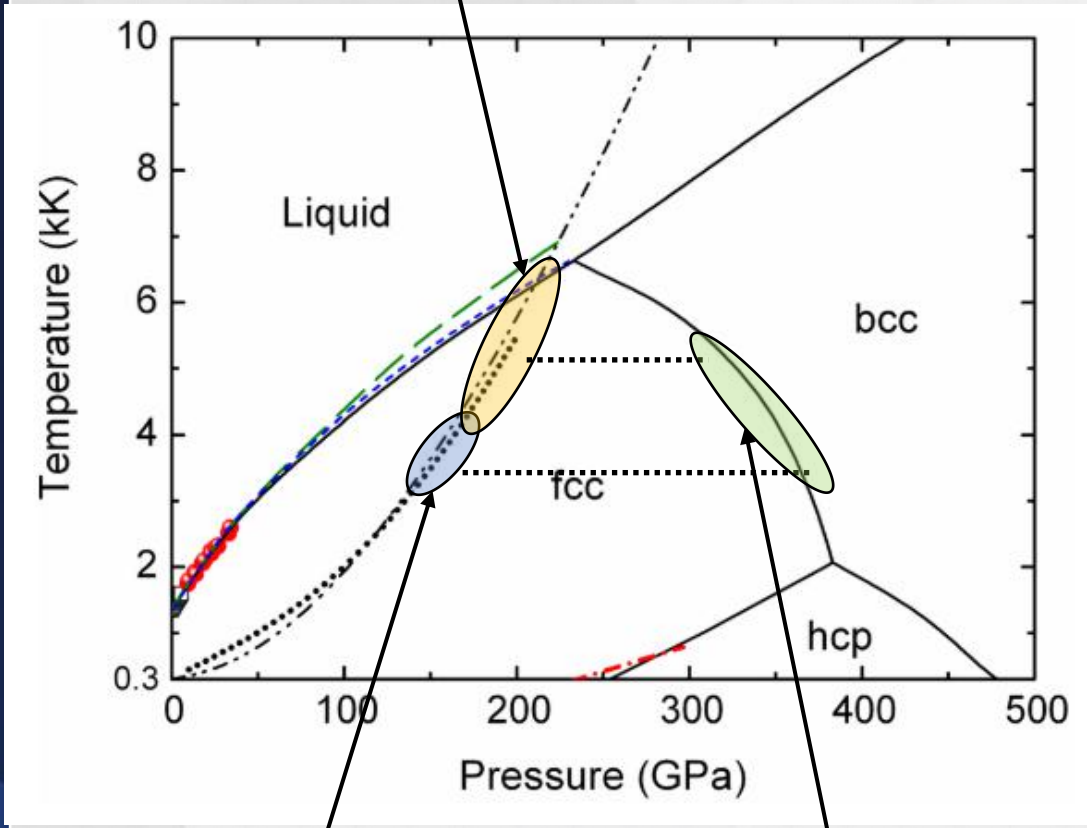

exp. by Sharma

DFT calculations

Laser-shock-wave combining with in-situ XRD experiments:

Phys. Rev. Lett. 124, 235701 (2020);

Phys. Rev. Lett. 123, 045702 (2019);

Phys. Rev. Lett. 123, 045701 (2019);

Nature Physics 15, 89 (2019);

Phys. Rev. X 10, 011010 (2020).

- 理论计算间的差异
- 实验与理论计算差异
- 不同实验间的差异

Methods – Machine Learning based Potential

- **Explicitly considered the electron temperature as an additional parameter**
- **Generate a many-body free energy surface**

$$E[\{\psi_i\},\{f_i\}] = U[\{\psi_i\},\{f_i\}] - T\cdot S[\{f_i\}],$$

$$E(\boldsymbol{R},T) = s(T)\tilde{E}(\boldsymbol{R},T) = s(T)\sum_I \tilde{E}_I(\mathcal{R}_I,T)$$

$$s(T) \equiv \hat{\sigma}_{\boldsymbol{F}}(T) = e^b \cdot T^a$$

DFT calculations + Machine Learning →

Deep Potential

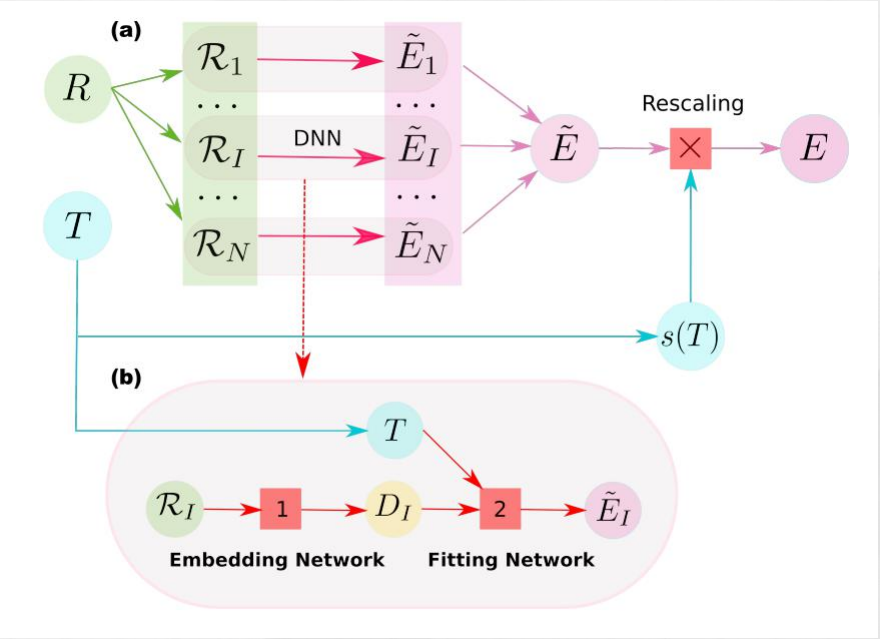

Wang H et al. 2018 Comput. Phys. Commun. 228 178–84

DP-GEN: an effective scheme for learning

主要流程：

- 搜索样本空间 *Exploration*
- 增加标记样本 *Labeling*
- 训练新的模型 *Training*
- 循环迭代至可靠模型

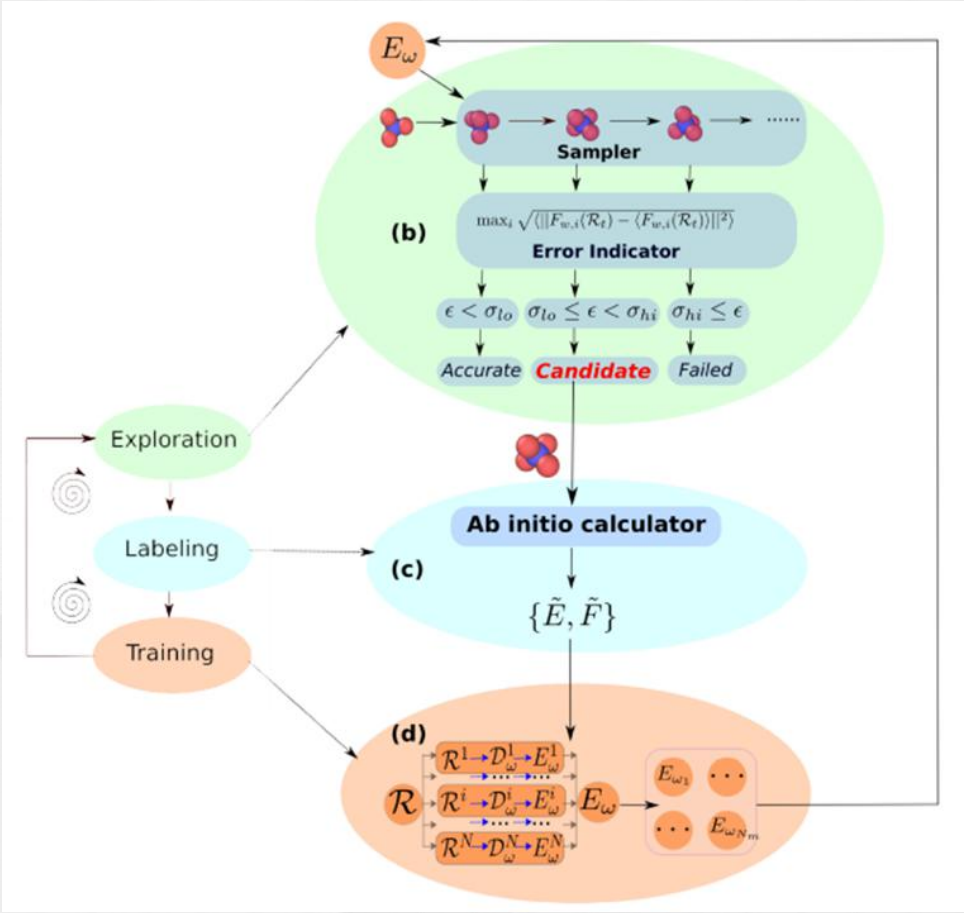

Zhang L, Lin D Y, Wang H, et al. Phys. Rev. Mater. 3, 023804 (2019)

DP-GEN: an effective scheme for learning

Sampling:

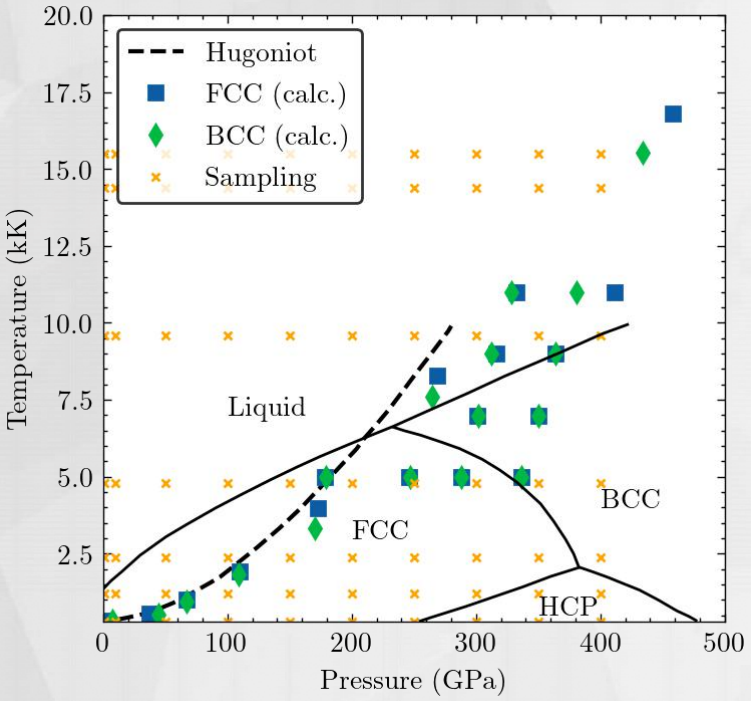

Model deviation:

eV/A

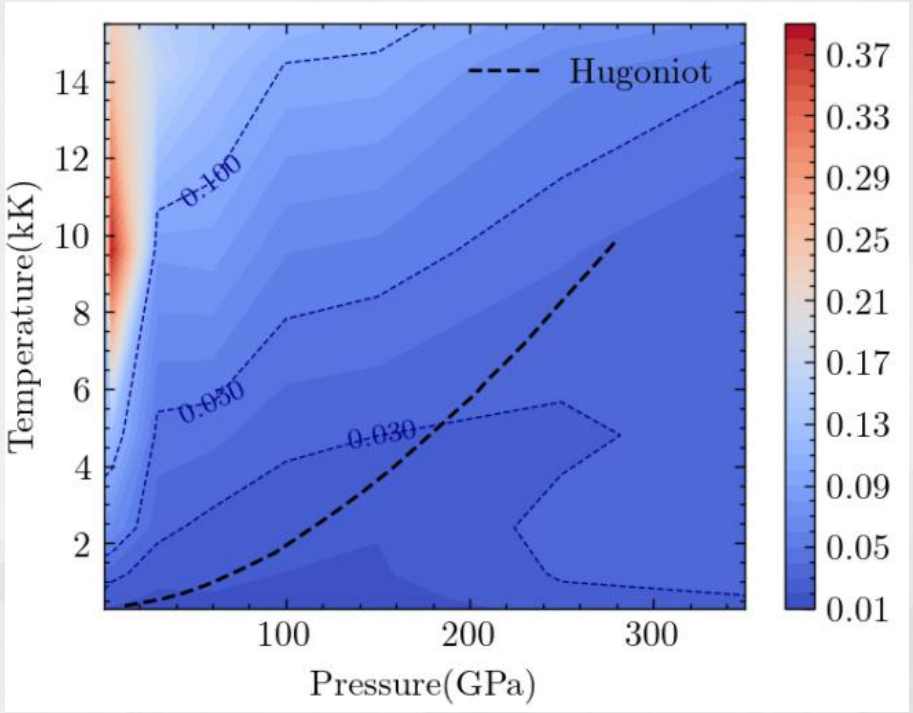

Temperature [300, 15500] K
Pressure [1, 350] GPa
Init surface : vacuum length from 0 to 9 Angstrom)

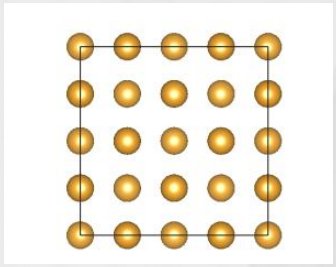

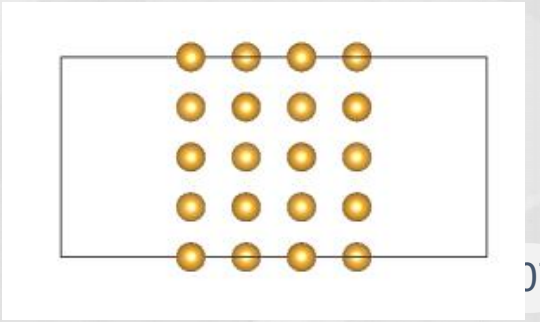

Methods - MSST (Multi Scale Shock Technology)

Hugoniot relations:

$$u = v_s\left(1-\frac{\rho_0}{\rho}\right)$$

$$p-p_0 = v_s^2 p_0\left(1-\frac{\rho_0}{\rho}\right)$$

$$e-e_0 = p_0\left(\frac{1}{\rho_0}-\frac{1}{\rho}\right)+\frac{v_s^2}{2}\left(1-\frac{\rho_0}{\rho}\right)^2$$

For molecular dynamics simulation employ the Lagrangian:

$$L = T\left(\{\dot{\vec{r}}_i\}\right)-V\left(\{\vec{r}_i\}\right)+\frac{1}{2}Q\dot{\upsilon}^2+\frac{1}{2}\frac{v_s^2}{\upsilon_0^2}(\upsilon_0-\upsilon)^2+p_0(\upsilon_0-\upsilon)$$

$$Q\ddot{\upsilon} = \frac{\partial T}{\partial \upsilon}-\frac{\partial V}{\partial \upsilon}-p_0-\frac{v_s^2}{\upsilon_0^2}(\upsilon_0-\upsilon)$$

where $\upsilon = \frac{1}{\rho}$ Q is a masslike parameter

Define shock speed v_s

Initial state: p_0, ρ_0, e_0

→ **Molecular dynamics simulation** ← **Hugoniot relations constraint**

→ **Time-independent steady state at the shock speed**

Output: p, ρ, e, u, T …

Evan J. Reed. et al. PRL, 2003, 90(23).

Dependence of Potentials

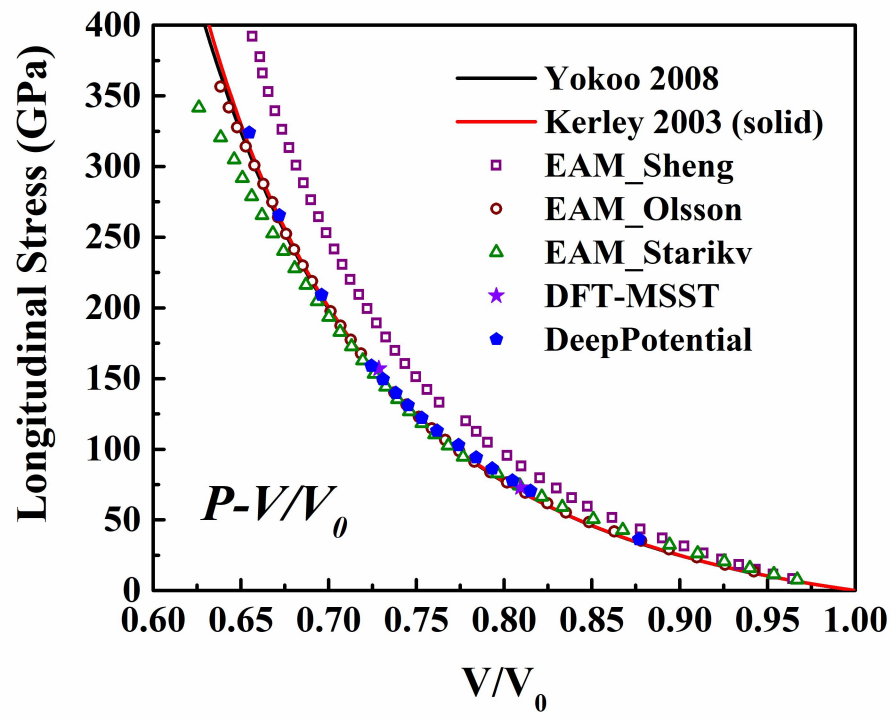

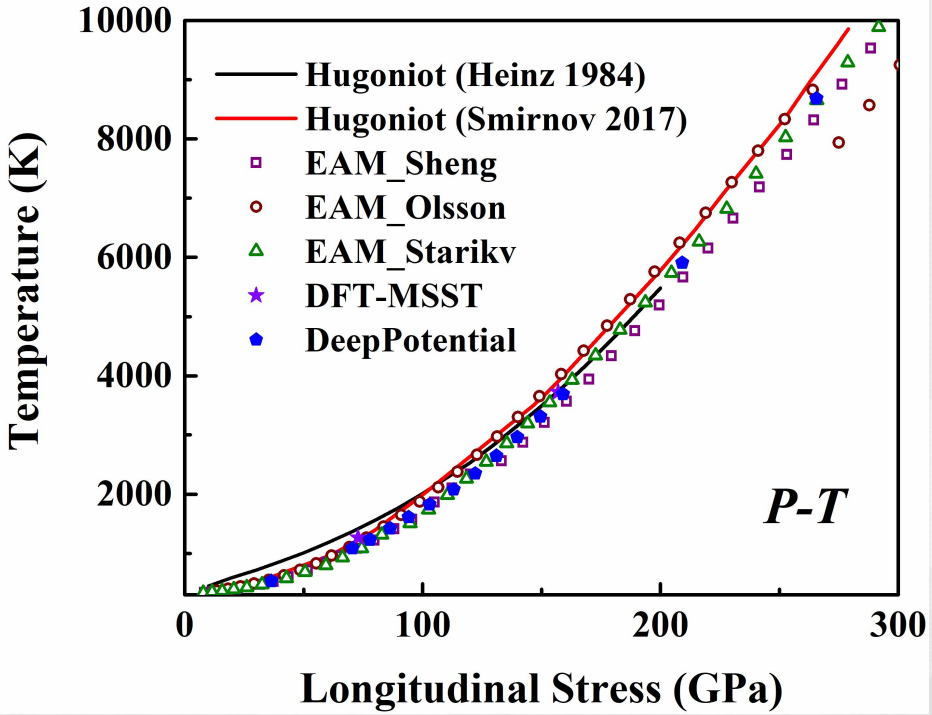

Method	Atoms	Hugoniot	Structure
Deep Potential	10000	√	√
EAM Potential	10000	×	√
DFT-MSST	96	√	×

Validation in NEMD Simulations

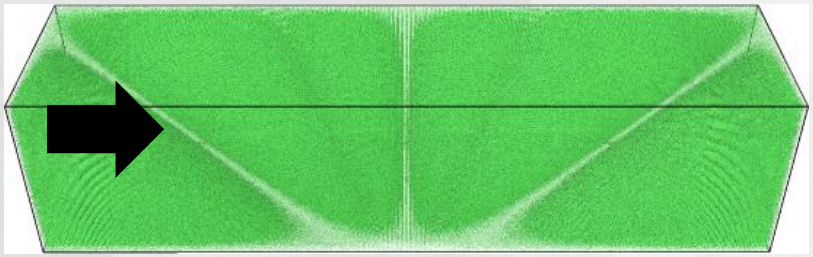

8320000 atoms

132×32.6×32.6 nm^3

Piston Velocity U_p = **0.6/1.4/2.5 km/s**

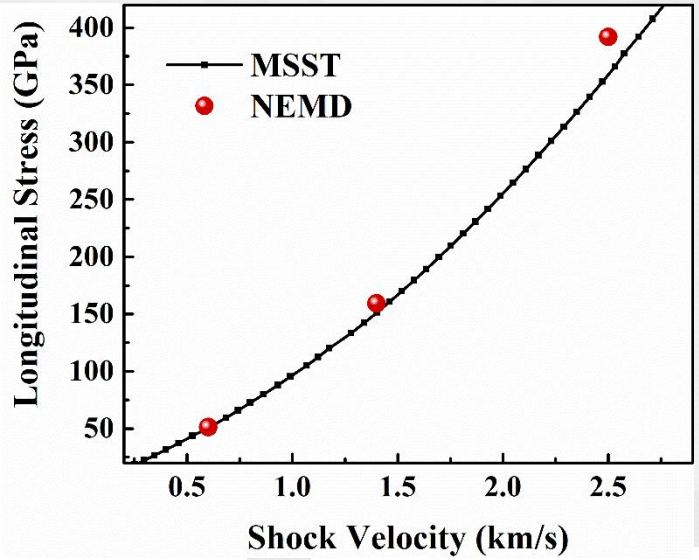

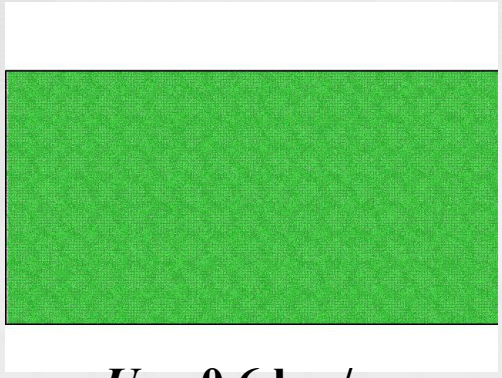

U_p = 0.6 km/s
P_{xx} = 51.5 GPa

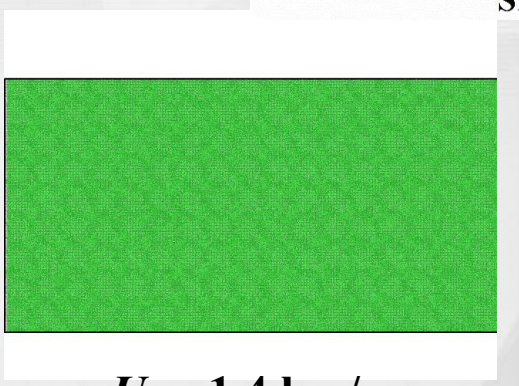

U_p = 1.4 km/s
P_{xx} = 159 GPa

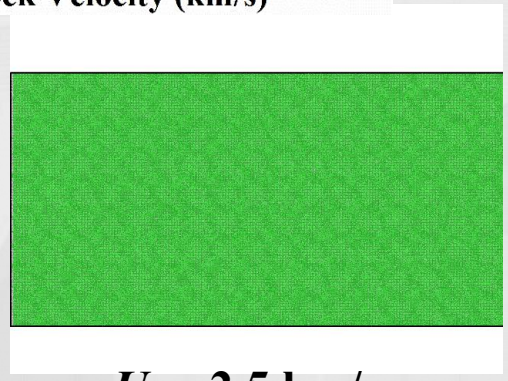

U_p = 2.5 km/s
P_{xx} = 392 GPa

Structural Transformation

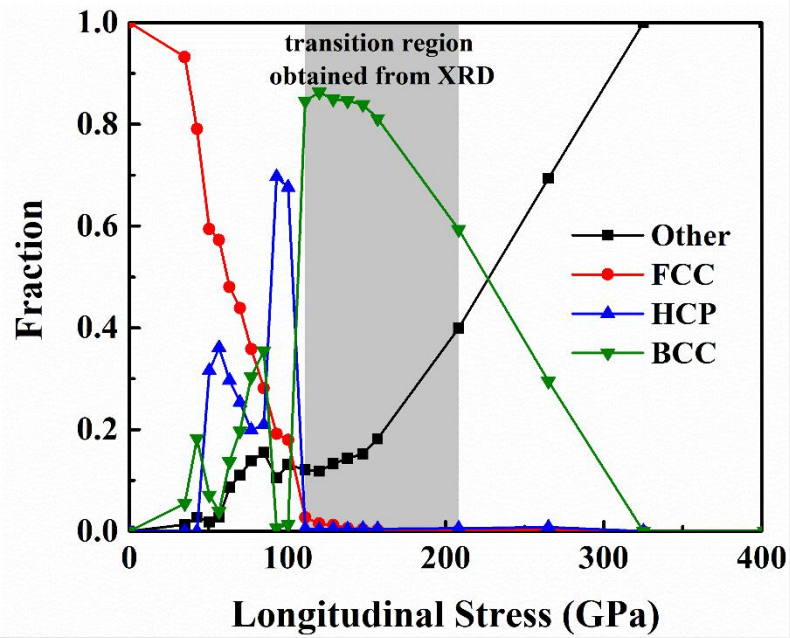

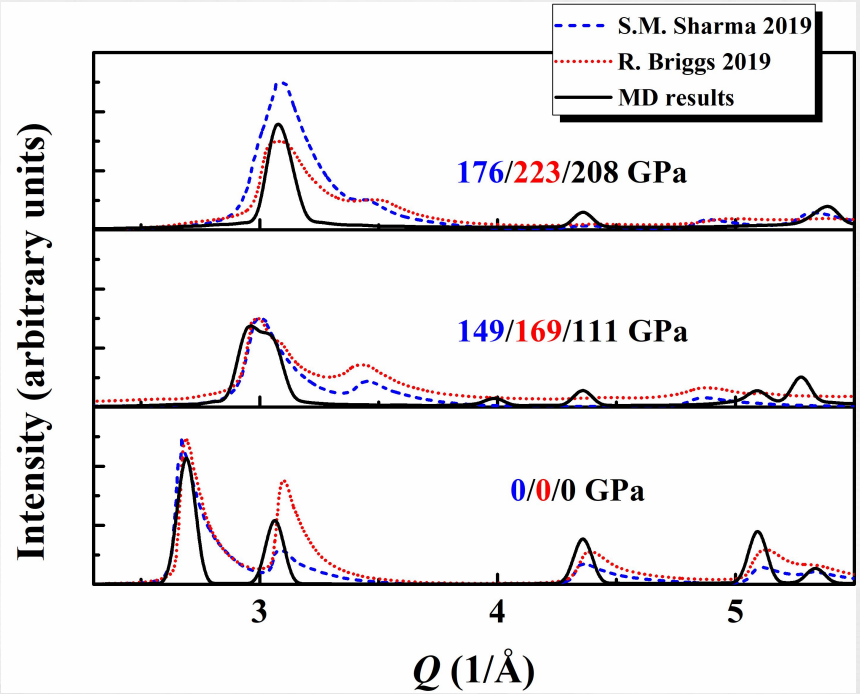

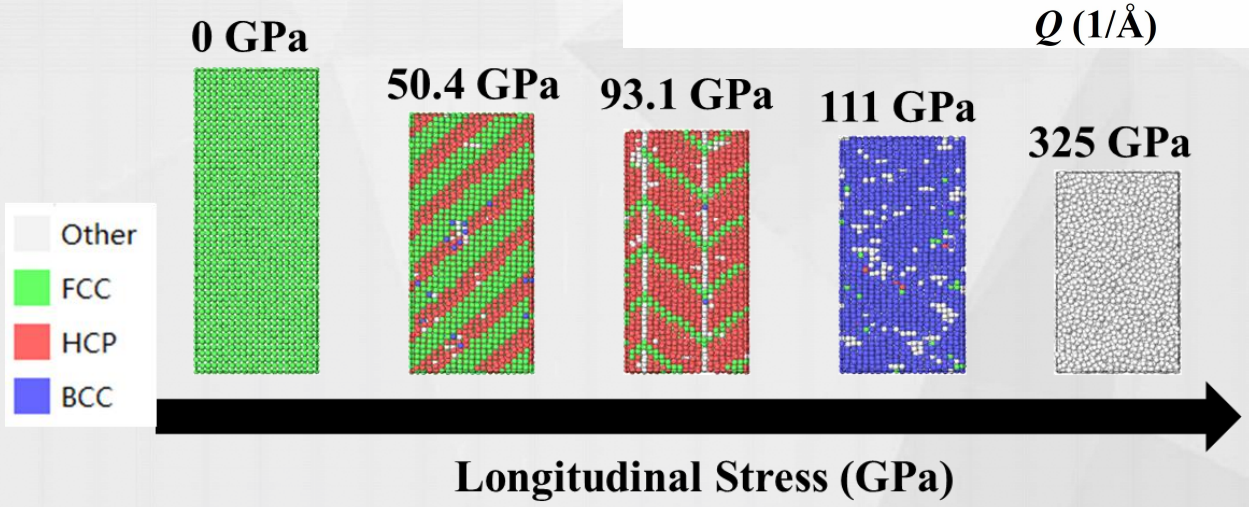

Free Energy Calculations

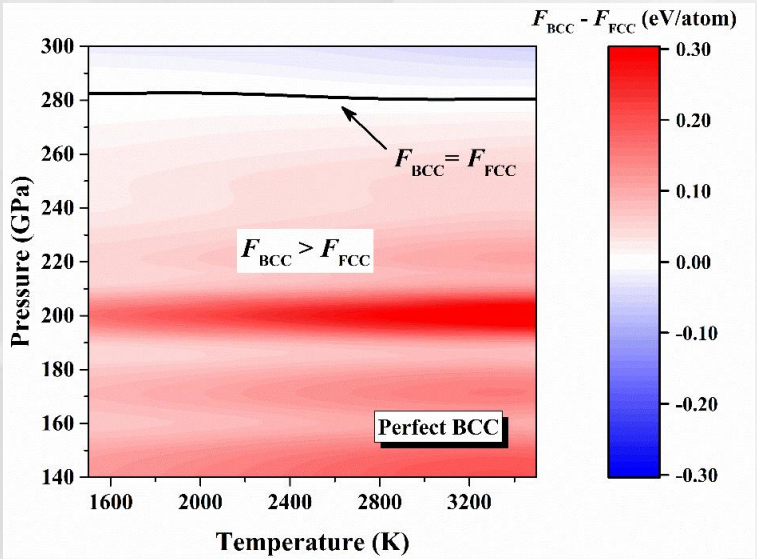

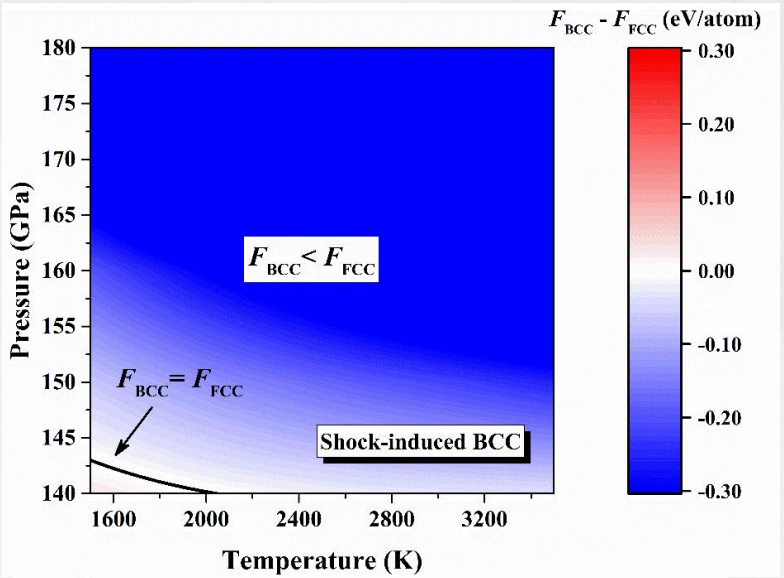

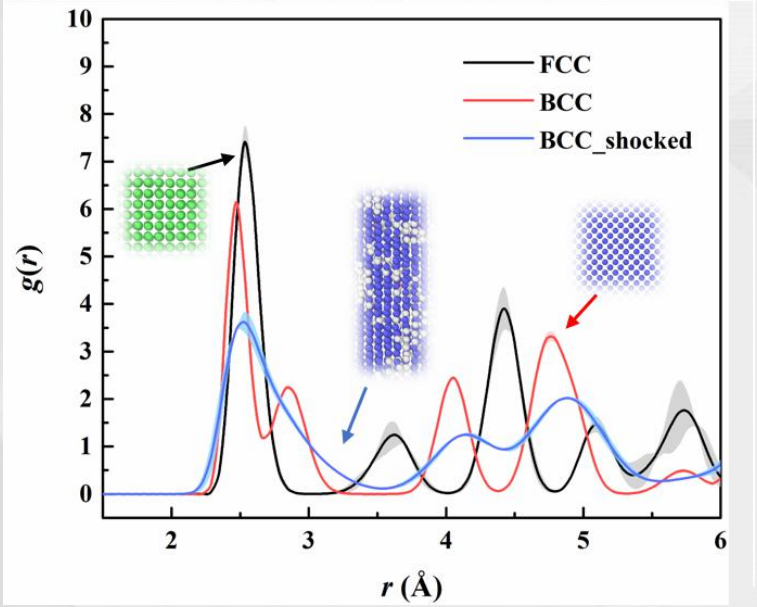

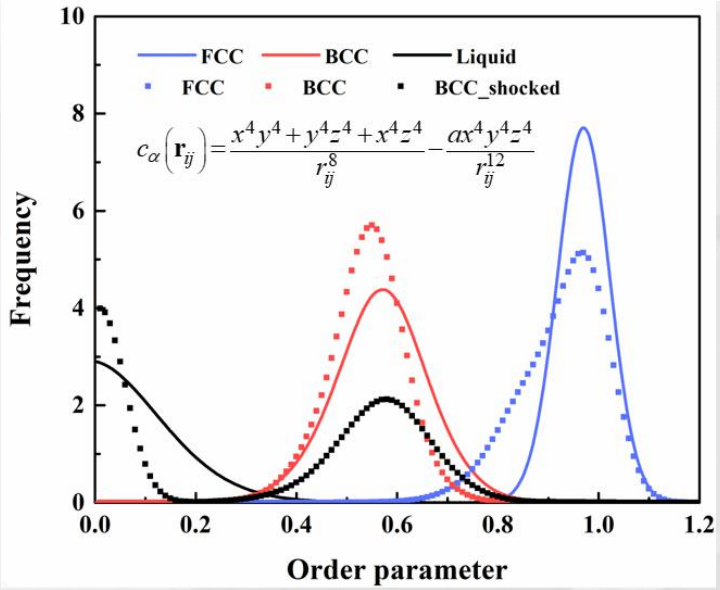

Effect of atomic defects

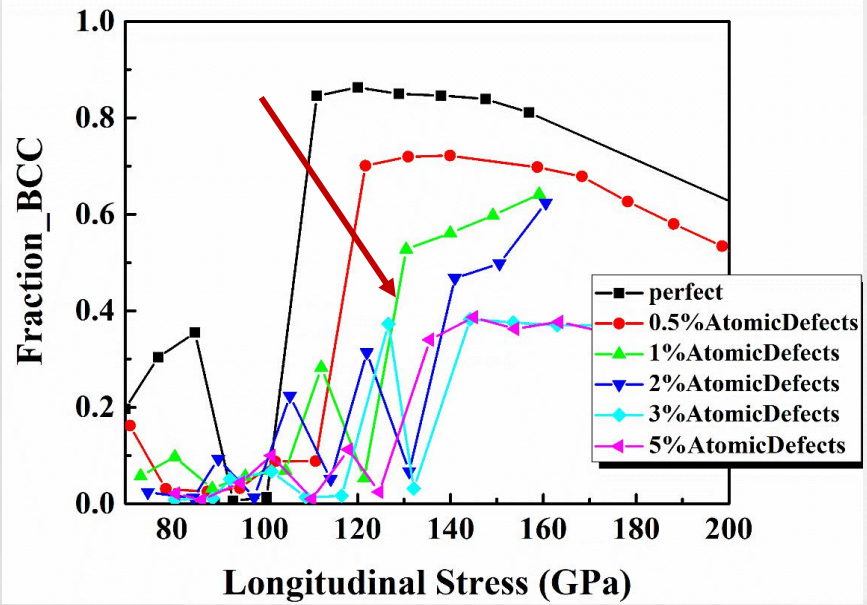

Effect of spherical defects

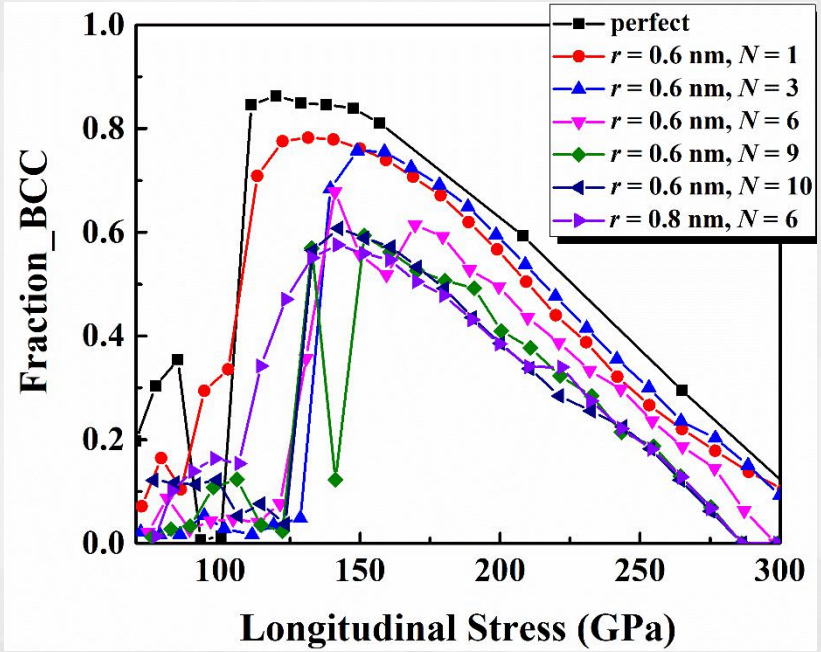

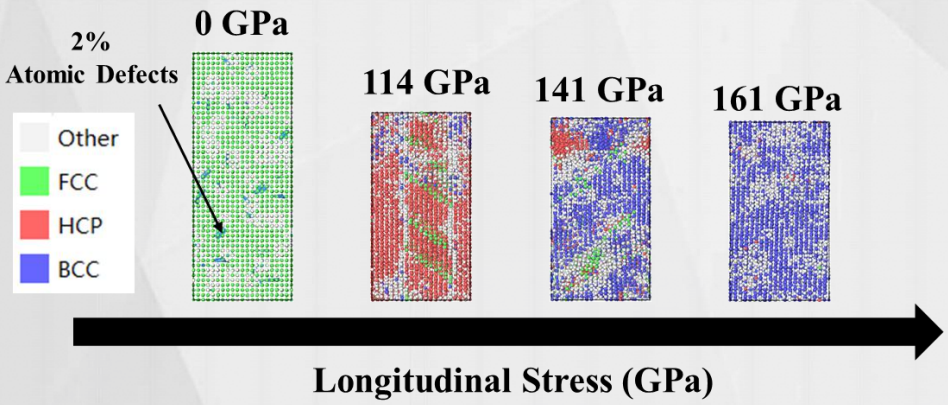

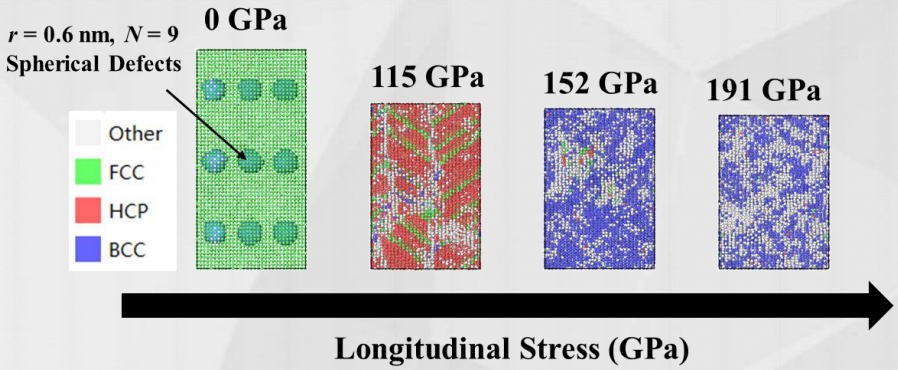

激光诱导物质结构相变

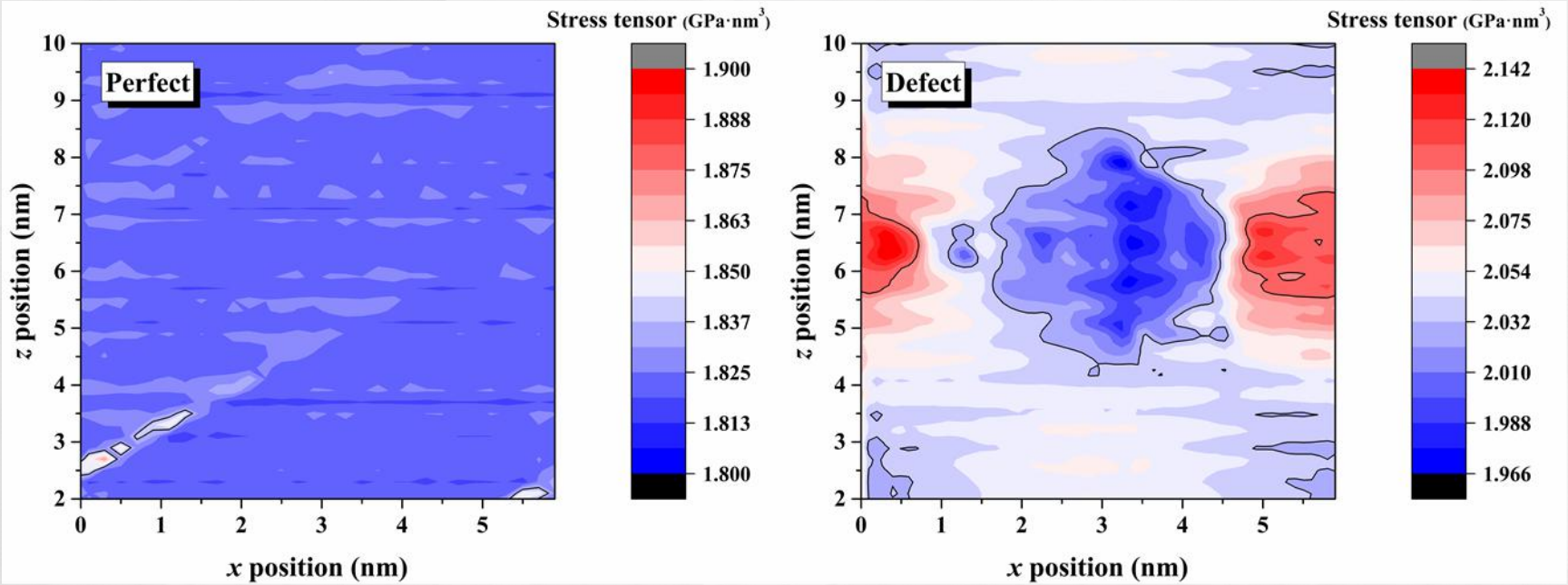

- 初始结构中含有缺陷会形成界面，增加界面能垒，降低内部应力，导致相变压力升高

- 无序结构 vs 缺陷的竞争机制共同决定了FCC→BCC相变压力

Chen, Dai* et al. arXiv:2006.13136

国防科技大学
National University of Defense Technology

Thanks for your attention!